

**EFFECTS OF PORTLAND CEMENT PARTICLE SIZE ON HEAT OF  
HYDRATION**

**Contract No. BDK84 977-13**

**Final Report**

**December 2013**

Submitted to  
Miss Sandra Bell (Sandra.bell@dot.state.fl.us)  
The Florida Department of Transportation  
Research Center  
605 Suwannee Street, MS 30  
Tallahassee, FL 32399

c/o Dr. Harvey DeFord, Ph.D.  
Structures Materials Research Specialist  
State Materials Office

Submitted by

Dr. Abla Zayed (zayed@usf.edu)  
Department of Civil & Environmental Engineering  
University of South Florida  
4202 E Fowler Avenue  
Tampa, Florida 33620

## **DISCLAIMER**

The opinions, findings, and conclusions expressed in this publication are those of the authors and not necessarily those of the State of Florida Department of Transportation (FDOT), the U.S. Department of Transportation (USDOT), or the Federal Highway Administration (FHWA).

**METRIC CONVERSION CHARTS**  
**APPROXIMATE CONVERSIONS TO SI UNITS**

<b>SYMBOL</b>	<b>WHEN YOU KNOW</b>	<b>MULTIPLY BY</b>	<b>TO FIND</b>	<b>SYMBOL</b>
<b>LENGTH</b>				
<b>in</b>	inches	25.4	millimeters	mm
<b>ft</b>	feet	0.305	meters	m
<b>yd</b>	yards	0.914	meters	m
<b>mi</b>	miles	1.61	kilometers	km

<b>SYMBOL</b>	<b>WHEN YOU KNOW</b>	<b>MULTIPLY BY</b>	<b>TO FIND</b>	<b>SYMBOL</b>
<b>AREA</b>				
<b>in<sup>2</sup></b>	Square inches	645.2	square millimeters	mm <sup>2</sup>
<b>ft<sup>2</sup></b>	Square feet	0.093	square meters	m <sup>2</sup>
<b>yd<sup>2</sup></b>	square yard	0.836	square meters	m <sup>2</sup>
<b>ac</b>	acres	0.405	hectares	ha
<b>mi<sup>2</sup></b>	square miles	2.59	square kilometers	km <sup>2</sup>

<b>SYMBOL</b>	<b>WHEN YOU KNOW</b>	<b>MULTIPLY BY</b>	<b>TO FIND</b>	<b>SYMBOL</b>
<b>VOLUME</b>				
<b>fl oz</b>	fluid ounces	29.57	milliliters	mL
<b>gal</b>	gallons	3.785	liters	L
<b>ft<sup>3</sup></b>	cubic feet	0.028	cubic meters	m <sup>3</sup>
<b>yd<sup>3</sup></b>	cubic yards	0.765	cubic meters	m <sup>3</sup>
NOTE: volumes greater than 1000 L shall be shown in m <sup>3</sup>				

<b>SYMBOL</b>	<b>WHEN YOU KNOW</b>	<b>MULTIPLY BY</b>	<b>TO FIND</b>	<b>SYMBOL</b>
<b>MASS</b>				
<b>oz</b>	ounces	28.35	grams	g
<b>lb</b>	pounds	0.454	kilograms	kg
<b>T</b>	short tons (2000 lb)	0.907	megagrams (or	Mg (or "t")

**APPROXIMATE CONVERSIONS TO SI UNITS**

<b>SYMBOL</b>	<b>WHEN YOU KNOW</b>	<b>MULTIPLY BY</b>	<b>TO FIND</b>	<b>SYMBOL</b>
<b>TEMPERATURE (exact degrees)</b>				
<b>°F</b>	Fahrenheit	5 (F-32)/9 or (F-32)/1.8	Celsius	<b>°C</b>

<b>SYMBOL</b>	<b>WHEN YOU KNOW</b>	<b>MULTIPLY BY</b>	<b>TO FIND</b>	<b>SYMBOL</b>
<b>ILLUMINATION</b>				
<b>fc</b>	foot-candles	10.76	lux	lx
<b>fl</b>	foot-Lamberts	3.426	candela/m <sup>2</sup>	cd/m <sup>2</sup>

<b>SYMBOL</b>	<b>WHEN YOU KNOW</b>	<b>MULTIPLY BY</b>	<b>TO FIND</b>	<b>SYMBOL</b>
<b>FORCE and PRESSURE or STRESS</b>				
<b>lbf</b>	poundforce	4.45	newtons	N
<b>lbf/in<sup>2</sup></b>	poundforce per square inch	6.89	kilopascals	kPa

**APPROXIMATE CONVERSIONS TO SI UNITS**

<b>SYMBOL</b>	<b>WHEN YOU KNOW</b>	<b>MULTIPLY BY</b>	<b>TO FIND</b>	<b>SYMBOL</b>
<b>LENGTH</b>				
<b>mm</b>	millimeters	0.039	inches	in
<b>m</b>	meters	3.28	feet	ft
<b>m</b>	meters	1.09	yards	yd
<b>km</b>	kilometers	0.621	miles	mi

<b>SYMBOL</b>	<b>WHEN YOU KNOW</b>	<b>MULTIPLY BY</b>	<b>TO FIND</b>	<b>SYMBOL</b>
<b>AREA</b>				
<b>mm<sup>2</sup></b>	square millimeters	0.0016	square inches	in <sup>2</sup>
<b>m<sup>2</sup></b>	square meters	10.764	square feet	ft <sup>2</sup>
<b>m<sup>2</sup></b>	square meters	1.195	square yards	yd <sup>2</sup>
<b>ha</b>	hectares	2.47	acres	ac
<b>km<sup>2</sup></b>	square kilometers	0.386	square miles	mi <sup>2</sup>

### APPROXIMATE CONVERSIONS TO SI UNITS

SYMBOL	WHEN YOU KNOW	MULTIPLY BY	TO FIND	SYMBOL
<b>VOLUME</b>				
<b>mL</b>	milliliters	0.034	fluid ounces	fl oz
<b>L</b>	liters	0.264	gallons	gal
<b>m<sup>3</sup></b>	cubic meters	35.314	cubic feet	ft <sup>3</sup>
<b>m<sup>3</sup></b>	cubic meters	1.307	cubic yards	yd <sup>3</sup>

SYMBOL	WHEN YOU KNOW	MULTIPLY BY	TO FIND	SYMBOL
<b>MASS</b>				
<b>g</b>	grams	0.035	ounces	oz
<b>kg</b>	kilograms	2.202	pounds	lb
<b>Mg (or "t")</b>	megagrams (or "metric ton")	1.103	short tons (2000 lb)	T

SYMBOL	WHEN YOU KNOW	MULTIPLY BY	TO FIND	SYMBOL
<b>TEMPERATURE (exact degrees)</b>				
<b>°C</b>	Celsius	1.8C+32	Fahrenheit	°F

SYMBOL	WHEN YOU KNOW	MULTIPLY BY	TO FIND	SYMBOL
<b>ILLUMINATION</b>				
<b>lx</b>	lux	0.0929	foot-candles	fc
<b>cd/m<sup>2</sup></b>	candela/m <sup>2</sup>	0.2919	foot-Lamberts	fl

SYMBOL	WHEN YOU KNOW	MULTIPLY BY	TO FIND	SYMBOL
<b>FORCE and PRESSURE or STRESS</b>				
<b>N</b>	newtons	0.225	poundforce	lbf
<b>kPa</b>	kilopascals	0.145	poundforce per square inch	lbf/in <sup>2</sup>

\*SI is the symbol for the International System of Units. Appropriate rounding should be made to comply with Section 4 of ASTM E380.  
(Revised March 2003)

**Technical Report Documentation Page**

1. Report No.	2. Government Accession No.	3. Recipient's Catalog No.	
4. Title and Subtitle EFFECT OF PORTLAND CEMENT PARTICLE SIZE ON HEAT OF HYDRATION		5. Report Date January 2014	
		6. Performing Organization Code	
7. Author(s) Abla Zayed, Ph.D. Ahmadreza Sedaghat, M.Sc., PE., Andre Bien-Aime, M.Sc., and Natalya Shanahan, M.Sc.		8. Performing Organization Report No.	
9. Performing Organization Name and Address Department of Civil and Environmental Engineering University of South Florida 4202 E Fowler Avenue; ENG 118 Tampa, FL 33620		10. Work Unit No. (TRAIS)	
		11. Contract or Grant No. BDK84 977-13	
12. Sponsoring Agency Name and Address Florida Department of Transportation Research Center 605 Suwannee Street, MS 30 Tallahassee, FL 32399		13. Type of Report and Period Covered Final Report June 2010 – December 2013	
		14. Sponsoring Agency Code	
15. Supplementary Notes			
16. Abstract Following specification harmonization for portland cements, FDOT engineers reported signs of deterioration in concrete elements due to temperature rise effects. One of the main factors that affect concrete temperature rise potential is the heat generated by portland cement during hydration. This study was initiated to identify the effect of cement fineness on the heat generated by portland cement. Eleven cements were selected for this study to address the effects of cement fineness and mineralogy. Several of the cements came from the same source but had different grinds. This was important in studying the fineness contribution to heat of hydration while maintaining similar cement mineralogy. The as-received cements from different suppliers had a wide range of mineralogical compositions which allowed the study of the effects of mineralogy on the heat of hydration. Cements were characterized through oxide chemical analysis, x-ray diffraction, Blaine fineness, laser particle size analysis, setting behavior, and strength measurements. Additionally, limited restrained shrinkage experiments were performed on two of the cements from the same source to determine the effect of cement fineness on restrained shrinkage. The findings indicate that cement fineness is better correlated to 7-day heat of hydration than the heat index expressed as $C_3S + 4.75 C_3A$ . Additionally, the results indicate that a finer cement experiences higher shrinkage than a coarser cement. Comparison of activation energies indicates that cements with higher fineness have lower activation energy. For Type II moderate heat (MH) portland cements that will be used in structural concrete elements where there is a risk of cracking due to thermal stresses, it is recommended that limits be placed on the heat of hydration, the Blaine fineness, and the heat index.			
17. Key Word Blaine fineness, mean particle size, heat index, heat of hydration, heat of solution, isothermal calorimeter, ASTM C186, ASTM C150, AASHTO M85, cement mineralogy, activation energy.		18. Distribution Statement	
19. Security Classif. (of this report) Unclassified	20. Security Classif. (of this page) Unclassified	21. No. of Pages 95	22. Price

## **AKNOWLEDGEMENTS**

This work has been supported by the Florida Department of Transportation and the Federal Highway Administration. The Principal Investigator appreciates the valuable discussions with Dr. Charles Ishee, PE, the initial Project Manager, who is currently with the United States Air Force Research Lab at Tyndall Air Force Base. The technical assistance offered throughout the course of this work by Mr. Michael Bergin, PE and Dr. Harvey DeFord, the current Project Manager, is greatly appreciated.

## EXECUTIVE SUMMARY

### Scope:

The objective of this study was to address the effect of cement fineness on the heat of hydration of portland cement. The significance of heat of hydration of portland cement is due to its role in thermal cracking of massive concrete structural elements. Heat generated through the hydration of portland cement is dependent on cement composition and fineness. Underestimating the amount of heat generated during the early hydration of a portland cement can have profound effects on the durability and service life of concrete structures that are designed and constructed using this cement. Current standard specifications for portland cement (ASTM C150 or AASHTO M85) present a heat index to quantify the amount of heat generated by a portland cement. The heat index uses the phase composition of a cement as the basis for assessing its potential for heat generation. This methodology does not take into account the effect of cement fineness on the heat generated. Data that validate this methodology are limited, and compiled from cements that have a substantially different mineralogical composition and particle size than the currently produced portland cements. This study was initiated to collect scientific data to establish the validity and limitations of the current methodology and to address the consequences of the exclusion of cement fineness as an important criterion for the estimation of the amount of heat generated during cement hydration at early ages.

To address the above objectives, 11 portland cements were used in this study. Of the eleven cements, three came from one source and were labeled CLEP, CLE02 and CLE03, six cements came from three different sources with 2 cements per source, and two cements came from two different sources. The cements obtained from the same source have different fineness, but share the same clinker mineralogy. Analyzing cements with essentially the same mineralogical composition enabled the determination of the effects of cement fineness. The cements selected for

this study had a wide range of fineness and mineralogy. Several characterization techniques were used, including: x-ray fluorescence for elemental and equivalent oxide composition, x-ray diffraction for mineralogical analysis, density measurements, heat of hydration using the solution method and isothermal calorimetry, Blaine fineness, and particle size distribution. Selected cements were used for activation energy determination and restrained shrinkage measurements.

The findings of this study indicate that the heat of hydration calculated from the heat index expression for a particular cement does not reliably correspond to the measured heat of hydration of the cement determined by either the heat of solution method or by isothermal conduction calorimetry. Blaine fineness and particle size distribution of portland cements were found to affect the heat generated by cement on hydration. Additionally, the experimental data show that coarser cements had a lower restrained shrinkage and experienced longer time to crack initiation. The findings indicate that Blaine fineness and heat of hydration obtained from direct heat measurements (isothermal calorimetry) are valuable indicators for assessing the thermal cracking potential of a moderate heat (MH) portland cement. Thus, for applications where the rate and magnitude of temperature rise is of concern and MH portland cements are specified, such as for mass concrete, measurement of heat of hydration should be required in the specifications.

**Recommendations:**

1. Require a maximum heat of hydration and a maximum fineness for Type II (MH) portland cements, where temperature rise is of concern for the service life and durability of structural elements.
2. In specifying a maximum value for the heat of hydration of Type II (MH) portland cement, direct measurement of the heat of hydration, in accordance with ASTM C186 and/or ASTM C1072, has to be also specified. The method used for heat measurement has to be reported.
3. For concrete mix design approval, heat of hydration has to be determined on the cementitious materials used in the mix including chemical admixtures, in the same

proportions used in the concrete mix. This composite heat of hydration should be more useful in predicting the thermal behavior when evaluating the cracking tendency of a mix design.

4. Evaluate which method of determining heat of hydration of portland cement, ASTM C186 or ASTM C1702, is most applicable for predicting the thermal behavior of cementitious structures that are susceptible to cracking from thermal stresses.
5. Investigate further the effects of particle size and fineness on the shrinkage of portland cements and blended portland cements.
6. Study the effects of blending portland cements, with commonly used pozzolanic materials, on the hydration kinetics, heat evolution, strength development, and microstructural development.
7. Evaluate the use of Rietveld analysis and scanning electron microscopy coupled with energy dispersive x-ray spectroscopy, for the mineralogical characterization of cementitious systems.

## TABLE OF CONTENTS

DISCLAIMER.....	ii
METRIC CONVERSION CHARTS.....	iii
TECHNICAL REPORT DOCUMENTATION PAGE.....	xvii
ACKNOWLEDGEMENTS.....	xviii
EXECUTIVE SUMMARY .....	xviii
LIST OF TABLES.....	xiii
LIST OF FIGURES .....	xiv
LIST OF ABBREVIATIONS.....	xvii
LIST OF SYMBOLS .....	xviii
CHAPTER 1: INTRODUCTION.....	1
CHAPTER 2: LITERATURE REVIEW .....	3
CHAPTER 3: METHODOLOGY .....	12
3.1 Materials .....	12
3.2 Oxide Chemical Analysis and Density Measurements of As-Received Cements.....	13
3.3 Mineralogical Analysis of Cements.....	13
3.4 Particle Size Analysis for Portland Cements .....	18
3.5 Heat of Hydration Measurements .....	21
3.6 Setting Time.....	23
3.7 Mortar Strength Measurements.....	24
3.8 Activation Energy .....	25
3.9 Restrained Shrinkage Measurements.....	25

CHAPTER 4: RESULTS AND DISCUSSION.....	27
4.1 Introduction.....	27
4.2 Chemical Characterization of As-Received Cements.....	27
4.3 Mineralogical Characterization of Portland Cements.....	32
4.4 Cement Particle Size Analysis .....	32
4.5 Heat of Hydration Using Isothermal Calorimeter.....	36
4.6 Activation Energy Determination.....	41
4.7 Density of As-Received Cements .....	60
4.8 Hydration Process and Cement Fineness.....	61
4.9 Restrained Shrinkage Measurements and Cement Fineness.....	64
 CHAPTER 5: CONCLUSIONS AND RECOMMENDATIONS.....	 67
REFERENCES.....	69
APPENDIX.....	76
Appendix A: Characteristics of Sand.....	77

## LIST OF TABLES

Table 3.1: Mix Proportions for Restrained Shrinkage Test .....	26
Table 4.1: Oxide Chemical Analysis for As-Received Cements .....	30
Table 4.2: Bogue-Calculated Potential Compound Content for As-Received Cements (ASTM C150-11) .....	31
Table 4.3: Heat of Hydration (kJ/kg)-ASTM C-186 .....	31
Table 4.4: Phase Content Using QXRD .....	35
Table 4.5: Particle Size Analysis of As-Received Cements .....	35
Table 4.6: Fineness and 7-Day Heat of Hydration for As-Received Cements .....	39
Table 4.7: Summary of Hyperbolic Function Parameters .....	56
Table 4.8: Summary of Exponential Function Parameters .....	57
Table 4.9: Activation Energy for As-Received Cements.....	59
Table 4.10: Density of As-Received Cements.....	61
Table 4.11: Restrained Shrinkage for AC Cement Mortar (w/c=0.485).....	64
Table 4.12: Restrained Shrinkage for AC Cement Mortar (w/c=0.45).....	65

## LIST OF FIGURES

Figure 3.1: One of the Windows Showing Differences between C <sub>3</sub> S Crystal Structure of the Cements.....	15
Figure 3.2: Internal Standard Calibration Curve for M1 Alite Polymorph.....	18
Figure 3.3: Example of Particle Size Distribution for Portland Cement .....	20
Figure 3.4: Measured Differential Particle Size Distribution for AC02 Cement .....	20
Figure 3.5: Profiles of Twin-Channel Isothermal Calorimeter (TAM Air).....	22
Figure 4.1: Variation of 7-Day Heat of Hydration with Heat Index.....	29
Figure 4.2: Effect of Blaine Fineness on the 7-Day Heat of Hydration .....	34
Figure 4.3: Effect of Cement Fineness on Cumulative Heat for CLE Cements .....	36
Figure 4.4: Effect of Cement Fineness on Cumulative Heat for AC Cements .....	37
Figure 4.5: Effect of Cement Fineness on Cumulative Heat for LG Cements .....	37
Figure 4.6: Effect of Cement Fineness on Cumulative Heat for ZR Cements .....	38
Figure 4.7: Effect of Cement Fineness on Cumulative Heat for CHC Cement.....	38
Figure 4.8: Effect of Cement Fineness on Cumulative Heat for ERD06 Cement .....	39
Figure 4.9: Relationship between Heat of Hydration Determined Using Heat of Solution Method and Isothermal Conduction Calorimetry.....	40
Figure 4.10: Setting Properties for AC02 Cement.....	42
Figure 4.11: Setting Properties for AC03 Cement.....	43
Figure 4.12: Setting Properties for ZR02 Cement .....	43
Figure 4.13: Setting Properties for ZR03 Cement .....	44
Figure 4.14: Setting Properties for LG01 Cement.....	44
Figure 4.15: Setting Properties for LG03 Cement.....	45
Figure 4.16: Effect of Cement Fineness on Setting Behavior of AC Cements.....	45

Figure 4.17: Effect of Cement Fineness on Setting Behavior of ZR Cements .....	46
Figure 4.18: Effect of Cement Fineness on Setting Behavior of LG Cements .....	46
Figure 4.19: Effect of Cement Mineralogy on Setting Behavior .....	47
Figure 4.20: Compressive Strength for AC02 Cement .....	48
Figure 4.21: Compressive Strength for AC03 Cement .....	48
Figure 4.22: Compressive Strength for ZR02 Cement .....	49
Figure 4.23: Compressive Strength for ZR03 .....	49
Figure 4.24: Compressive Strength for LG01 .....	50
Figure 4.25: Strength Gain over Time for LG03 .....	50
Figure 4.26: Effect of Cement Fineness on Strength for AC Cements .....	51
Figure 4.27: Effect of Cement Fineness on Strength for ZR Cements .....	51
Figure 4.28: Effect of Cement Fineness on Strength for LG Cements .....	52
Figure 4.29: Effect of Cement Composition on Strength .....	52
Figure 4.30: Strength Data Fitting Using Exponential and Hyperbolic Functions on AC02 at 22°C .....	54
Figure 4.31: Strength Data Fitting Using Exponential and Hyperbolic Functions on AC02 at 30°C .....	55
Figure 4.32: Strength Data Fitting Using Exponential and Hyperbolic Functions on AC02 at 40°C .....	55
Figure 4.33: Activation Energy Determination $E_a$ Using Hyperbolic Function on AC02 .....	58
Figure 4.34: Activation Energy Determination $E_a$ Using Exponential Function on AC02 .....	58
Figure 4.35: Variation of Calcium Hydroxide with Hydration Time for AC Cements .....	62
Figure 4.36: Variation of Calcium Hydroxide with Hydration Time for ZR Cements .....	63
Figure 4.37: Variation of Calcium Hydroxide with Hydration Time for LG Cements .....	64

Figure 4.38: Development of Steel Ring Strain as a Function of Age for AC03 Mortar Mix ..... 66

Figure 4.39: Development of Steel Ring Strain as a Function of Age for AC02 Mortar Mix ..... 66

## LIST OF ABBREVIATIONS

AASHTO	American Association of State Highway and Transportation Officials
ASTM	American Society of Testing and Materials
$E_a$	Activation Energy
HOH	Heat of Hydration
MPa	Megapascal
MPS	Mean Particle Size
PSD	Particle Size Distribution
XRD	X-Ray Diffraction
XRF	X-Ray Fluorescence
QXRD	Quantitative X-Ray Diffraction

## LIST OF SYMBOLS

A	Alumina, $\text{Al}_2\text{O}_3$
C	Calcium Oxide, free lime $\text{CaO}$
F	Ferric Oxide, $\text{Fe}_2\text{O}_3$
H	Water, $\text{H}_2\text{O}$
S	Silica, $\text{SiO}_2$
$\text{C}_3\text{A}$	Tricalcium Aluminate, $3\text{CaO}\cdot\text{Al}_2\text{O}_3$
$\text{C}_4\text{AF}$	Tetracalcium Aluminoferrite, $4\text{CaO}\cdot\text{Al}_2\text{O}_3\cdot\text{Fe}_2\text{O}_3$
$\text{C}_2\text{S}$	Dicalcium Silicate, $2\text{CaO}\cdot\text{SiO}_2$
$\text{C}_3\text{S}$	Tricalcium Silicate, $3\text{CaO}\cdot\text{SiO}_2$
$\text{C}\bar{\text{S}}\text{H}_2$	Gypsum, $\text{CaSO}_4\cdot 2\text{H}_2\text{O}$
$\text{SO}_3, \bar{\text{S}}$	Sulfur Trioxide

## CHAPTER 1: INTRODUCTION

Recently, standard specifications for portland cement, ASTM C150 and AASHTO M85, have gone through several modifications. This is due to the harmonization efforts undertaken by the Joint AASHTO-ASTM Harmonizing Task Group. The implemented changes resulting from the harmonization efforts triggered concerns with some state agencies. The Florida Department of Transportation (FDOT) Structures Materials Laboratory issued a report [1] indicating adverse performance characteristics in some Florida concrete elements fabricated with Type II cements. The report noted that this adverse performance was due to an increase in the heat of hydration of Type II cements resulting from standard specification changes following the harmonization efforts. The report identified the necessity of proposing “revisions to FDOT Specification 921, Portland Cement and Blended Cement, to mitigate the adverse effects of Type II cements.”

The harmonized specifications for portland cements were based on the findings of a study relating standard test properties of portland cement to its heat of hydration [2]. Current Type II cement specifications do not have maximum limits on  $C_3S$  or maximum limits on Blaine fineness. The effects of tricalcium silicate and aluminate content on the heat generated by portland cement have been long recognized [3]. However, the studies were typically conducted on cements with similar fineness, or fineness was not considered as a factor in the heat generated. A moderate heat (MH) Type II cement was introduced into the specifications, following harmonization, as an alternative cement to be used in applications where moderate heat generation is needed. The heat index, defined by the left-hand side of Equation 1.1, is used as the only standard requirement to classify cement as moderate heat. As indicated in ASTM C150-12 [4], Note 5 “The limit on the sum,  $C_3S + 4.75C_3A$ , in Table 1 provides control on the heat of hydration of the cement and is consistent with Test Method C186-05 [8] 7-day heat of hydration limit of 335 kJ/kg (80 cal/g)”. The heat index expression identifies the significance of the tricalcium compounds on the amount of heat produced by portland cements, but does not address the effect of cement fineness.

$$C_3S + 4.75 C_3A \leq 100 \qquad \text{Equation 1.1}$$

where  $C_3S$  = percentage of tricalcium silicate (Bogue calculated)  
 $C_3A$  = percentage of tricalcium aluminate (Bogue calculated)

$$C_3S + 4.75 C_3A = \text{heat index}$$

According to current specifications on cements, if a portland cement Type II (MH) has a heat index less than or equal to 90, the Blaine fineness limit of 430 m<sup>2</sup>/kg set per Standard Physical Requirements (Table 3 ASTM C150-12 [4]) does not apply.

The current study was initiated in order to address the effects of cement particle size and fineness on heat of hydration. Additionally, the study evaluated the effectiveness of the heat index to estimate the heat of hydration of portland cements. Establishing these relationships was considered necessary to insure the durability of Florida concrete structures.

## CHAPTER 2: LITERATURE REVIEW

Temperature rise in concrete elements is primarily driven by the heat generated by the hydration of portland cement. Heat of hydration of cement is affected by several parameters; namely, cement composition, fineness, temperature, and w/c ratio [5]. All cement phases generate heat on reacting with water; that is, the hydration process is exothermic in nature. The heat of hydration of portland cement is mainly attributed to the contributions of the tricalcium silicate and aluminate phases. In spite of that, current standard portland cement specifications for Type II or Type II (MH) do not directly limit  $C_3S$  content for moderate heat cements. However, a heat index expression has been employed (see Equation 1.1) to aid in quantifying the total heat of hydration. The heat index is calculated based on the phases quantified indirectly from Bogue calculations. Previous research and published literature [6, 7] indicate that there are significant differences between actual phase quantification through direct measurements, such as with petrographic analysis or quantitative x-ray diffraction, and the indirect phase quantification through Bogue calculations.

The heat of hydration measurement, which is an optional requirement for Type II (MH) portland cements, references ASTM C186-05 [8] as the procedure for measuring heat generated by cement during hydration. There is general consensus, in the industry and also in the published literature [9], that this test has poor precision (among labs) and can provide conflicting results. This test requires the use of hazardous chemicals, is expensive to run, and few labs are certified to run the test. All these concerns have initiated efforts to provide other means by which heat of hydration of portland cement can be assessed. A new specification for heat of hydration measurements using isothermal conduction calorimetry has been specified under ASTM C1702-13 [10]. However, portland cement standard specification ASTM C150-12 [4] has not yet implemented the use of this test, which is simpler to run and has better precision than the currently adopted heat of solution method [9].

In an attempt to develop a method to estimate the ASTM C186 heat of hydration of a portland cement, Poole [9] conducted a study in which he examined data from the Cement and Concrete Reference laboratory (CCRL) and the US Army Corps of Engineers. In this study, data from 38 Type II cements with measured heats of hydration higher than 290 kJ/kg at 7 days were analyzed. It is worth noting that 34 of the 38 cements used in this study had Blaine fineness values

in the range of 316-400 m<sup>2</sup>/kg. An analysis performed using a proposed equation of “unknown origin” [9] on two hypothetical cements indicate that varying Blaine fineness gave an approximate effect on the 7-day heat of hydration of 0.08 kJ/kg per unit change in Blaine fineness (m<sup>2</sup>/kg). Stated differently, a change of 4 kJ/kg was calculated for a change in Blaine fineness of 50 m<sup>2</sup>/kg using the hypothetical cements. The study concluded that fineness appears to have an effect on the 7-day heat of hydration, but to have any practical value a relatively large change in fineness would be required. No specifics were given to define what could be considered as a significant change in fineness. However, when cements from Verbeck and Foster [11] were statistically analyzed, Blaine fineness was identified as a variable of significance. In the latter, the Blaine fineness ranged from 285-490 m<sup>2</sup>/kg. It was also found that an increase in Blaine fineness of 50 m<sup>2</sup>/kg results in an increase in 7-day heat of hydration of 20 kJ/kg, which is significantly higher than the previous prediction based on the two hypothetical cements.

Blended cements were also considered in the same study. In the case of blended cements, the analyses included a wider range of Blaine fineness (336-534 m<sup>2</sup>/kg). It was concluded that Blaine fineness did not appear to correlate well with the 7-day heat of hydration. However, the 7-day strength showed some correlation with the 7-day heat of hydration but the correlation had a low R<sup>2</sup> value. This was explained by the possible variable contribution of different fly ashes to strength development or heat of hydration. The study concluded that for portland cements a combination of cement composition and fineness might be useful in predicting heat of hydration. For blended cements, the study concluded that none of the commonly measured properties, including fineness and strength, appear to correlate well with 7-day heat of hydration.

A recent study [12] focused on establishing a heat of hydration relationship in terms of cement composition, fineness, and cement mineralogy (determined by quantitative x-ray diffraction techniques) using statistical methods. The study also explored predictive models for 7-day heat of hydration of portland cements. No single strong model emerged from this study; however, it was concluded that mineralogical cement composition and fineness appear to be of significance on heat of hydration.

Several studies concluded that the effect of cement fineness on early-age properties of concrete and cement-based materials was significant [13-15]. The properties studied by Benz et al. [13] included heat release, temperature rise and shrinkage. It was indicated that the current emphasis on high early strength may result in susceptibility to early-age cracking. Fineness of

portland cement has received much attention due to its successive increase over the past 50 years [16]. The common conclusion among those studies [13-15, 17] was to advocate the use of coarser cements for better durability. While cement fineness has a significant impact on its heat of hydration and, therefore, temperature rise in concrete elements, another issue of significance is the shrinkage associated with finer portland cements. It was found that coarser cements are at a lower risk of experiencing early age cracking than finer cements [17].

The effect of cement composition and fineness extends to the concept of activation energy ( $E_a$ ) and equivalent age. The activation energy of concrete is an important concept that is widely implemented in predicting concrete strength and temperature rise. The concept was first introduced in 1889 by Svante Arrhenius as the energy that must be supplied to a system for a reaction to commence [18]. Later research [19-21] indicates that it can be considered as the parameter that describes the temperature sensitivity of the hydration process of a cementitious system. Others [22-25] used different qualifiers in describing the activation energy. However, there is agreement that the term quantifies the energy barrier for reactions and it defines the reaction rate-temperature relationship in a cementitious system. The concept of activation energy is very useful as it can help engineers predict the performance of concrete elements under variable field conditions, including the coupled effect of temperature and time. Examples of concrete hardened properties that can be predicted using activation energy concept are strength, temperature rise and thermal cracking.

As the physical and chemical processes that control heat generation are different than those that control strength gain, several researchers have contemplated if there can be a single activation energy value that can be used in predicting strength and heat of hydration at various ages and temperatures. Two different testing regimes are proposed in the literature for predicting activation energy of cement; namely, compressive strength and heat of hydration. The appropriateness of using the activation energy calculated from heat of hydration measurements to predict strength or using the activation energy calculated from strength measurements to predict temperature rise has been questioned [19, 26]. The consensus is that the activation energy determined through strength measurements should only be used to predict strength while that determined through heat of hydration should only be used for predicting temperature rise. This is due to the fact that though it has been established that all clinker phases contribute to strength development and heat of hydration, the extent of their individual contribution to each property is different. As an example, while  $C_3S$  is primarily responsible for early strength gain,  $C_3A$  is the most effective phase in

controlling early heat release of cement. The contribution of the latter to strength is of limited effect.

D'Aloia et al. [25] used  $E_a$  simulation models while varying  $C_3A$  (3 & 10%) with sulfate content (3 & 4%) and  $C_3S$  (54 & 48%). Experimental work used isothermal calorimetric testing over a temperature range of 10 to 28°C for 50 hours to investigate the influence of individual compounds on activation energy. It was concluded that varying  $C_3S$ , within this range, did not affect the determined  $E_a$  while the effect of varying  $C_3A$  for similar amounts was of significance. Furthermore, this work indicated that the sulfate content and type affect the contribution of  $C_3A$  to activation energy. The role of sulfates on  $C_3A$  hydration was also confirmed recently [27] on work conducted on high alumina cements.

Strength-based methods for activation energy prediction rely on the maturity concept, which uses the principle that concrete strength is directly related to both its time and temperature history. The maturity concept was proposed in the late 1940s and early 1950s. Carino and Carino et al. [28-30] provided a historic timeline of the maturity concept and maturity functions. These functions are used to translate the measured temperature history of concrete into a numerical index, which can then serve as an indicator for strength gain. ASTM C1074-11 “Standard Practice for Estimating Concrete Strength by Maturity Method” [31] provides two maturity functions, one of which incorporates activation energy. Additionally, this ASTM standard provides the procedures for determination of activation energy.

In 1949, McIntosh [32] defined maturity as the product of time and temperature (above a certain reference temperature of -1.1°C or 30°F); this product would define the curing history. However, it was concluded that there was no simple or unique relationship that can define maturity because strength development of concrete is governed by more complex factors than a simple product of time and temperature. In the same year, Nurse [33] provided experimental evidence supporting McIntosh. Nurse's evidence came from low-pressure steam curing testing. It was shown that for different concrete mixtures, the relative strength as a function of time-temperature and curing cycles fell reasonably close to a single non-linear curve. A critical concern regarding this research was that the concept of datum or reference temperature was not taken into consideration; therefore, one cannot be sure whether the temperature history reflects the temperature of the chamber or the concrete itself.

Saul [34] introduced the principle of maturity concept and defined it as “Two concretes of the same composition with the same value of maturity will have the same strength irrespective of the temperature history that lead to this value of maturity”. Saul considered the datum temperature to be -10.5°C and suggested that upon setting, concrete will continue to harden or gain strength at temperatures below 0°C; therefore, maturity should be calculated with respect to the lowest temperature at which hardening is observed. The concept was implemented in ASTM C1074-11 [31] and defined by Equation 2.1.

$$M\{t\} = \sum (T_a - T_o) \Delta t \quad \text{Equation 2.1}$$

where  $M\{t\}$  = Maturity as defined by the temperature-time factor at age  $t$  (degree-days or degree-hours)  
 $\Delta t$  = Time interval (days or hours)  
 $T_a$  = Average temperature of concrete over time interval  $\Delta t$  (°C)  
 $T_o$  = Datum temperature (°C)

Equation 2.1, also known as the Nurse-Saul function, defines the value of maturity as the total area under time-temperature history curves of the concrete. Saul is credited for recognizing that during early ages, temperature has a greater effect on strength development while time has the greater effect at later ages, and that ultimately maturity is an approximation. Carino et al. [28-30] concluded that some form of a rate constant-temperature function is needed to describe the combined effect of time and temperature on strength development for a specific concrete mix. A detailed procedure that relates maturity and strength was later implemented in ASTM C1074-11 [31]. The specification uses the linear hyperbolic function (Equation 2.2), to correlate the asymptotic relation between strength and the age of the concrete mixture. Activation energy is then determined using Equation 2.2 and 2.3.

$$S = S_u \frac{k(t-t_o)}{1+k(t-t_o)} \quad \text{Equation 2.2}$$

where  $S$  = Average compressive strength at age  $t$  (MPa)  
 $t$  = Test age (days)  
 $S_u$  = Limiting strength (MPa)  
 $k$  = Rate constant or rate of reaction ( $\text{days}^{-1}$ )  
 $t_o$  = Age at which strength development is assumed to begin (days)

$$k(T) = A \exp \left[ \frac{-E_a}{R(T+273)} \right] \quad \text{Equation 2.3}$$

where  $k$  = Rate of reaction ( $\text{day}^{-1}$ )  
 $A$  = Frequency factor ( $\text{day}^{-1}$ )  
 $E_a$  = Activation energy (kJ/mol)  
 $R$  = Universal gas constant [8.314 J/ (mol•K)]  
 $T$  = Curing temperature (kelvin)

The hyperbolic function provides a good fit while maintaining the profile of the actual strength data. Overall, the procedure outlined in ASTM C1074-11 [31] is straight forward, but its inconsistency is often cited as a liability. In addition, initial research pertaining to development of this method only considered ASTM Type I cement. ASTM C1074 appears to be too vague in terms of when strength measurements should start for each temperature or for that matter when should initial measurement be made for cements of different composition or different classifications. Similarly, the parameter  $t_o$  in the hyperbolic expression indicates that the period of gradual strength development during setting is not considered. The assumption of zero strength gain is cited as a limitation of the hyperbolic function in modeling the hydration behavior of concrete [19, 20, 35, 36]. Carino also indicated that the hyperbolic function was limited to strength predictions up to 28-day equivalent ages. As a result, an exponential function was proposed.

The exponential function [19, 21, 28-30] is presented in Equation 2.4. It is also known as the “exponential method” and is often used in lieu of a hyperbolic function to describe the relationship between the rate of strength gain, the curing time, and the curing temperature. This idea is not new but rather follows the function proposed by Hansen and Pedersen [37] (Equation

2.5), an empirical alternative to the hyperbolic equation relating strength development and maturity.

$$S = S_u e^{-\left(\frac{\tau}{t}\right)^\alpha} \text{ or } S = S_u e^{-\left(\frac{\tau}{t}\right)^\beta} \quad \text{Equation 2.4}$$

where  $S$  = Average compressive strength at age  $t$  (MPa)  
 $t$  = Test age (days)  
 $S_u$  = Limiting strength (MPa)  
 $\tau$  = Time constant (days)  
 $\alpha$  or  $\beta$  = Shape parameters, (dimensionless)

$$S = S_\infty e^{-\left(\frac{\tau}{M}\right)^a} \quad \text{Equation 2.5}$$

where  $S$  = Strength at a given age (MPa)  
 $S_\infty$  = Limiting strength (MPa)  
 $M$  = Maturity (Time-°C)  
 $\tau$  = Characteristic time constant (time)  
 $a$  = Shape parameter (dimensionless)

According to Schindler and Poole, Equation 2.4 can model the gradual strength development during the setting period and provides a better understanding of the hydration process in a cementitious system, as it is not dependent on the setting time,  $t_o$ , as in the case of the hyperbolic function. Carino [30] showed that the hyperbolic and the exponential models fit data well and the curves were indistinguishable up to 28 days.

The maturity method is used extensively to estimate in-place strength of concrete. ASTM C1074-11 [31] provides two maturity functions, which allow the conversion of maturity index from reference temperatures to different curing conditions. It was suggested [28-30] that traditional maturity defined by the Nurse-Saul function (Equation 2.1) was accurate only over some limited temperature range. The second function, which is based on the Arrhenius concept, has been considered to be more scientifically accurate as it makes use of the mixture's activation energy, which is determined using at least 3 curing temperatures. The above conclusions on both maturity

functions were made based on observed deviations between actual strength development and that predicted by the Nurse-Saul relationship.

The principle of Nurse-Saul implies that mixtures with the same value of maturity will have the same strength irrespective of temperature. In other words, only a horizontal shift in strength data should be observed; however, in some mixtures there is an additional vertical shift, which results in an intersection of the strength curves for the same concrete mix cured at different temperatures. The phenomenon is known as the “cross-over effect” [19, 28-30]. The underlying factor responsible for this behavior was identified as the temperature [22, 23]. Pinto et al. [38] stipulated that in some mixtures, lower curing temperatures often led to higher later age strength, and vice versa.

There are many explanations provided in the literature on the cross-over effect. In general, there is agreement that strength development of cements depends on the capillary porosity or degree of space filling as well as the uniformity of the developed microstructure. Verbeck et al. [39] suggested that there is a strong relationship between strength gain, capillary porosity, and the uniformity of the distribution of the hydration products within the microstructure of the paste. It was ultimately illustrated that the cross-over effect exists due to the increase in temperature. Moreover, it was indicated that while an increase of hydration temperature would increase the initial rate of hydration and therefore contribute to early hydration and early strength gain, the opposite is true at later ages.. The formed hydration products will, in effect, make it more difficult for hydration to proceed at later ages, which may explain the decrease in ultimate strength. These conclusions were based on tests conducted over temperature ranges from 4.4°C to 110°C (40°F to 230°F) for 28 days.

Review of the literature indicates that there are several aspects of concrete properties that are influenced by fineness and phase composition of portland cements. The most prominent trend is that an increase in cement fineness increases the rate of hydration (as more surface area becomes available for the reaction [40]), which consequently results in a higher rate of strength gain. It is further indicated that fineness affects heat of hydration. The effect is more pronounced at early ages where temperature rise is very critical [17, 41, 42]. Additionally, the trend was consistent regardless of the curing temperature.

The primary focus of this study was to establish the effect of fineness on heat of hydration of portland cements with a wide range of composition. In examining the contribution of fineness

to heat of hydration, different methods of heat measurement were implemented to document the effectiveness of different methods in correlating fineness and cement mineralogy to heat of hydration.

## CHAPTER 3: METHODOLOGY

This chapter presents the experimental techniques and methodology implemented in satisfying the objectives of this research.

### 3.1 Materials

Several cement producers were contacted in an effort to acquire portland cements in sufficient quantities and with varied mineralogical composition to successfully accomplish the different project tasks. The objective was to work with different suppliers that could provide the same cement source (clinker) processed to different grinds to ensure the ability to study cement fineness effects while maintaining the same or similar cement composition. Initially, 9 cements were obtained from 4 different sources. The first three sources provided 2 grinds per single cement source, and these cements were labeled AC02, AC03, ZR02, ZR03, LG01, and LG03. The fourth source provided 3 different grinds of the same cement, labeled CLEP, CL02, and CL03, but the quantities were limited, preventing a full round of testing. After initial testing, it was decided to add 2 more cements in an attempt to widen the mineralogical range of the cements tested, and these were labeled CHC and ERD06.

The cements used in this study, with the objective of assessing the effect of fineness and cement mineralogical composition, were selected to reflect a wide range in Blaine fineness, about 200 m<sup>2</sup>/kg, and a substantial variation in tricalcium aluminate and tricalcium silicate contents. Emphasis on these two phases is due to the fact that cement heat of hydration is primarily affected by the tricalcium phases' contents. Careful consideration was made in selecting the cements in order to isolate these effects. Each set of cements had similar compositions, but different fineness. The as-received cements conformed to ASTM C150-12 "Standard Specification for Portland Cement Classification" [4] and the identical American Association of State Highway and Transportation Officials (AASHTO) M85-12.

The sand used in this study for mortar mixtures preparation and as a reference material in the isothermal calorimeter was obtained from U.S. Silica Company, 701 Boyce Memorial Drive, Ottawa, Illinois 61350. The Ottawa Sand is finely graded sand conforming to ASTM C778-13 "Standard Specification for Standard Sand" [43]. Sand properties are presented in Appendix A.

Distilled water was used for all mixtures. Additionally, all specimens were cured in saturated lime solution using 98% extra pure calcium hydroxide. This was done to eliminate leaching of calcium hydroxide from the hydrated paste during extended curing periods, especially at high curing temperatures.

### **3.2 Oxide Chemical Analysis and Density Measurements of As-Received Cements**

Oxide chemical analysis of the as-received cements was conducted using x-ray fluorescence spectroscopy (XRF) and performed by a certified commercial laboratory (CCL) according to ASTM C114-13 [44]. XRF was used for elemental oxide quantification. ASTM C150-12 [4] was used to determine potential mineralogical composition. The density measurements for all of the as-received cements were conducted in accordance to ASTM C188-09 [45].

### **3.3 Mineralogical Analysis of Cements**

Apart from the bulk elemental oxide analysis, the phase content of portland cement is of great significance. It is understood that different cement phases have different contributions to concrete properties. Stutzman [46] suggested that the application of accurate measurement techniques for cement phase quantification would improve the knowledge of their influences on cement hydration characteristics, concrete strength development, and durability of structures. Additionally, it renders concrete as a more predictable construction material. X-ray diffraction (XRD) is a direct method of identification and quantification of the crystalline compounds in portland cements [47-49]. In this study, quantitative x-ray diffraction was adopted in identifying and quantifying crystalline phases present in all the cements used.

XRD scans of as-received cements were collected in accordance with ASTM C1365-06 (Reapproved 2011) "Standard Test Method for Determination of the Proportion of Phases in Portland Cement and Portland-Cement Clinker Using X-ray Powder Diffraction Analysis" [50]. Mixtures of cement and ethanol 200 (99.5% pure) were prepared and wet ground in a McCrone micronizing mill to an average particle size between 1 and 10 micrometers. The wet grinding method was used to avoid the effect of temperature on gypsum and its possible phase transformation to hemihydrate or anhydrite. The samples were then dried at 43°C using a Buchner funnel and were later stored in desiccators to assist in the evaporation of ethanol and eliminate

possible hydration problems. After drying, the samples were placed in a sample holder and compressed to provide a smooth and flat surface for XRD measurements. A Phillips X'Pert PW3040 Pro diffractometer using Cu K $\alpha$  radiation was used in collecting the scans. The samples were scanned with a step size of 0.02 degrees per step and a counting time of 4 seconds per step. The tension and current were set at 45 kV and 40 mA. The divergence slit was fixed at 1°, the receiving slit had a height of 0.2 mm, and the anti-scatter slit was fixed at 1°. Rietveld refinement was utilized for phase quantification of the as-received cements. The Rietveld method is a full-pattern analysis method that uses a complex mathematical algorithm [51]. Duplicated tests were conducted on each sample and the average was reported.

Quantification of cement phase composition presents a number of challenges. Although the presence of the four major phases (C<sub>3</sub>S, C<sub>2</sub>S, C<sub>3</sub>A and C<sub>4</sub>AF) in the sample is guaranteed together with some form of calcium sulfate, the major peaks for these phases suffer from peak overlap. This overlap makes it difficult to determine the individual peak heights and positions, making identification of the correct crystal structure complicated for constituents that can be present in more than one crystalline form. For example, C<sub>3</sub>S has monoclinic polymorphs, and C<sub>3</sub>A has a cubic and orthorhombic form. In addition, cements contain a number of minor phases, such as alkali sulfates, periclase, and free lime that are present in small quantities, making their detection by x-ray diffraction analysis rather challenging.

In order to aid the identification of the minor phases as well as the C<sub>3</sub>S and C<sub>3</sub>A crystal structures, selective dissolutions of the major phases (extractions) were performed for all cements. Salicylic acid/methanol (SAM) extraction dissolves the silicates and free lime leaving a residue of aluminates, ferrites, and minor phases, such as periclase, carbonates, alkali sulfates and double alkali sulfates [47, 52]. X-ray diffraction scans of the SAM extraction residues were collected for all the cements used in this study. In addition to minor phase identification, SAM residues were used to determine the presence of the C<sub>3</sub>A polymorph. Tricalcium aluminate can be present in cement either in cubic or orthorhombic form or a combination of both. Although the XRD patterns of cubic and orthorhombic C<sub>3</sub>A are very similar, orthorhombic C<sub>3</sub>A does not have a peak at 2 $\theta$  of 21.8°. In addition, cubic C<sub>3</sub>A has only one peak at 2 $\theta$  of 33.3°, while orthorhombic C<sub>3</sub>A has two peaks in this angular range, one at 2 $\theta$  of 32.9° and another at 2 $\theta$  of 33.2° [47, 53]. By observing

the  $21.8^\circ 2\theta$  angle for cubic  $C_3A$  and  $32.9^\circ 2\theta$  angle for orthorhombic  $C_3A$ , it was determined that the cements contained only cubic  $C_3A$ .

Potassium hydroxide/sucrose extraction dissolves aluminates and ferrites, thus leaving a residue of  $C_3S$ ,  $C_2S$ , alkali sulfates and  $MgO$  [47]. Potassium hydroxide/sucrose extraction residues were used to identify the alite polymorph present in cements. Although alite has a number of polymorphs, triclinic, monoclinic, and rhombohedral [7], only monoclinic polymorphs are generally present in cements. Monoclinic alite has three polymorphs: M1, M2, and M3 [54], although it is generally accepted that only M1 and M3 polymorphs exist in commercial clinkers [53, 55]. X-ray diffraction scans were collected for the 5 angular windows recommended by Courtial et al. for alite polymorph identification [55]. The 5 angular windows consist of the following  $2\theta$  ranges:  $24.5-26.5$ ,  $26.5-28.5$ ,  $31.5-33.5$ ,  $36.0-38.0$ , and  $51.0-53.0$  degrees. It was determined that in cements AC02, AC03, ZR02 and ZR03, alite was present in the M1 form, and in cements LG01 and LG03 alite was present as M3 as shown in Figure 3.1.

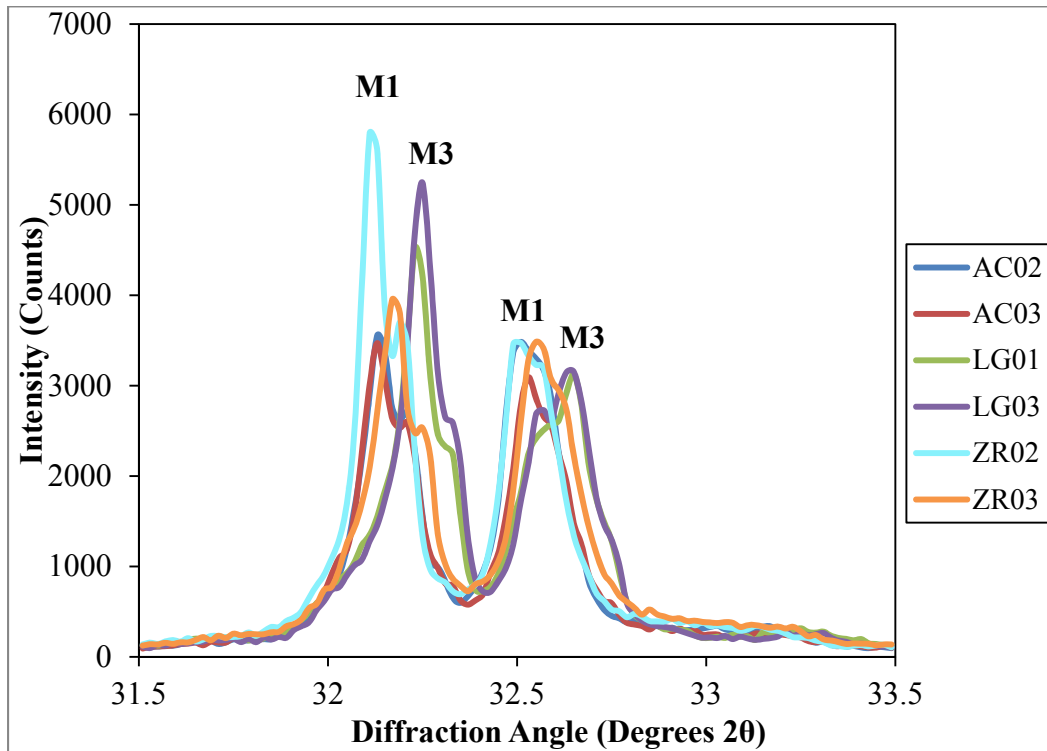


**Figure 3.1: One of the Windows Showing Differences between  $C_3S$  Crystal Structures of the Cements**

In addition, both the M1 and M3 polymorphs can have either a regular unit cell or a superstructure unit cell, the superstructure cell being significantly larger than the regular cell [55]. Since the larger superstructure is going to have additional reflections, the presence of extra peaks in these windows identifies the presence of a superstructure unit cell. Based on observing the peak shapes for the cements with the M1 polymorph (AC02, AC03, ZR02 and ZR03), it was concluded that M1 has a regular unit cell in all these cements. The presence of extra peaks for the LG01 and LG03 cements indicate that M3 alite in these cements has a superstructure cell.

Rietveld refinement is a well-established technique for cement phase quantification. Quantitative analysis via the Rietveld method is based on the assumption that all the phases present in the samples have been identified and included in the analysis and that all the phases are crystalline. The accuracy of the analysis depends on how true these assumptions are for a particular sample. In multiphase materials suffering from peak overlap, like cements and clinkers, it is often challenging to identify minor phases that may be present in amounts of 1-2% or less. When the minor phases are excluded from the analysis or when amorphous material is present, the weights of the identified phases are normalized to 100%, which can lead to overestimation. Even though identification of the minor phases can be aided by performing selective dissolutions, as Chung pointed out, “even when all the peaks in the x-ray diffraction pattern are accounted for, one is still not sure whether there is any amorphous material present” [56]. This is particularly true of cements since some researchers have reported a significant amount of unidentified/amorphous material [57] while others found no amorphous material [58].

Because of the possibility of overestimation of the cement phase composition by the Rietveld analysis, a C<sub>3</sub>S calibration curve was established, using internal standard analysis, in order to confirm the results of Rietveld refinement with respect to the alite content of the cement. Since alite usually constitutes at least half of the total mass of Types I, II and III portland cements, it is plausible that the effect of overestimation would be most evident in the quantification of this phase.

Internal standard analysis is based on the principle that the peak intensity of a phase, determined either as peak height or peak area, is directly proportional to the amount of this phase in the sample, as described by the following equation:

$$\frac{I_{ij}}{I_{ks}} = K \frac{x_j}{x_s} \quad \text{Equation 3.1}$$

where  $I_{ij}$  = Intensity of peak  $i$  of phase  $j$ ,  
 $I_{ks}$  = Intensity of peak  $k$  of the internal standard,  
 $x_j$  = Weight fraction of phase  $j$ ,  
 $x_s$  = Weight fraction of the internal standard, and  
 $K$  = A constant [59].

The advantage of the single-peak internal standard analysis is that quantification of the phase of interest is not affected by any other phases present in the sample, meaning that unlike Rietveld analysis, it is not affected by unidentified or amorphous content.

The alite calibration curve was prepared by mixing samples of known C<sub>3</sub>S content with 10% of internal standard by total weight of sample following the general procedures described by Klug and Alexander [59]. Titanium dioxide (TiO<sub>2</sub>) obtained from the National Institute of Standards and Technology (NIST) as part of the Standard Reference Material (SRM) 674b set was selected as an internal standard. TiO<sub>2</sub> was selected for two reasons: it has a mass absorption coefficient (MAC) close to that of cements, and most of the TiO<sub>2</sub> diffraction peaks do not interfere with the major peaks of portland cement.

Standard reference clinkers SRM 2686a, SRM 2687 and SRM 2688 were obtained from NIST and were used as a source of C<sub>3</sub>S for the standardization mixtures. These clinkers have certified phase compositions and are representative of the modern-day clinkers produced by the cement industry. The clinkers were first ground with a mortar and pestle to reduce the particle size to below 45 microns and then ground in the McCrone micronizing mill for 10 minutes with ethanol prior to collecting x-ray diffraction scans.

After observing 5 angular alite windows for these clinkers as described previously, it was determined that SRM 2688 contained the M1 alite polymorph and was suitable for the preparation of the M1-C<sub>3</sub>S calibration curve. SRM 2688 contains 64.95% of alite. Ground SRM 2688 was mixed with 10% TiO<sub>2</sub> to produce the 65% point on the calibration curve. In order to produce the 40 and 50% points for the calibration curve, SRM 2688 was diluted with C<sub>3</sub>A in order to achieve the required alite content. Alite content of the sample was calculated for the SRM 2688/C<sub>3</sub>A mixture excluding the TiO<sub>2</sub> addition.

The samples were mixed in the McCrone micronizing mill for 10 minutes with 5 mL of ethanol per every gram of sample as recommended by ASTM C1365-06 (Reapproved 2011) [50]. This was done to achieve homogeneous dispersion of the internal standard throughout the sample. After mixing, the sample was dried in an oven at 40°C in order to evaporate the ethanol. Samples were loaded into the sample holder using the back-loading technique and scanned using the settings described previously. Three samples were analyzed for each point on the calibration curve.

The diffraction pattern collected for each sample was analyzed with HighScore Plus software in order to determine the areas of the 51.8° 2θ peak of alite and the 54.3° 2θ peak of TiO<sub>2</sub>. The area ratios of the alite peak to the TiO<sub>2</sub> peak were plotted against the alite content of the sample fraction excluding TiO<sub>2</sub> as shown in Figure 3.2. Subsequently, ground cements were mixed with 10% TiO<sub>2</sub> to determine the area ratios in the as-received cements.

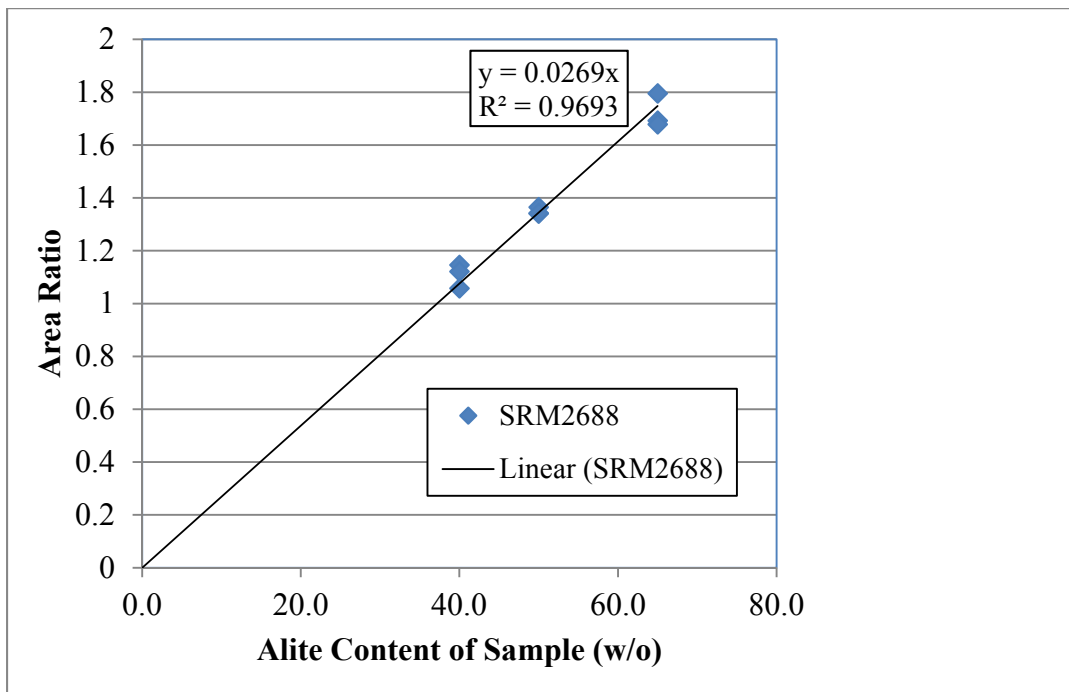


**Figure 3.2: Internal Standard Calibration Curve for M1 Alite Polymorph**

### 3.4 Particle Size Analysis for Portland Cements

The last step in manufacturing portland cement involves grinding of portland cement clinker with calcium sulfate or one of its hydrates. The product of this grinding stage is known as

portland cement. The fineness to which cement is ground has a significant effect on the behavior of cement, especially during the early stages of hydration [60]. For cements, there are two basic measures of fineness; namely, Blaine (air permeability) and Turbidimetry. Blaine fineness was used in this study. It is an indirect measure of the total surface area of each cement sample and can be determined by the air permeability apparatus according to ASTM C204-11 “Standard Test Method for Fineness of Hydraulic Cement by Air Permeability Apparatus” [61].

Prior to conducting Blaine fineness measurements on the as-received cements, the air-permeability apparatus was calibrated in accordance with ASTM C204-11 section 4 [61]. A sample bed of standard cement SRM 114 obtained from the National Institute of Standards and Technology (NIST) was used. The calibration was run at 21.1°C (70°F) and a relative humidity of 61%. Using the same settings, Blaine fineness for the as-received cements was quantified using triplicate trials as indicated in the specifications. The results satisfied the bias and precision of the test standard. While the method is widely used in the cement industry for quality control, it offers some drawbacks. For example, a single averaged value may be given to two cements with different proportion of fines; that is, two different cements having the same surface area can give the same Blaine value even though they have very different particle size distributions (PSD) [62, 63]. In contrast, particle size distribution measurements provide more accurate insight on the quality and grading of the cement [63].

PSD measurement describes the frequency and size of particles contained in a sample [64]. Typical particle sizes in portland cement vary from  $<1 \mu\text{m}$  to  $100 \mu\text{m}$  in diameter [62]. Particle size influences the hydration rate and strength; it is also a valuable indicator for predicting cement quality and performance [65, 66]. The characterization of the particles of the as-received cements was conducted using the principle of laser diffraction. That is, a particle will scatter light at an angle determined by its particle size. The angle of scattering increases as the particle size decreases; this method is particularly effective in the particle size range of 0.1 to  $3,000 \mu\text{m}$  [64]. An LA-950 laser scattering particle size analyzer manufactured by HORIBA Instruments was used to analyze the particle size distribution of the cements. The instrument has the capacity to measure wet and dry samples in the range of 10 nm to 3 mm.

Sample preparation was conducted per manufacturer procedures. An adequate amount of dry cement was homogenized by mechanical agitation through the flow cell of the instrument at the start of measurement [65]. Figure 3.3 and 3.4 depict examples of data collected for one of the

cements used in this study. It is worth noting that the results presented in Figures 3.3 and 3.4 are for 3 runs conducted on the same cement. The obvious overlap is indicative of the accuracy and precision of the testing technique.

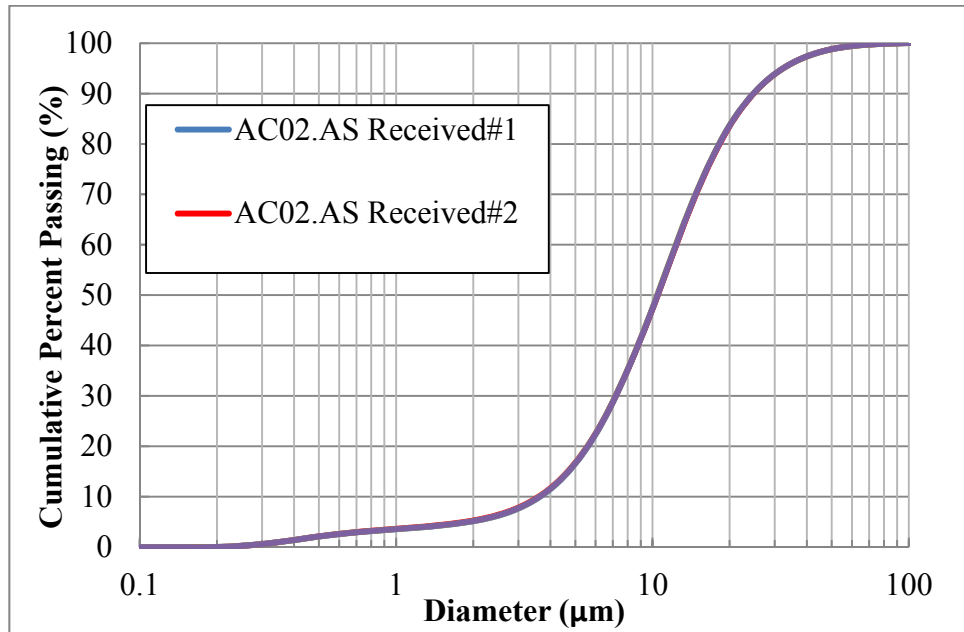


**Figure 3.3: Example of Particle Size Distribution for AC02 Cement**

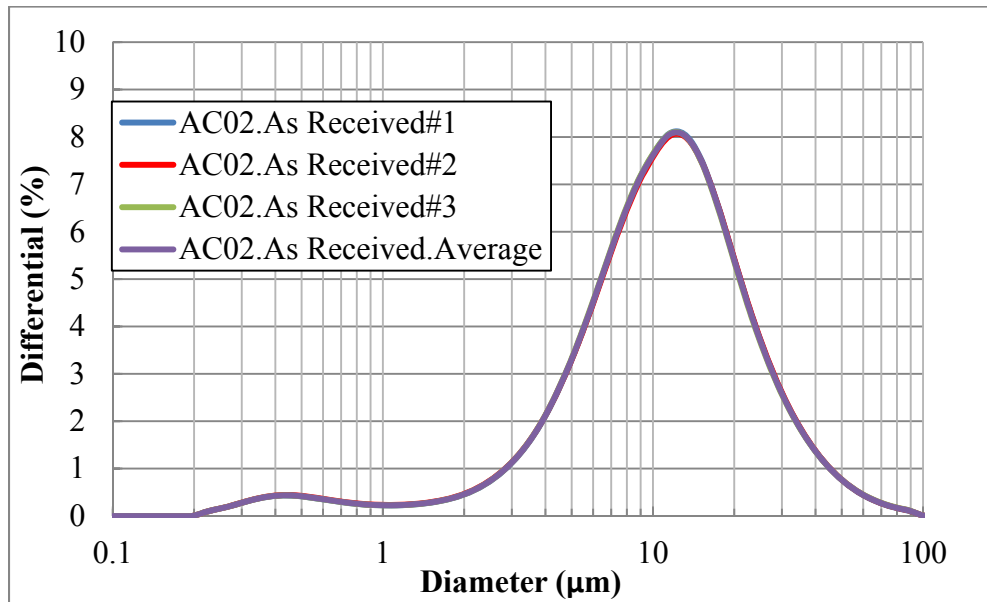


**Figure 3.4: Measured Differential Particle Size Distribution for AC02 Cement**

The expressions of PSD results are based on a volume distribution using measures of  $D_{10}$ ,  $D_{50}$ , and  $D_{90}$  (under size %) which identify the 10th, 50th, and 90th percentiles below a given particle diameter [12].  $D_{50}$  is also defined as the median size; that is, the size that splits the size distribution with half above and half below the specified diameter. Similar to the concept of average, the mean size or mean particle size (MPS) expresses the volume mean as an average of  $D_{10}$ ,  $D_{50}$ , and  $D_{90}$  [66]. In other words, MPS provides an approximation of the central point of the particle size distribution of an entire sample on volume basis [12, 65, 66]. Triplicate tests were conducted on all as-received cements and averages of the 3 tests were reported.

### **3.5 Heat of Hydration Measurements**

In this study, two techniques were used to measure the heat of hydration of portland cements; namely, isothermal conduction calorimeter and the heat of solution method. TAM Air, an 8-channel isothermal heat conduction calorimeter by TA Instruments, was used for heat flow measurements (Figure 3.4). Measurements were conducted according to ASTM C1072-13 “Standard Test Method for Measurement of Heat of Hydration of Hydraulic Cementitious Materials Using Isothermal Conduction Calorimetry” internal mixing protocol [10]. The calorimeter has an operating temperature range of 5 to 90°C. The calorimetric channels are of twin type, consisting of a sample and a reference vessel, each with a volume of 20 ml. As shown in Figure 3.5, the channels that are labeled “A” were used for actual mixtures while the “B” channels contained the reference material. The thermostat uses circulating air with advanced temperature regulating system to maintain the temperature very stable within  $\pm 0.02^\circ\text{C}$ . The temperature change between the sample and the surroundings (kept at constant temperature) results in heat flow [67]. This is the heat that was monitored continuously. The high accuracy and stability of the thermostat makes the calorimeter well suited for heat flow measurements over extended periods of time [68]. Built-in calibration heaters were used for calibration of the calorimetric units and general performance testing. Calibration tests are performed on a regular basis following manufacturer directions. Pico Log™, which is a commercial software package, was used for data collection and analysis.

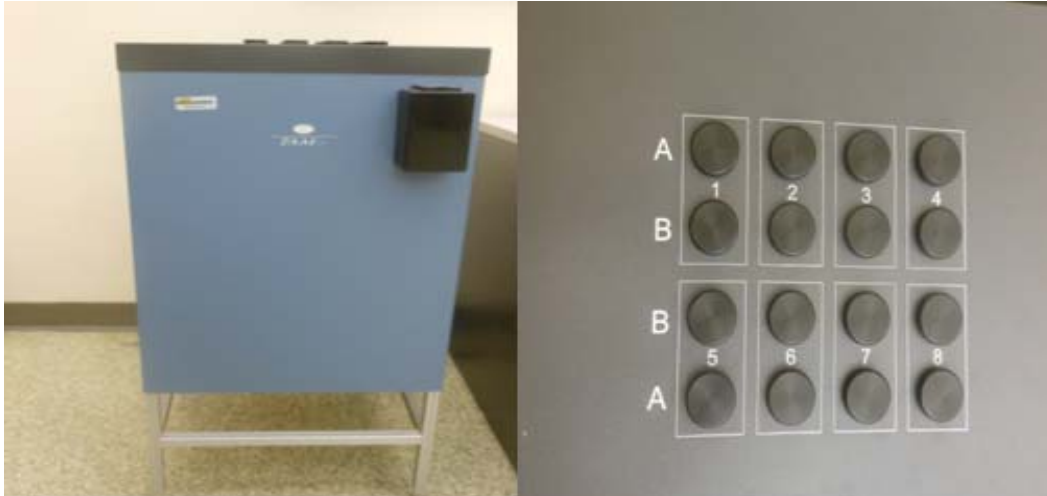


**Figure 3.5: Profiles of Twin-Channel Isothermal Calorimeter (TAM Air)**

Paste samples were prepared using 3.3007 grams of cement mixed with 1.650 grams of water. A fixed water-to-cement ratio (w/c) of 0.5 was maintained for all the mixtures to ensure proper mixing for cements, especially those that have a high tricalcium silicate or aluminate content or a high fineness. Several w/c ratios were experimented with, and it was concluded that 0.5 was appropriate for all cements used here [69]. The objective was to use a ratio that can provide adequate paste mixing using the internal mixing protocol while maintaining a constant w/c ratio for all cements. A mass of 12.33 grams of Ottawa sand was placed in the reference cell as the inert sample during testing as well. The weight of the sand used in the reference cell is based on the equivalent heat capacity of the paste mixture. In addition, the same amount of reference material was used in the gain calibration of the calorimeter. The dry cement was loaded into an ampoule (Figure 3.6). The ampoule contained a stirring fixture and a syringe that was loaded with the appropriate amount of water to achieve the desired w/c ratio. The ampoule was then positioned in a channel or a compartment of TAM Air maintained at the desired testing temperature of 23° C. Figure 3.6 also shows the typical configuration of the ampoule and 20 ml glass with dry sample inside the calorimeter. When the system reached the desired temperature, water was added using the syringe. The mixture was stirred inside the calorimeter constantly for 60 seconds. Due to the exothermic nature of cement hydration, heat is released once water touches cement [68]. Consequently, internal mixing was used as it provided the ability to record the heat of hydration of cements right from the instant of mixing water with cement. The rate of heat production was

continuously monitored for a period of 7 days. All heat of hydration values reported here are based on the average values collected for duplicate runs.



**Figure 3.6: Ampoule and Typical Ampoule-Glass Container Configuration**

The isothermal calorimeter used in this study has eight twin channels that partially share the same heat sink; evidently, there is a possibility that thermal power in one channel might possibly affect the power in neighboring channels. Wadsö [70] indicated that this might occur when two adjacent channels have a significant difference in thermal power, or if a sample is at a significantly different temperature than the calorimeter when it is inserted into the calorimeter. Thus, efforts were made to minimize this effect by allowing the system to equilibrate once the sample was inserted and initiating water injection only after the system had stabilized. It is worth noting that all duplicate runs had less than 1% heat deviation at 1, 3 and 7 days. Heat evolution and cumulative heat of hydration were normalized to the original mass of the anhydrous cement in the mixture.

### **3.6 Setting Time**

The gradual stiffening or increase in rigidity of freshly mixed concrete is commonly referred to as setting. Cement chemistry, temperature, fineness, and water-to-cement ratio are among the important factors that affect concrete setting time. Although setting is caused primarily by the chemical reaction between cement and water, the setting time of concrete or mortar does not correspond to the setting time of its cement component [62]. The initial and final setting times

of concrete are defined arbitrarily by the test method ASTM C403-08 “Standard Test Method for Time of Setting of Concrete Mixtures by Penetration Resistance” [71]. In general, the initial and final set points indicate loss of flow and the ability to sustain load for a given mix [60]. According to Dodson [72], time of setting is a critical period where concrete is vulnerable to environmental influences. In fact, setting time dictates appropriate times for placement, compaction, finishing, or loading of the concrete. Initial set and final set times for mortar mixes were measured using procedures outlined in ASTM C403-08 [71]. The time of setting was determined for the as-received cements at three temperatures; namely, 23°C, 30°C, and 40°C. A water-to-cement ratio (w/c) of 0.485 and a sand-to-cement ratio of 2.75 were used for mortar mixtures used in compressive strength measurements. The mortar raw materials were preconditioned to match the curing temperatures. The mixing procedures followed were those given in ASTM C305-13 “Standard Practice for Mechanical Mixing of Hydraulic Cement Pastes and Mortars of Plastic Consistency” [73]. Exceptions were made at 40°C because it was difficult to maintain the room temperature at 40°C. In addition, the penetration resistance measurements were conducted at the corresponding temperatures except for 40°C. However, mixtures were kept at their respective temperatures between measurements by placing the test containers in an oven set at the test temperature. Precautions were taken to minimize the time between removing and returning the specimen to the curing chamber.

Initial and final setting times were marked at 500 psi (3.5 MPa) and at 4000 psi (27.6 MPa), respectively, per ASTM C403-08 [71]. The setting times were calculated from linear interpolation of the penetration resistance versus elapsed time. Duplicate runs were conducted on all cement mortar mixtures, and the averages of the two tests were reported. Even though setting times do not reflect the actual compressive strength at those arbitrary points, they were used to determine the initial compressive strength testing age for mortar cubes used in the activation energy determination per specification requirements [31].

### **3.7 Mortar Strength Measurements**

Mortar cubes were proportioned according to ASTM C109-13 “Standard Test Method for Compressive Strength of Hydraulic Cement Mortars” [74]. Mortars were made with a w/c of 0.485 and a sand-to-cement ratio of 2.75. Distilled water was used for all mixtures. Mortar cubes were mixed according to ASTM C305-13 [73]. The cubes were then cured in saturated lime solution

baths maintained at 3 different temperatures (22, 30, and 40°C) in accordance to Annex A.1 of the ASTM C1074-11 [31] “Standard Practice for Estimating Concrete Strength by Maturity Method”. A Blue M Magni Whirl 1120A-1 constant temperature bath with an agitation system was used in curing mortar cubes. The motion of the agitator provided gentle circulation throughout the bath to maintain constant curing temperature. The compressive strength was determined per ASTM C109-13 [74] using an MTS 809 Axial/Torsional Test System. The strength was determined at a constant loading rate per specifications. Strength averages were reported accordingly and checked against the precision and bias of the testing method. For this study, any deviation of more than 6% within a strength test average prompted reruns of that test. Average strengths were determined for at least 2 runs at each curing temperature for the selected cement, and the results were used for activation energy determination.

### **3.8 Activation Energy**

ASTM C1074-11 [31] procedures were used in determining the activation energies for six of the cements studied, namely AC02, AC03, ZR02, ZR03, LG01, and LG03. These were the cements that were supplied in enough quantities to conduct the extensive testing matrix required to determine the activation energy. The data were analyzed using hyperbolic and exponential functions on mortar cube strength data collected at the three temperatures of 22, 30 and 40°C. Microsoft Excel solver was used to determine the necessary parameters in both functions. Each strength data point represents the average of three mortar cube strength tests. The initial testing age for each mix at each temperature was dictated by the setting tests per ASTM C1074 protocol.

### **3.9 Restrained Shrinkage Measurements**

The effect of cement fineness on the potential of concrete and mortar to crack under restrained shrinkage conditions was also addressed in this study. Two cements were used here, AC02 and AC03. The mix proportions used are presented in Table 3.1. Three ring specimens were prepared for each cement and the average values reported in the next chapter.

**Table 3.1: Mix Proportions for Restrained Shrinkage Test**

Material	Weight (lb)
Cement	9.0
Ottawa sand	24.75
Distilled water	4.365
w/c	0.485
Mortar flow	118
Mortar Density	2.14 g/cm <sup>3</sup>

Two strain gauges were placed diametrically, in each ring, for strain measurements. The specimens were cured for 24 hours using wet burlap followed by air-drying. The flow and density reported in Table 3.1 were for both cement mixes. In addressing the effect of w/c on restrained shrinkage potential of a particular cement, additional tests were conducted at a lower w/c ratio of 0.45.

## CHAPTER 4: RESULTS AND DISCUSSION

### 4.1 Introduction

The experimental data and discussion of the observed trends are presented in this chapter. First, the properties and characteristics of the as-received cements are presented. The characterization techniques entail chemical, mineralogical, and physical tests. Following that, heat of hydration data are presented and correlated to cement characteristics. Next, the activation energies determined through mortar strength testing are presented and analyzed. Finally, the effect of cement particle fineness on restrained shrinkage and kinetics are addressed.

### 4.2 Chemical Characterization of As-Received Cements

As the purpose of this study was to assess the effects of cement fineness on heat of hydration of portland cements, it was critical to select cements of the same mineralogical composition, but of different grinds. Cements with two different grinds were obtained from each of three cement producers. Cements from the same producer had similar mineralogy, but were ground to different fineness. These 6 cements from 3 different producers were available in sufficient quantities to satisfy the requirements of the desired testing protocol. These cements were coded ZR (ZR02 and ZR03), AC (AC02 and AC03), and LG (LG01 and LG03). Cements were obtained from an additional supplier, CLE (CLEP, CLE02, CLE03), but the amounts made available were insufficient for all the planned testing. After initial testing, it was decided to expand the range of cement mineralogy evaluated for this study. Two additional single-grind cements, designated CHC and ERD06, were obtained, but the available quantities were insufficient for all the planned testing.

The oxide chemical compositions, in weight percent (w/o), of the as-received cements are presented in Table 4.1. Table 4.2 presents the potential phases in addition to the heat index currently used in the specifications to assess the potential of portland cements to generate heat on hydration. No corrections were made for possible additions. Typically, MH cements with a heat index of less or equal to 90 do not have to be subjected to the maximum fineness requirement of 430 m<sup>2</sup>/kg (Blaine fineness). The data depicted in both tables indicate that the cements have a wide range of alkali contents (0.25-1.13 Na<sub>2</sub>O<sub>eq</sub>), SO<sub>3</sub>/Al<sub>2</sub>O<sub>3</sub> ratio (0.45-0.85), tricalcium silicate (47-65), and tricalcium aluminate (5-11). The heat indices reported for the cements also indicate a wide range from a low of 83 to a high of 101. Note that, among the cements studied, the ZR cements

and the CHC cement had the highest LOI values. LG cements had the highest alkali and sulfate content, while CLE cements had the lowest alkali and sulfate content.

The calculated potential phase contents, in weight percent (w/o), determined from Bogue equations are listed in Table 4.2 where it can be seen that the cements had a wide range of phase contents:  $C_3S = 47-65$ ,  $C_2S = 7-20$ ,  $C_3A = 5-11$ , and  $C_4AF = 8-12$ . Tricalcium silicates and aluminates are known for their significant effect on the amount of heat generated by a portland cement. This is why the heat index expression in current standard specifications incorporates only those two phases. Accordingly, it would be expected that cements with the highest heat index would have the highest heat of hydration. However, there is not necessarily a direct correlation between the heat index and the heat of hydration determined by the heat of solution method (ASTM C186). This can be seen by comparing heat index values ( $C_3S+4.75C_3A$ ) in Table 4.2 with the heat of hydration values determined per ASTM C186-05 [8], shown in Table 4.3. For example, comparing the data for cements CLE03, CHC, ZR03, and LG03, it can be seen that these cements had a wide range of heat indices, ranging from 83 to 101. However, these cements had about the same 28-day heat of hydration values, 387 kJ/kg (+/- 1). At 7 days, the cement with the lowest heat index of 83 (CLE03) had a heat value of 366 kJ/kg (87.4 cal/g) which exceeds the 80 cal/g value listed as the maximum HOH for cements with Heat Indices of  $\leq 100$  in ASTM C150-12 [4]. The AC02 cement had a heat index of 91 and a HOH of 349 kJ/kg (83.4 cal/g), while cement ER06 had a heat index of 90 and HOH of 382 kJ/kg (91.3 cal/g). According to specifications, cement ER06 was not required to satisfy the fineness limit of 4300  $m^2/kg$  since its heat index was 90. Also, cement AC03, with a heat index of 89 did not have a fineness requirement though its HOH was 370 kJ/kg (88.4 cal/g), which was also above the 80 cal/g value. While the LG cements tested would not be classified as Type II cements or Type II (MH) due to their high  $C_3A$  contents, they are valuable for comparison purposes.

Figure 4.1 shows the 7-day heat of hydration measured by the solution method plotted against the heat index. The best linear fit determined using the data collected here indicates that for a heat index of 100, cement heat of hydration is 376 kJ/kg (89.9 cal/g) and for a heat index of 90, cement heat of hydration would be about 357 kJ/kg (85.3 cal/g). This finding is not in agreement with the data analysis conducted on CCRL cements [2]. A possible explanation is CCRL cements might not be similar to the currently produced portland cements, which have considerably higher fineness values.

In conclusion, the data presented here show that there is no consistent relationship between the reported heat index as determined per ASTM C150-12 [4] and the HOH measurements per ASTM C186-05 [8] at 7 days. Additionally, based on the chemical requirements of ASTM C150-12, all cements used here can be classified as Type II (MH) with the exception of the LG series. For the nine cements that satisfied the chemical requirements for MH classification, 7 had a heat index of less than or equal to 90 and therefore would not have been required to satisfy the maximum fineness limit of 430 m<sup>2</sup>/kg. All but one cement had a HOH value, at 7 days, above 80 cal/g. The exception, CLEP, had a Blaine fineness of 325 m<sup>2</sup>/kg and HOH of 75 cal/g. The other two cements had heat indices greater than 90, and therefore would have been subjected to the fineness limit of 430 m<sup>2</sup>/kg. AC02 and CHC both satisfied the maximum fineness requirement but had HOH values of 83 and 87 cal/g, respectively.

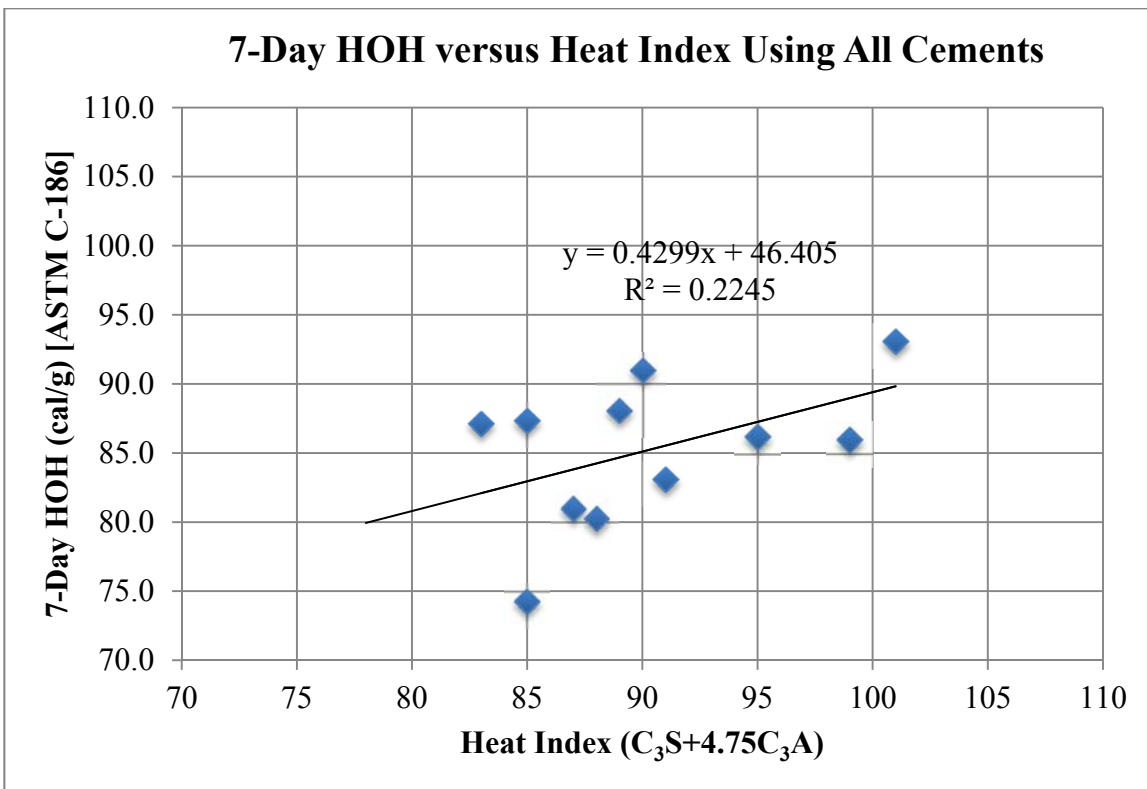


**Figure 4.1: Variation of 7-Day Heat of Hydration with Heat Index**

**Table 4.1: Oxide Chemical Analysis (w/o) for As-Received Cements \***

<b>Analyte</b>	<b>CLEP</b>	<b>CLE02</b>	<b>CLE03</b>	<b>CHC</b>	<b>AC02</b>	<b>AC03</b>	<b>ZR02</b>	<b>ZR03</b>	<b>ERD06</b>	<b>LG01</b>	<b>LG03</b>
SiO <sub>2</sub>	20.83	20.74	20.86	19.67	20.01	20.02	20.51	20.85	20.44	18.67	19.01
Al <sub>2</sub> O <sub>3</sub>	4.61	4.45	4.42	4.17	5.15	5.32	4.91	4.9	4.61	5.7	5.66
Fe <sub>2</sub> O <sub>3</sub>	4.2	4.07	3.86	2.89	3.86	3.88	3.7	3.62	3.14	2.63	2.55
CaO	64.33	64.83	64.02	62.94	63.52	63.43	63.54	63.5	63.45	60.15	60.89
MgO	0.83	0.92	1.12	2.58	0.92	0.93	0.63	0.64	1.06	2.92	2.76
SO <sub>3</sub>	2.06	2.58	2.82	3.23	3.18	3.99	3.03	3.33	3.7	4.83	4.6
Na <sub>2</sub> O	0.07	0.07	0.11	0.25	0.12	0.12	0.09	0.09	0.12	0.41	0.37
K <sub>2</sub> O	0.29	0.28	0.28	1.07	0.42	0.43	0.45	0.45	0.51	1.1	1.02
TiO <sub>2</sub>	0.29	0.28	0.26	0.22	0.26	0.27	0.31	0.29	0.18	0.25	0.26
P <sub>2</sub> O <sub>5</sub>	0.11	0.1	0.1	0.05	0.13	0.13	0.12	0.11	0.17	0.26	0.25
Mn <sub>2</sub> O <sub>3</sub>	0.08	0.08	0.08	0.05	0.01	0.01	0.04	0.03	0.22	0.07	0.08
SrO	0.04	0.04	0.04	0.04	0.06	0.06	0.06	0.06	0.18	0.28	0.28
Cr <sub>2</sub> O <sub>3</sub>	0.01	0.01	0.01	0.01	0.01	0.01	0.01	0.01	<0.01	0.01	0.01
ZnO	0.05	0.05	0.05	0.03	0.01	0.01	0.05	0.05	0.01	0.06	0.07
L.O.I(950°C)	1.36	1.22	1.44	2.77	2.4	1.68	2.70	2.3	1.92	2.58	2.54
Total	99.13	99.72	99.47	99.98	100.07	100.31	100.16	100.23	99.72	99.91	100.33
Na <sub>2</sub> O <sub>eq</sub>	0.26	0.25	0.3	0.95	0.4	0.41	0.39	0.38	0.45	1.13	1.04
SO <sub>3</sub> /Al <sub>2</sub> O <sub>3</sub>	0.45	0.58	0.64	0.77	0.62	0.75	0.62	0.68	0.80	0.85	0.81

\* Tests conducted by a certified commercial laboratory

**Table 4.2: Bogue-Calculated Potential Compound Content (w/o) for As-Received Cements (ASTM C150-12)**

Phase	CLEP	CLE02	CLE03	CHC	AC02	AC03	ZR02	ZR03	ERD06	LG01	LG03
C <sub>3</sub> S	61	63	59	65	57	53	56	52	57	47	49
C <sub>2</sub> S	14	12	15	7	14	17	17	20	16	18	18
C <sub>3</sub> A	5	5	5	6	7	8	7	7	7	11	11
C <sub>4</sub> AF	13	12	12	9	12	12	11	11	10	8	8
C <sub>4</sub> AF+2C <sub>3</sub> A	23	22	22	21	26	28	25	25	24	30	30
C <sub>3</sub> S+4.75C <sub>3</sub> A*	85	87	83	95	91	89	88	85	90	99	101

\* Heat Index

**Table 4.3: Heat of Hydration (kJ/kg)[cal/g]-ASTM C186\***

Age	CLEP	CLE02	CLE03	CHC	AC02	AC03	ZR02	ZR03	ERD06	LG01	LG03
7 days	(312)	(340)	(366)	(362)	(349)	(370)	(337)	(367)	(382)	(361)	(391)
	[74.6]	[81.3]	[87.5]	[86.5]	[83.4]	[88.4]	[80.5]	[87.7]	[91.3]	[86.3]	[93.5]
28 days	(360)	(374)	(387)	(388)	(391)	(398)	(370)	(386)	(403)	(365)	(388)
	[86.1]	[89.5]	[92.5]	[92.8]	[93.5]	[95.2]	[88.5]	[92.3]	[96.4]	[87.3]	[92.8]

\* Tests conducted by certified commercial laboratory

### **4.3 Mineralogical Characterization of Portland Cements**

In order to address the effect of different cement phases on cement properties, quantitative x-ray diffraction (QXRD) was performed on all the as-received cements. Rietveld analysis was adopted here for phase quantification and the results are depicted in Table 4.4. It is noted that tricalcium silicate quantified through XRD was in general higher than that determined through Bogue calculations, while tricalcium aluminate was in general lower. The disagreement between the phase content determined through XRD and potential phase content determined through ASTM C150-12 [4] is expected as indicated in the published literature [46, 47, 76, 77]. It is also noted that cement mineralogy alone cannot explain fully the 7-day heat of hydration trends as measured per ASTM C186-05 [8].

### **4.4 Cement Particle Size Analysis**

Two methods were used in characterizing cement particle size; namely, Blaine fineness and laser particle size analysis. In the first, the total specific surface area of particles is quantified while in the second the mass fraction or volume fraction is quantified for specific particle diameters. Both the specific surface area and the particle size distribution affect the water demand for a given flow. Also, for the same specific surface area, two cements of significantly different particle size distribution will have different water demands. A higher proportion of fines would also indicate a higher early strength gain [60, 62]. In addition to the effect of cement mineral composition on its properties, cement fineness affects the rate of its reaction with water, or hydration kinetics. The published literature indicates that the effect of higher fineness is to increase the rate of hydration due to a corresponding increase in surface area [40]. In terms of strength gain, the effect of fineness is more pronounced on early age strength than on the ultimate strength [17, 41].

Particle size distribution (PSD) defines the relative amount of particles at specific sizes or size ranges. Typically, particle sizes of portland cements vary from  $<1 \mu\text{m}$  to  $100 \mu\text{m}$  in diameter [5]. Moreover, PSD affects fresh and hardened concrete properties [17]. It

has been reported that a wider size distribution increases the packing density of the system and effectively reduces water demand [76]. Consequently, it is expected that increasing the packing density would have a positive contribution to strength gain potential. The effect of fineness is also extended to the amount of heat generated by portland cement, which increases with increasing fineness [5].

The results of particle size analysis for all as-received cements are presented in Table 4.5 using Blaine fineness and particle size distribution values. The results depicted in Table 4.5 indicate that there is in general a decrease in mean particle size with increasing Blaine fineness. However, there are several exceptions, such as the case of CHC, where the Blaine fineness was 575 m<sup>2</sup>/kg with a mean particle size of about 8.7 μm, compared to AC03 cement with a higher fineness of 612 m<sup>2</sup>/kg and a higher mean particle size of about 10 μm.

As to the effect of cement fineness on the 7-day heat of hydration [8], Figure 4.2 indicates a better relationship between Blaine fineness and heat of hydration than the heat index defined by ASTM C150-12 [4] for the cements studied here. However, it is to be noted that the combined effect of mineralogy and fineness needs to be explored to improve the coefficient of correlation.

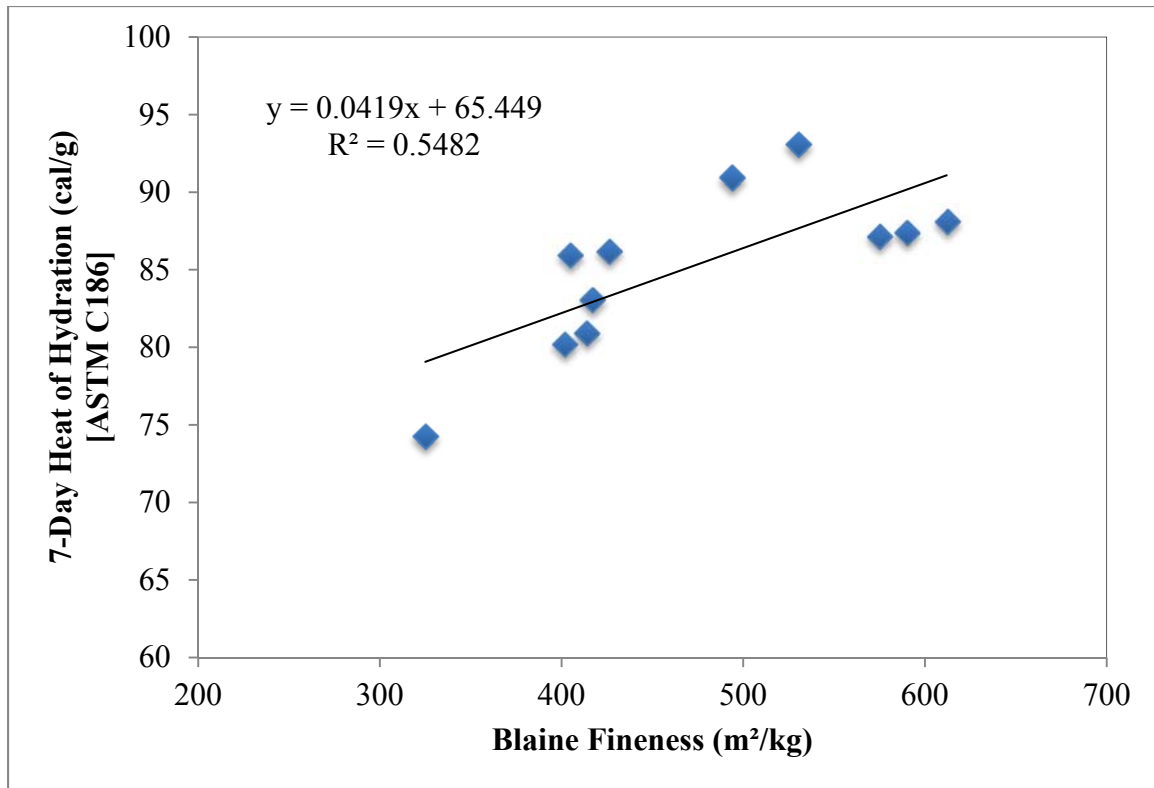


**Figure 4.2: Effect of Blaine Fineness on the 7-Day Heat of Hydration (ASTM C186)**

**Table 4.4: Phase Content (w/o) Using Quantitative X-Ray Diffraction**

Cement Phase	Source	CLEP	CLE02	CLE03	CHC	AC02	AC03	ZR02	ZR03	ERD06	LG01	LG03
C <sub>3</sub> S (%)	Rietveld	62	62	59	69	61	62	57	57	62	57	59
C <sub>2</sub> S (%)	Rietveld	16	17	20	7	13	14	16	20	16	13	13
C <sub>3</sub> A (%)	Rietveld	4	4	3	5	7	7	7	7	5	10	11
C <sub>4</sub> AF (%)	Rietveld	13	13	13	7	12	13	11	11	10	6	6

**Table 4.5: Particle Size Analysis of As-Received Cements**

Physical Properties	CLEP	CLE02	CLE03	CHC	AC02	AC03	ZR02	ZR03	ERD06	LG01	LG03
D <sub>10</sub> (μm)	3.31	2.63	1.76	2.43	3.61	1.33	2.51	1.43	2.76	3.21	2.55
D <sub>50</sub> (μm)	12.75	10.67	7.90	11.11	10.45	8.23	9.85	7.65	8.90	10.78	9.08
D <sub>90</sub> (μm)	40.71	26.30	16.08	32.21	24.86	19.94	23.39	19.19	19.43	29.74	19.18
Median size (μm)	12.75	10.67	7.90	11.11	10.45	8.23	9.85	7.65	8.90	10.78	9.08
Mean size (MPS) [μm]	18.38	13.15	8.65	15.00	12.90	10.05	11.95	9.61	10.41	14.35	10.27
ASTM C204-Blaine Fineness (m <sup>2</sup> /kg)	325	414	575	426	417	612	402	590	494	405	530

#### 4.5 Heat of Hydration Using Isothermal Calorimeter

Heat of hydration (HOH) was also determined using an isothermal calorimeter as another method of assessing heat generation during cement hydration. As indicated previously in Chapter 3, internal mixing was adopted here in order to capture the reaction process from the time of water addition. The results are reported in Table 4.6 and Figures 4.3 through 4.8. The results indicate the significance of cement fineness as well as mineralogy on the amount of heat generated by cements during hydration. It is noted that increasing the fineness for cement from the same source, and therefore same cement mineralogy, increased the measured heat at 7 days whether heat measurements were conducted using procedures outlined in ASTM C186 or C1702. The results also indicate that for cements of similar Blaine fineness, the higher the  $C_3A$  and/or  $C_3S$  content of cement, the higher the heat generated at 7 days. The findings are in agreement with what has been published in the literature on the parameters that affect heat of hydration of portland cement; namely, cement fineness, and  $C_3A$  and  $C_3S$  content.

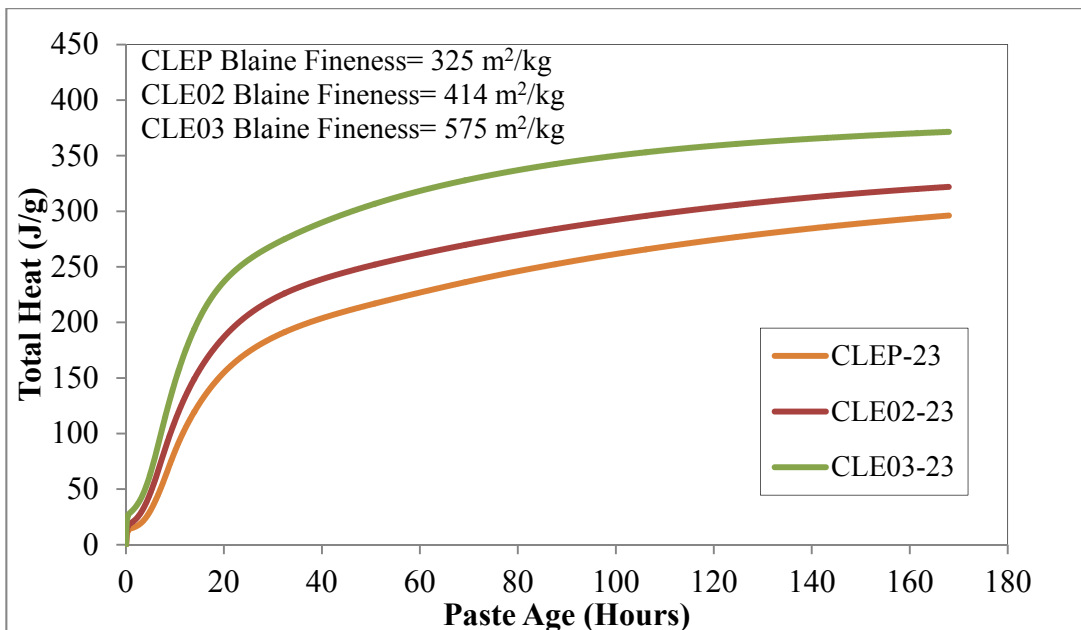


**Figure 4.3: Effect of Cement Blaine Fineness on Cumulative Heat (ASTM C 1702) for CLE Cements**

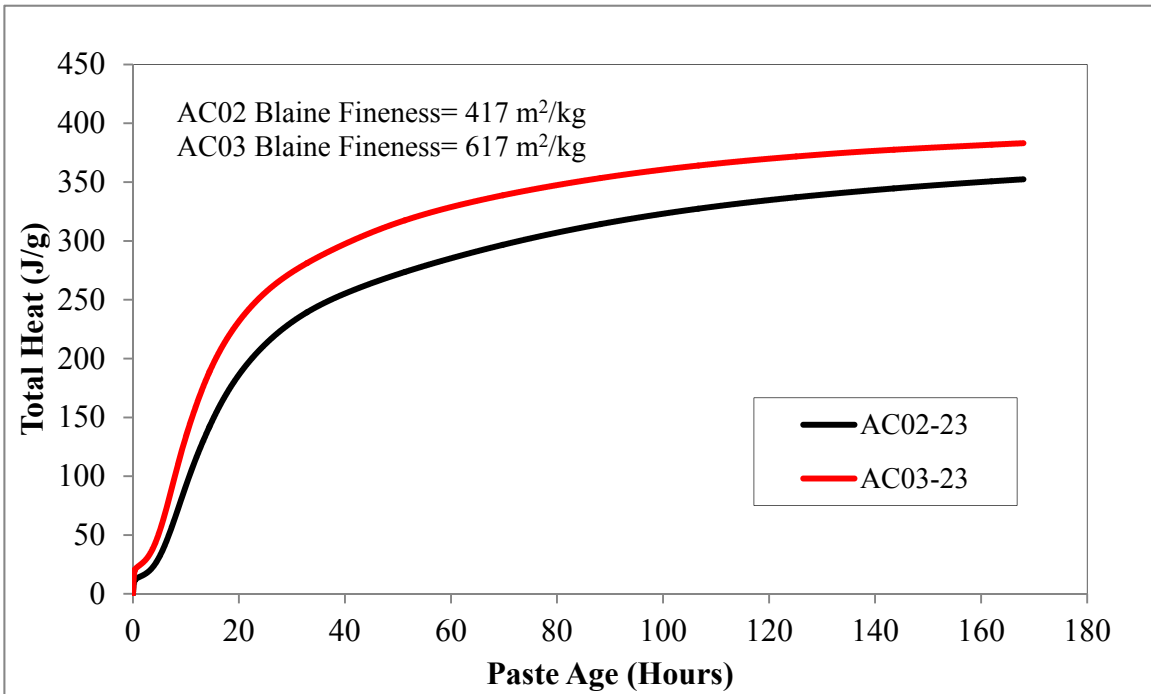


**Figure 4.4: Effect of Cement Blaine Fineness on Cumulative Heat (ASTM C 1702) for AC Cements**

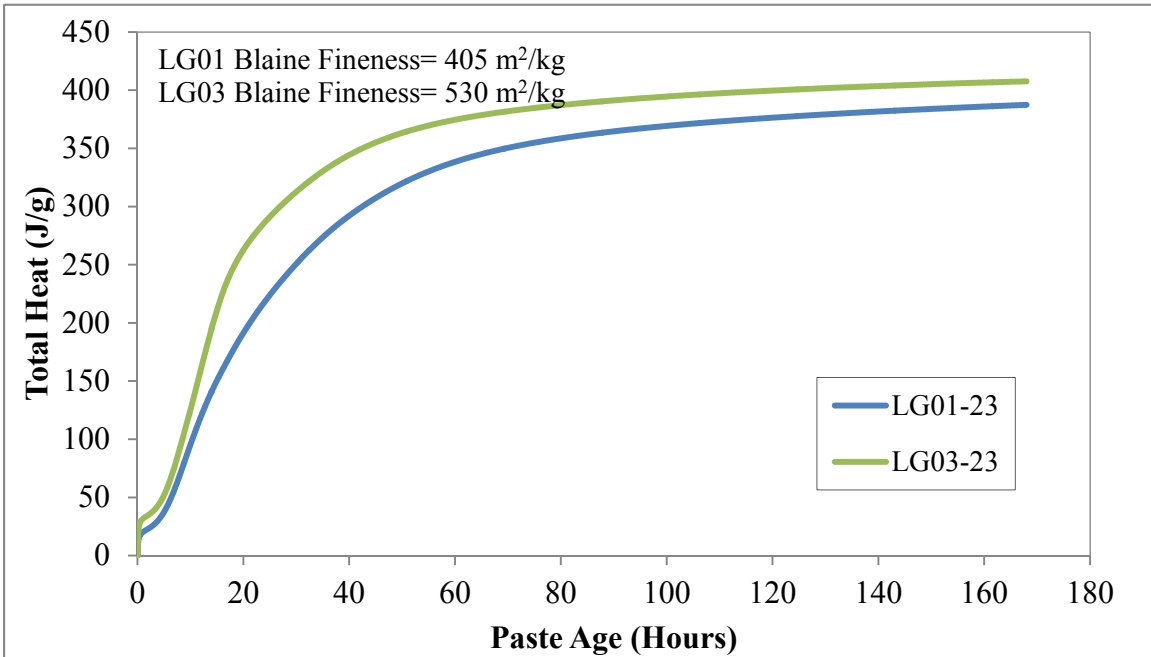


**Figure 4.5: Effect of Cement Blaine Fineness on Cumulative Heat (ASTM C 1702) for LG Cements**

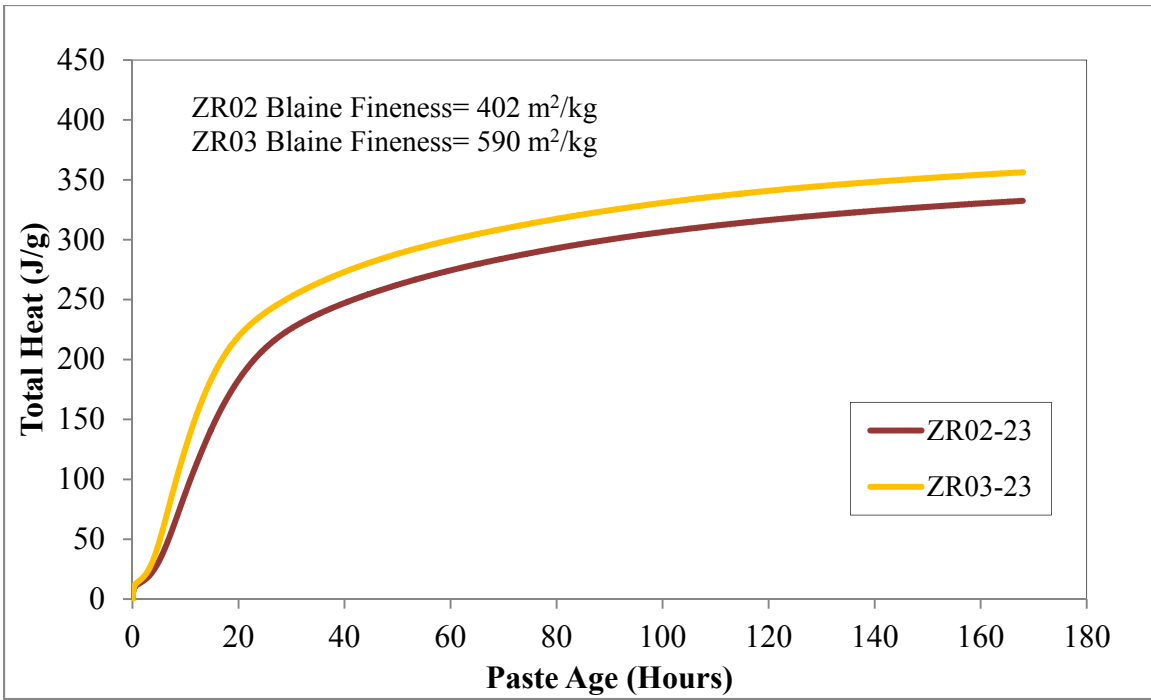


**Figure 4.6: Effect of Cement Blaine Fineness on Cumulative Heat (ASTM C 1702) for ZR Cements**

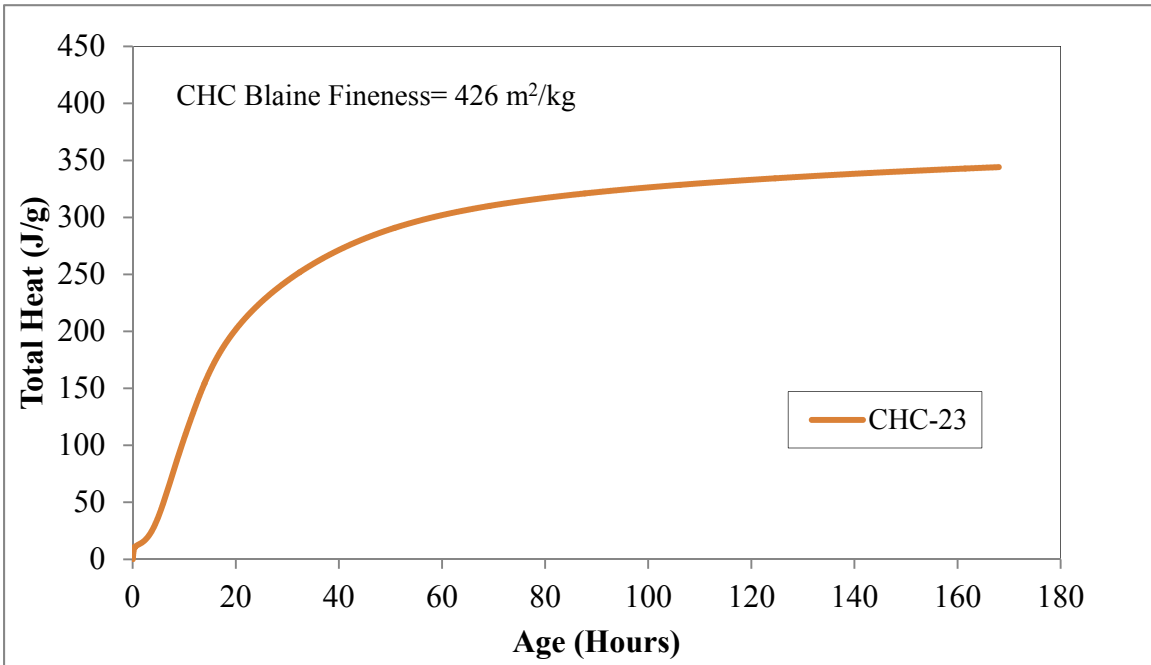


**Figure 4.7: Cumulative Heat (ASTM C 1702) for CHC Cement**

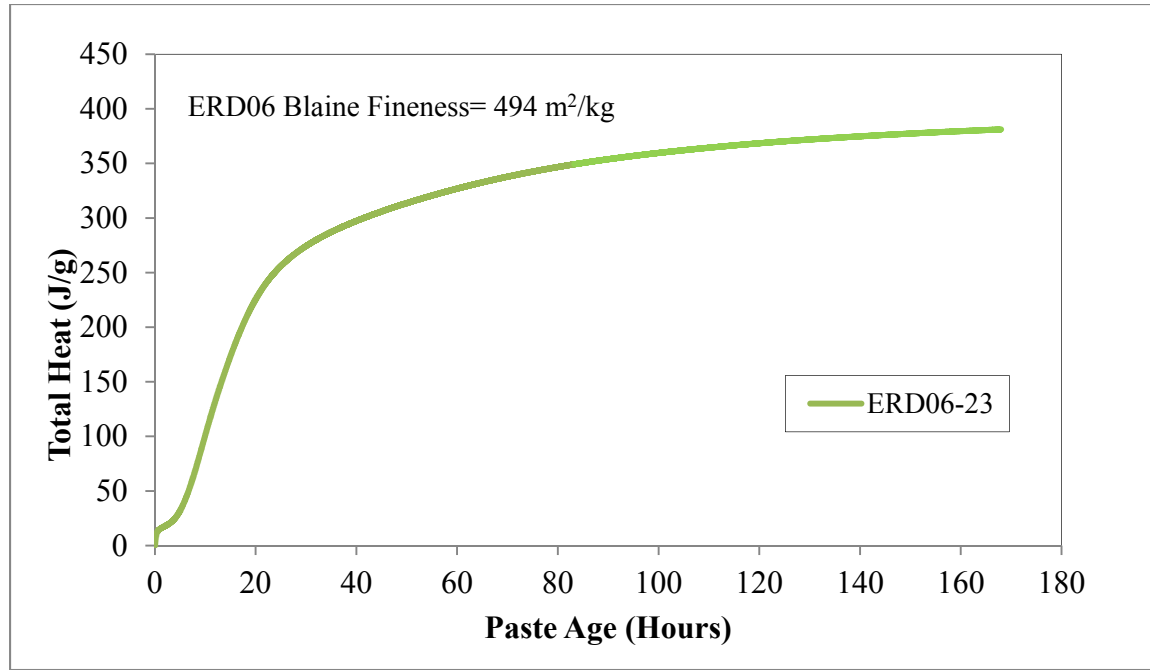


**Figure 4.8: Cumulative Heat (ASTM C 1702) for ERD06 Cement**

**Table 4.6: Fineness and 7-Day Heat of Hydration for As-Received Cements**

Property	CLEP	CLE02	CLE03	CHC	AC02	AC03	ZR02	ZR03	LG01	LG03	ERD06
Blaine Fineness (m <sup>2</sup> /kg)	325	414	575	426	417	612	402	590	405	530	494
ASTM C186 (J/g)	312	340	366	362	349	370	337	367	361	391	382
[cal/g]	[75]	[81]	[87]	[87]	[83]	[88]	[81]	[88]	[86]	[93]	[91]
ASTM C1702 (J/g)	297	326	368	340	350	385	331	354	386	407	384
[cal/g]	[71]	[78]	[88]	[81]	[84]	[92]	[79]	[85]	[92]	[97]	[92]

Figure 4.9 examines the relationship between HOH determined using ASTM C186 and C1702. The data indicate that there is a reasonable relationship between the two measurement methods. The heat of solution method appears to yield lower values than the conduction method for cements with heat of hydration values above 360 kJ/kg. However, for values less than 360, heat of solution method gave higher heat values than those collected using isothermal calorimetry. It is recognized that both heat measurement methods are not necessarily equivalent and used different w/c ratios, with the heat of solution method at 0.40 and the isothermal conduction calorimetry method at 0.50. This w/c difference could have affected the degree of hydration; however, the effect of w/c ratio has been reported to be minimal at 7 days of hydration [79, 80]. The higher heat values measured through calorimetry are for cements that have high fineness or high tricalcium aluminate content. For those cements, it appears that the C186 method produced heat of hydration values that were less than those collected through isothermal calorimetry. It would be interesting to see if this effect would be observed at shorter hydration times; that is, at an age of 3 days.

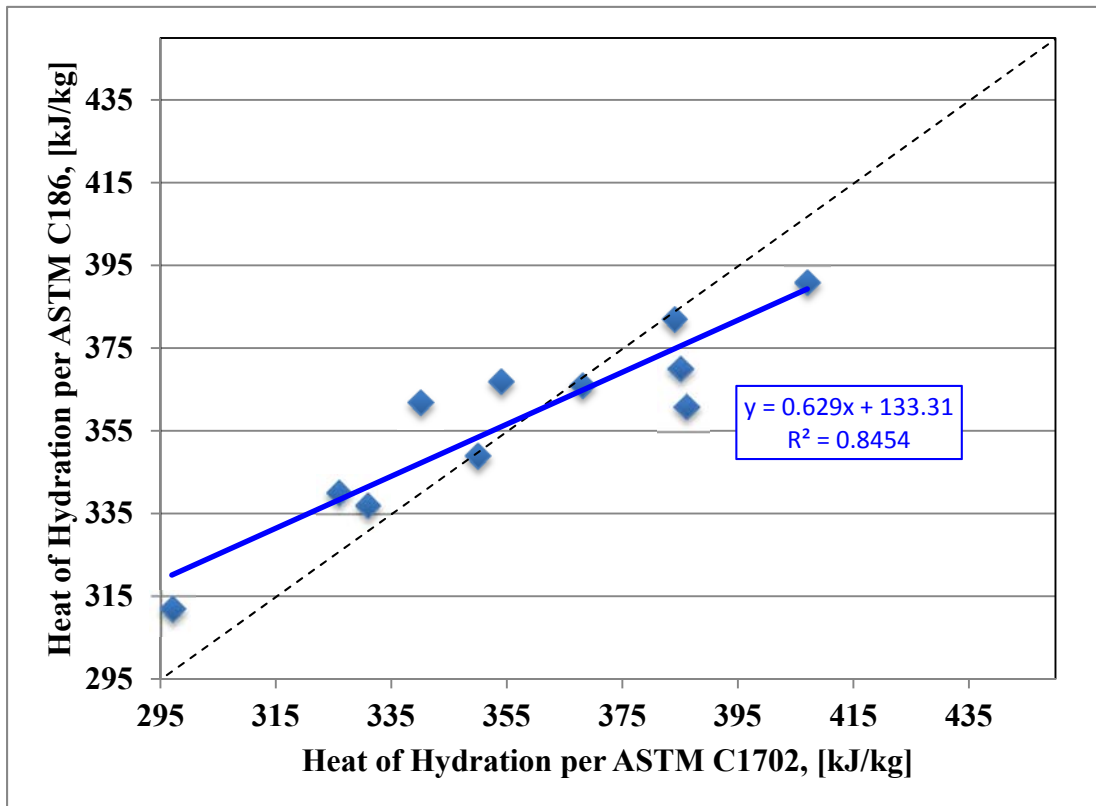


**Figure 4.9: Relationship Between Heat of Hydration Determined Using Heat of Solution Method and Isothermal Conduction Calorimetry**

The experimental data showed that for 2 cements that had the same heat index of 85, CLEP and ZR03, the 7-day HOH differed by 13-14 cal/g. It is also noted that these two cements had Blaine fineness values of 325 and 590 m<sup>2</sup>/kg, with the cement of higher Blaine fineness generating higher HOH. Additionally, for cements of similar heat index, between 87 and 89 (CLE02, ZR02, AC03), the measured HOH varied between 7 and 14 cal/g, with corresponding Blaine fineness values ranging between 410 and 610 m<sup>2</sup>/kg. For cements with high fineness values and/or high tricalcium aluminate contents, the heat measured at 7 days using C186 was lower than that reported using C1702. This finding could indicate that for cements of high fineness, C1702 might be a better technique in assessing the heat of hydration, and subsequently predicting temperature rise, in portland cement concrete mixes used for massive elements.

#### **4.6 Activation Energy Determination**

The concept of activation energy has been used in predicting concrete field properties. However, the calculation is usually based on data collected in the laboratory at different ambient temperatures than those experienced in the field. The concept has been used widely in practice and the procedures for its implementation and data collection are outlined in ASTM C1074-11 [31]. Strength data for mortar cubes were collected at three temperatures. Additionally, the age at which strength data were collected was based on the setting time for each mortar at each testing temperature. As indicated in Chapter 3, the curing temperatures used in this study were 22, 30 and 40°C. The effects of curing temperature on the setting profile (change in penetration resistance with time) are depicted in Figures 4.10 through 4.15.

Increasing the curing temperature shortened the initial and final set times due to the increased rate of hydration, especially during the early stages of the reaction where the reactions were chemically controlled. In addressing the effect of fineness on the setting time behavior of cements, it can be noticed that increasing fineness resulted in a consistently shorter setting time as can be observed from the data presented in Figures 4.16 through 4.18. Figure 4.19 shows that cement composition affected the setting behavior. LG01 and AC02 were chosen because they have similar Blaine fineness values and mean particle sizes. The data indicate that for cements of similar fineness and mean particle size, setting behavior appeared to be affected by the C<sub>3</sub>A, C<sub>3</sub>S, and alkali contents, and the SO<sub>3</sub>/C<sub>3</sub>A ratio. The AC02 cement had a higher tricalcium silicate content

while LG01 had higher contents of tricalcium aluminate and alkali oxides, and a higher  $SO_3/C_3A$ . The literature indicates that the setting time increases with increasing gypsum content. While the early rate of reaction of tricalcium silicate is not affected by alkali oxide content, tricalcium aluminates initial reaction rate appears to be affected by both sulfates and alkalis [6, 7].

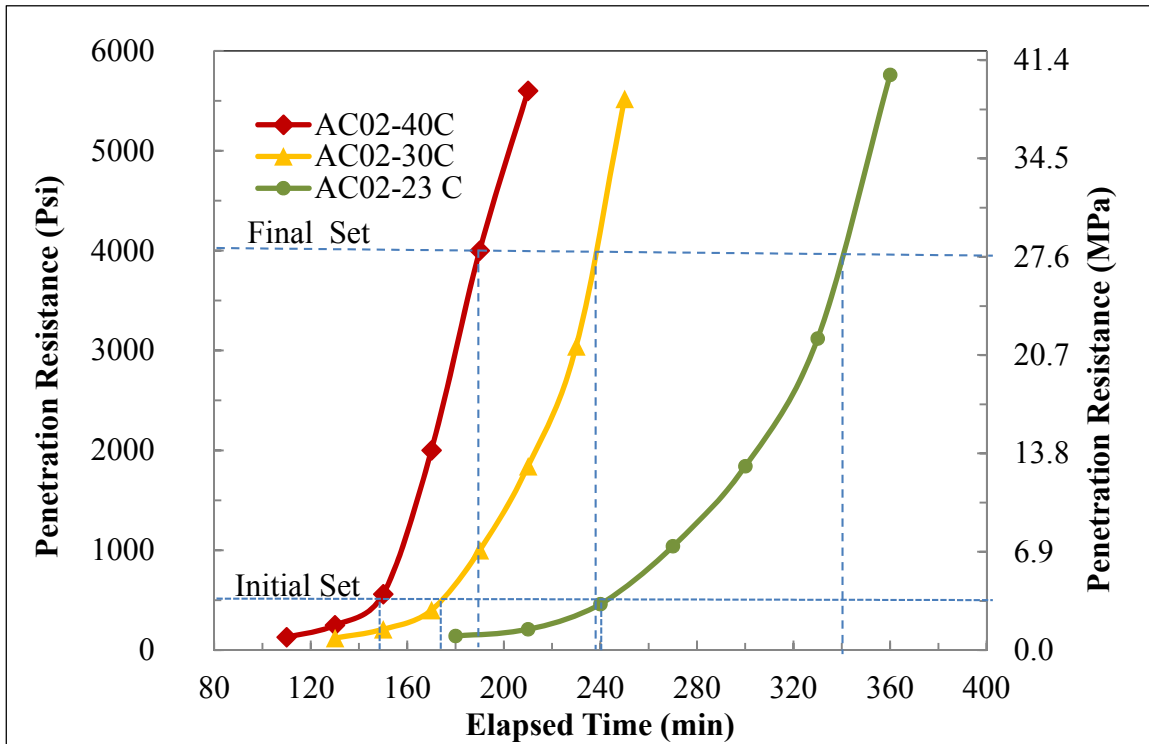


**Figure 4.10: Effect of Temperature on Setting Properties for AC02 Cement**

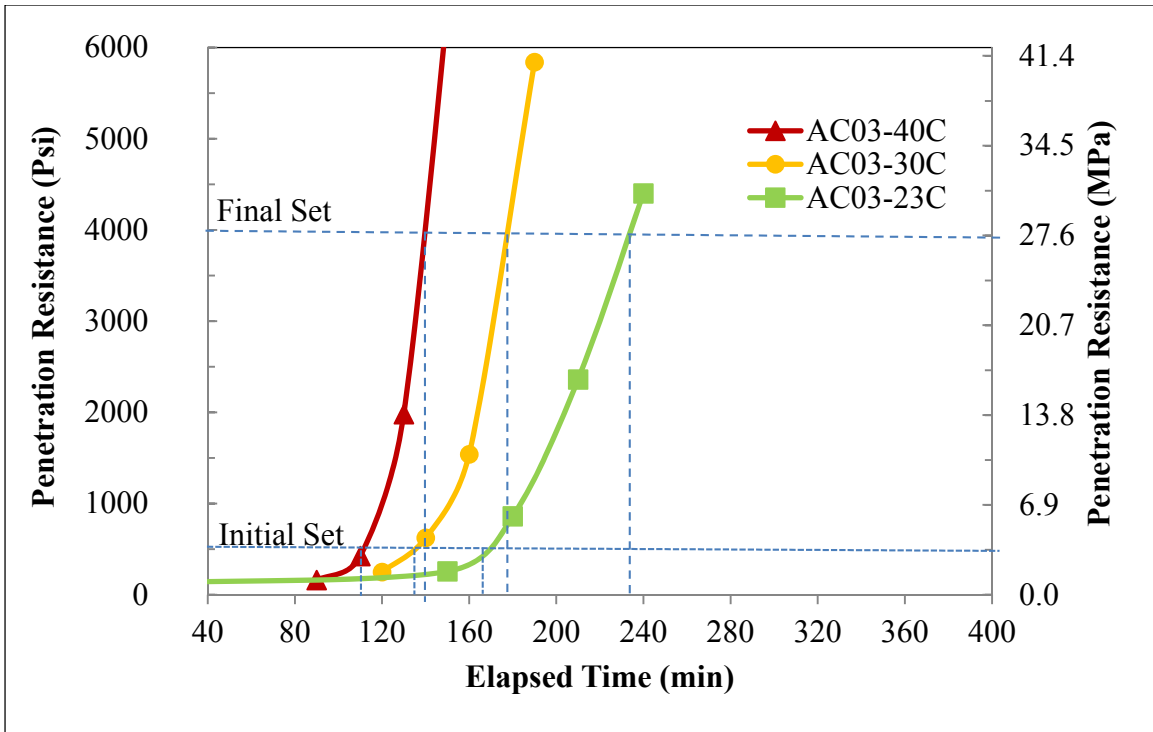


Figure 4.11: Effect of Temperature on Setting Properties for AC03 Cement

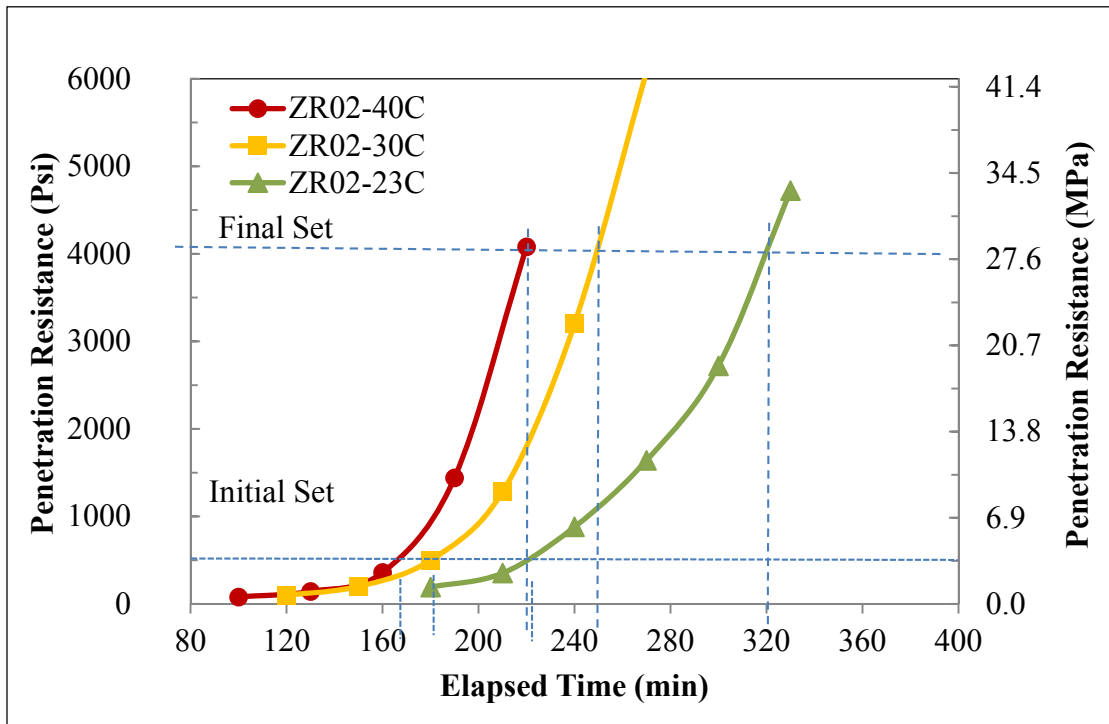


Figure 4.12: Effect of Temperature on Setting Properties for ZR02 Cement

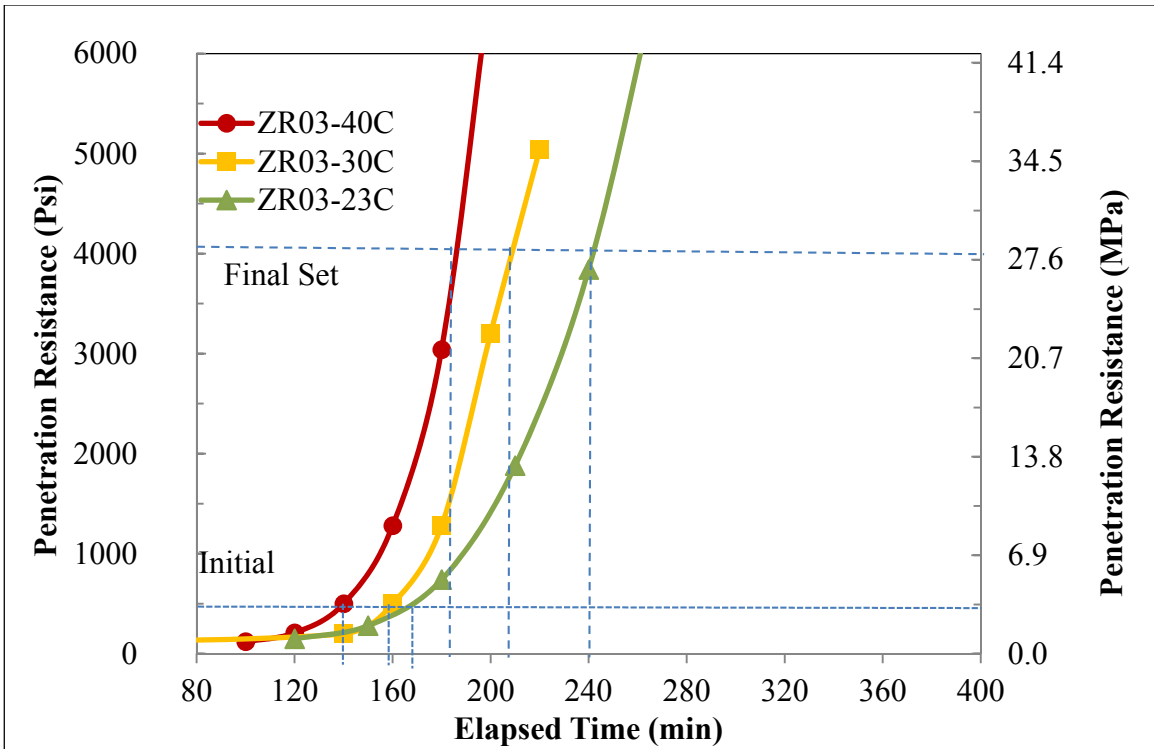


Figure 4.13: Effect of Temperature on Setting Properties for ZR03 Cement

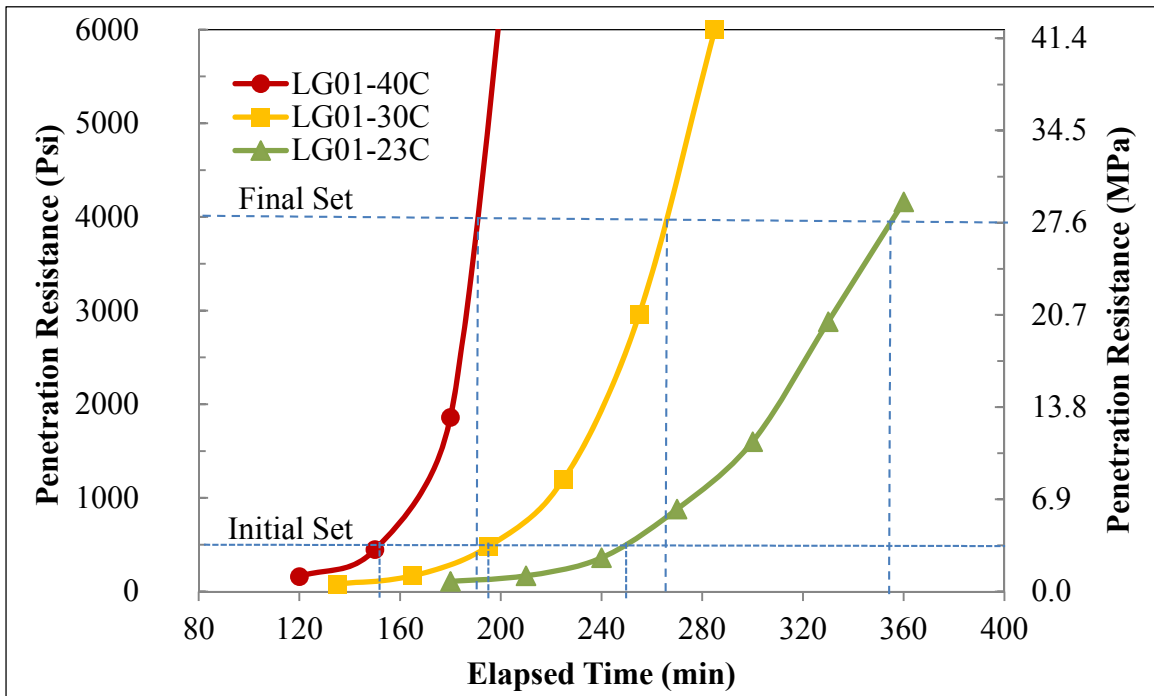


Figure 4.14: Effect of Temperature on Setting Properties for LG01 Cement

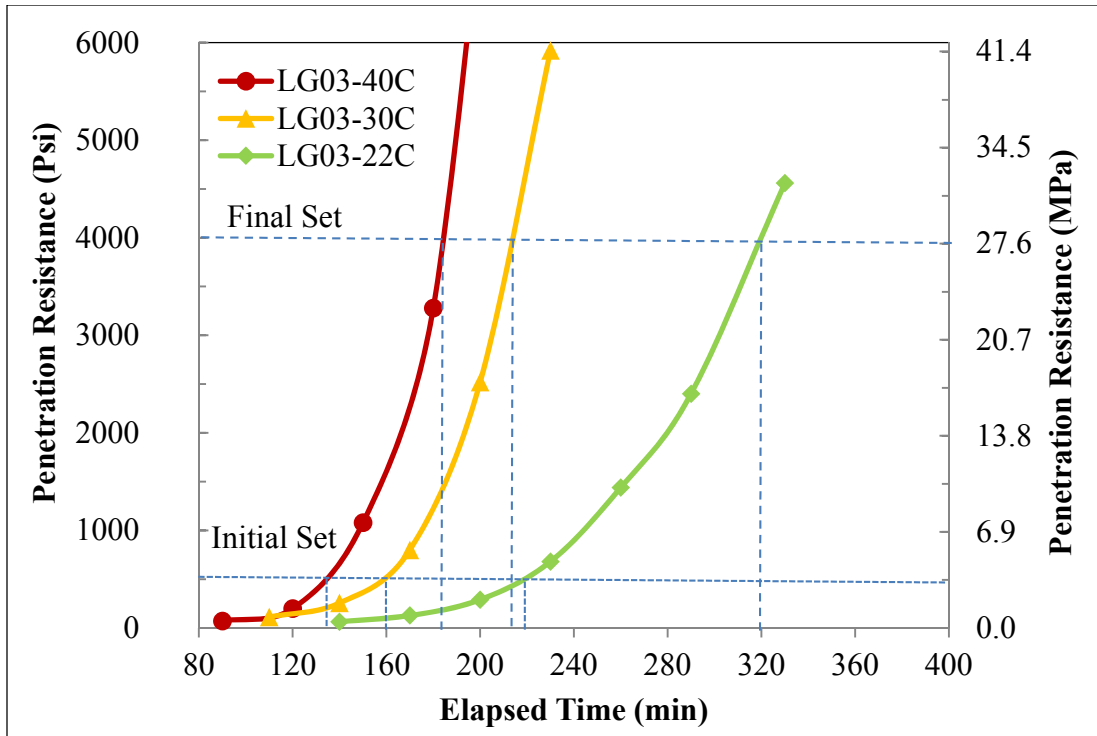


Figure 4.15: Effect of Temperature on Setting Properties for LG03 Cement

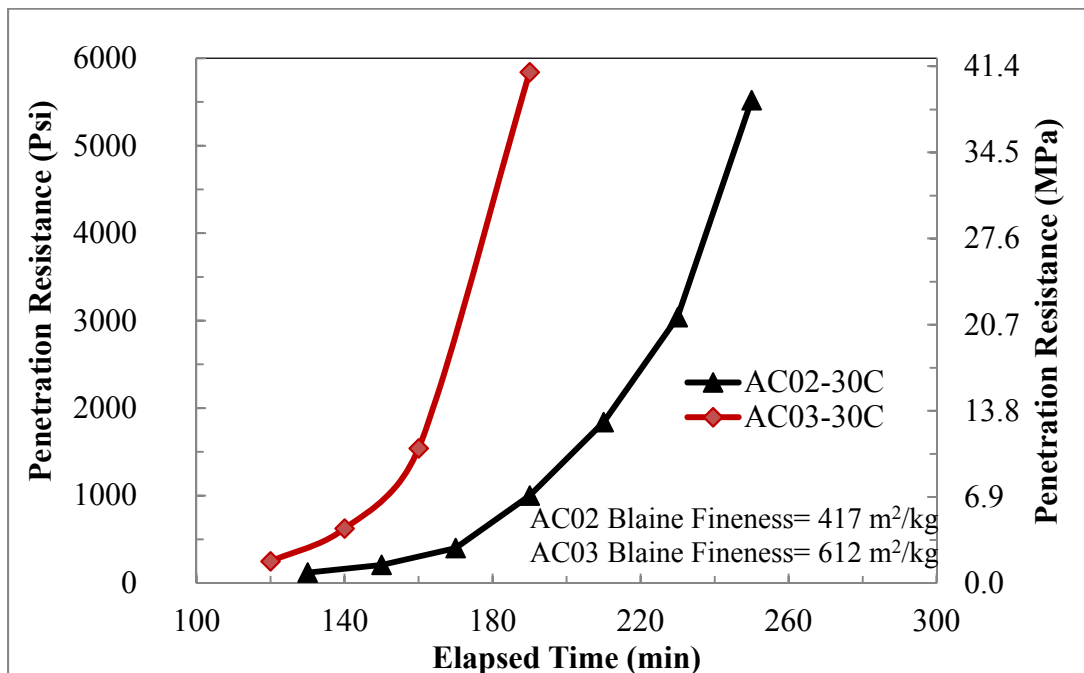


Figure 4.16: Effect of Cement Fineness on Setting Behavior of AC Cements

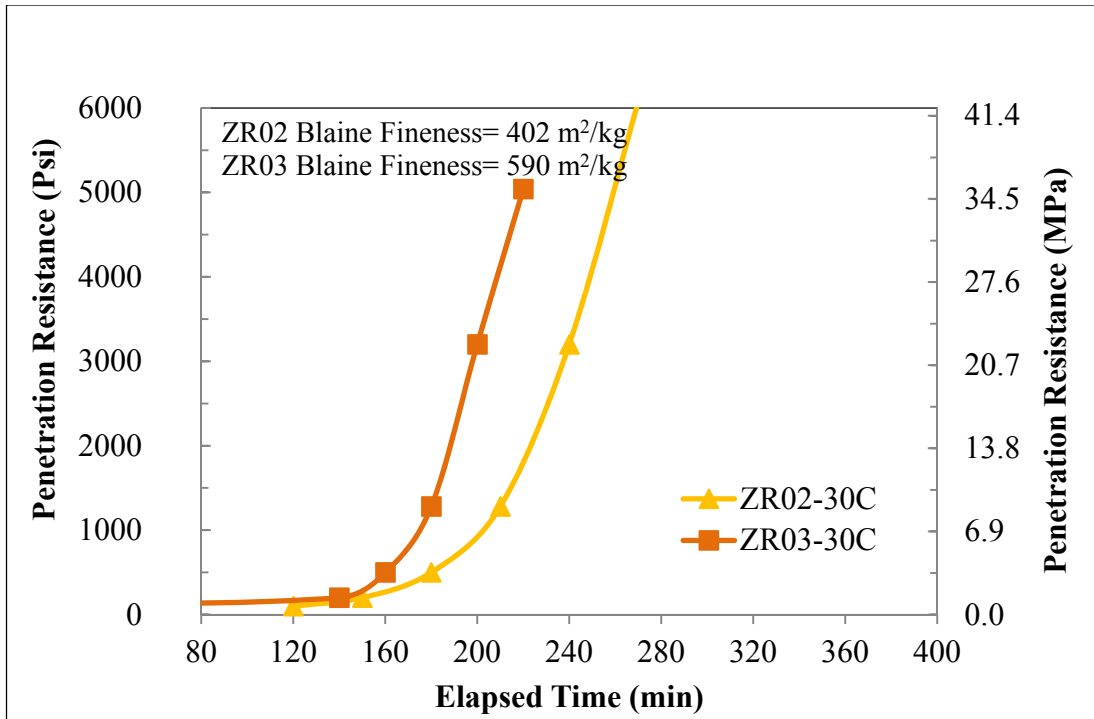


Figure 4.17: Effect of Cement Fineness on Setting Behavior of ZR Cements

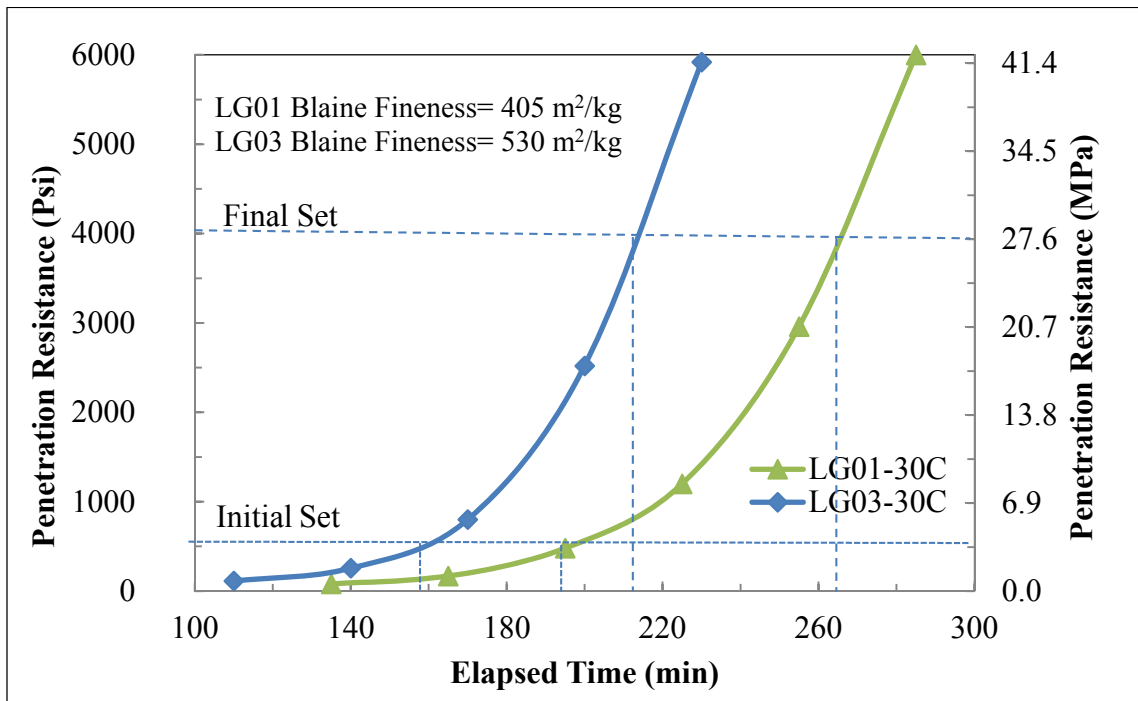
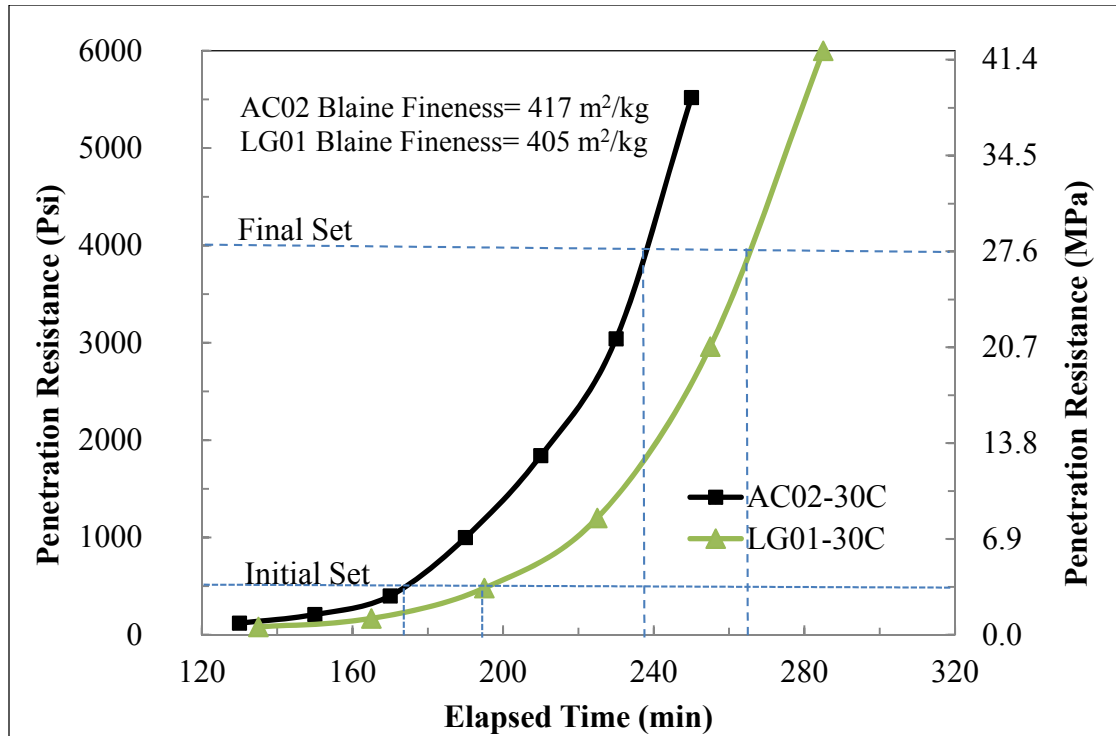


Figure 4.18: Effect of Cement Fineness on Setting Behavior of LG Cements



**Figure 4.19: Effect of Cement Mineralogy on Setting Behavior for Cements of Similar Fineness**

Following setting time determination, the compressive strengths for mortar cubes prepared using those 6 cements were determined at 3 different curing temperatures. The data are presented in Figure 4.20 through Figure 4.25. For all cements tested here, it appears that increasing the temperature had the effect of increasing early strength but not necessarily the later strength. This is in agreement with the findings in the literature on the effect of curing temperature on strength gain; that is, increasing the temperature increases early strength while the later strength decreases. This was attributed to the more rapid production of hydration products, which resulted in a nonuniform distribution of the hydration phases in the hydrated cement paste.

To address the effects of cement fineness and mineralogy on strength gain, several cements were evaluated and the data are presented in Figure 4.26 through Figure 4.28. The literature indicates that cement fineness affects compressive strength of portland cement mortar up to an age of 7 days. However, the results presented here indicate that for cements of the same mineralogy, the significance of cement fineness may be persistent up to an age of about 28 days. Also, comparing cements of similar fineness but different composition, Figure 4.29 shows that for LG01

and AC02 of similar Blaine fineness (405 and 417 m<sup>2</sup>/kg respectively), the calcium silicate content affects strength gain up to an age of 28 days.

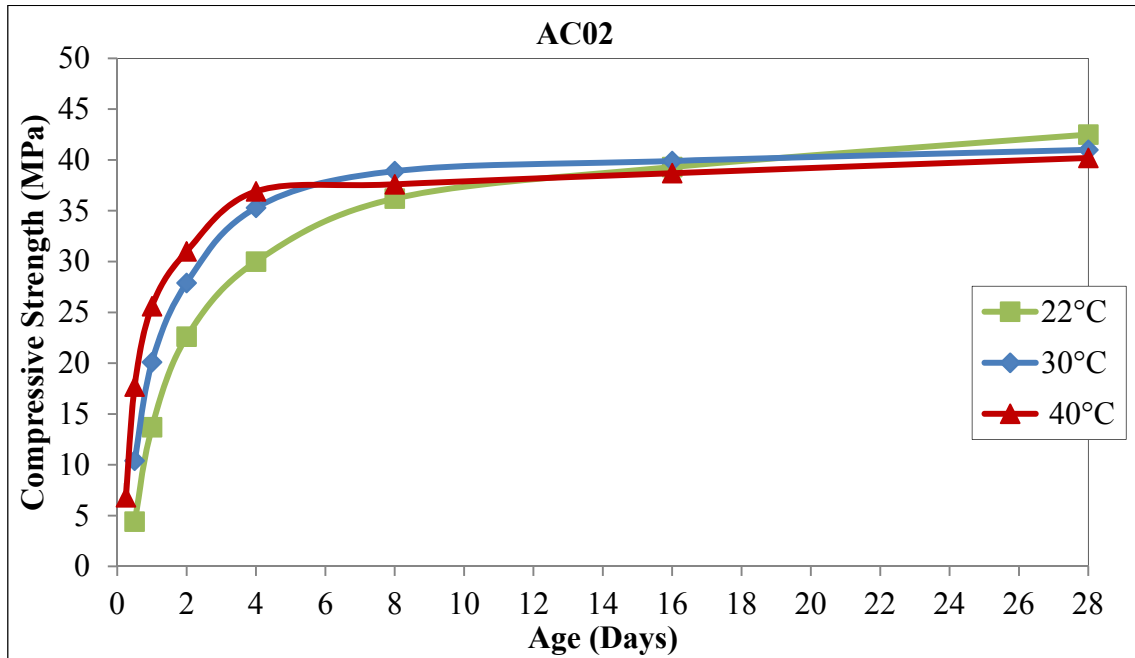


Figure 4.20: Effect of Curing Temperature on Compressive Strength Gain with Time for AC02 Cement

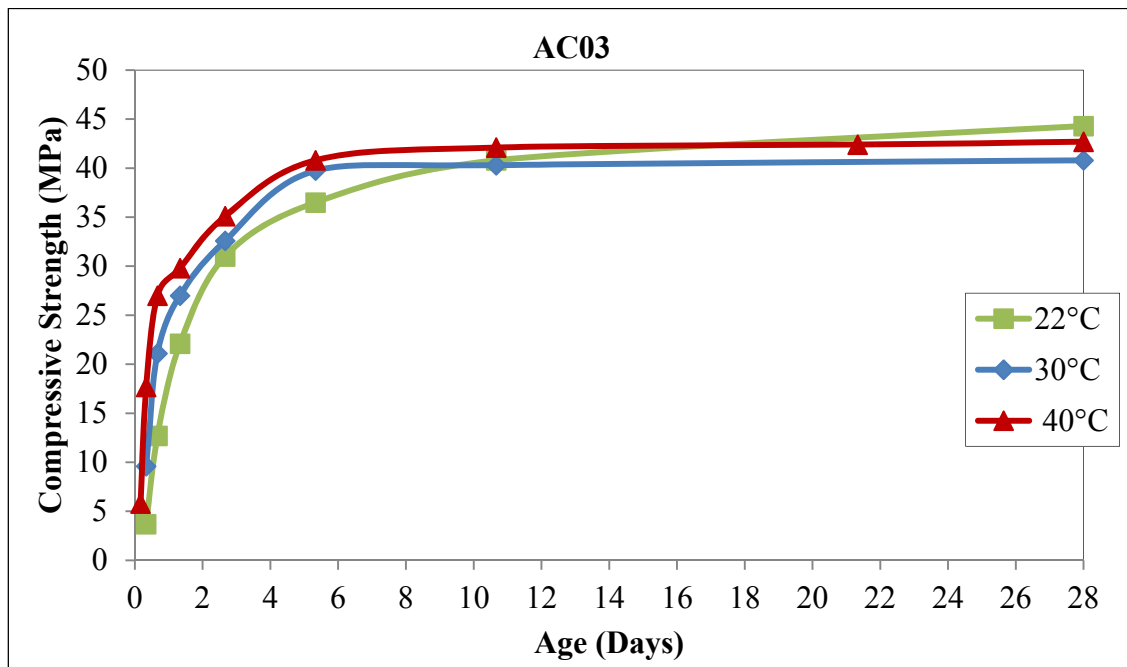
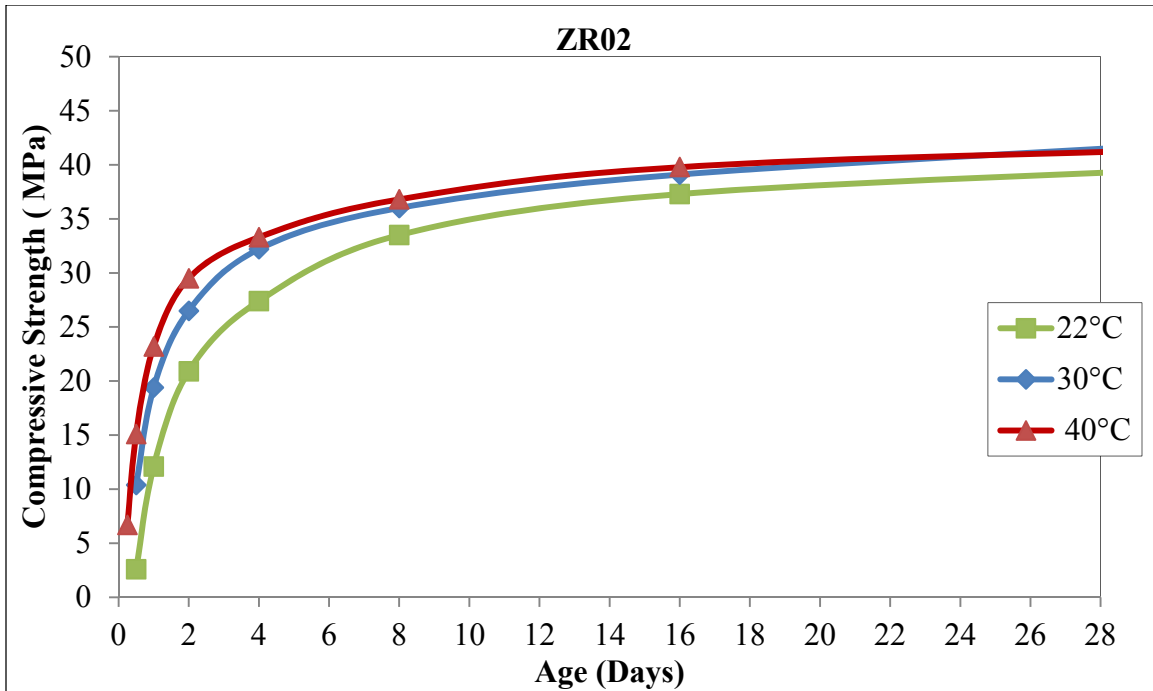
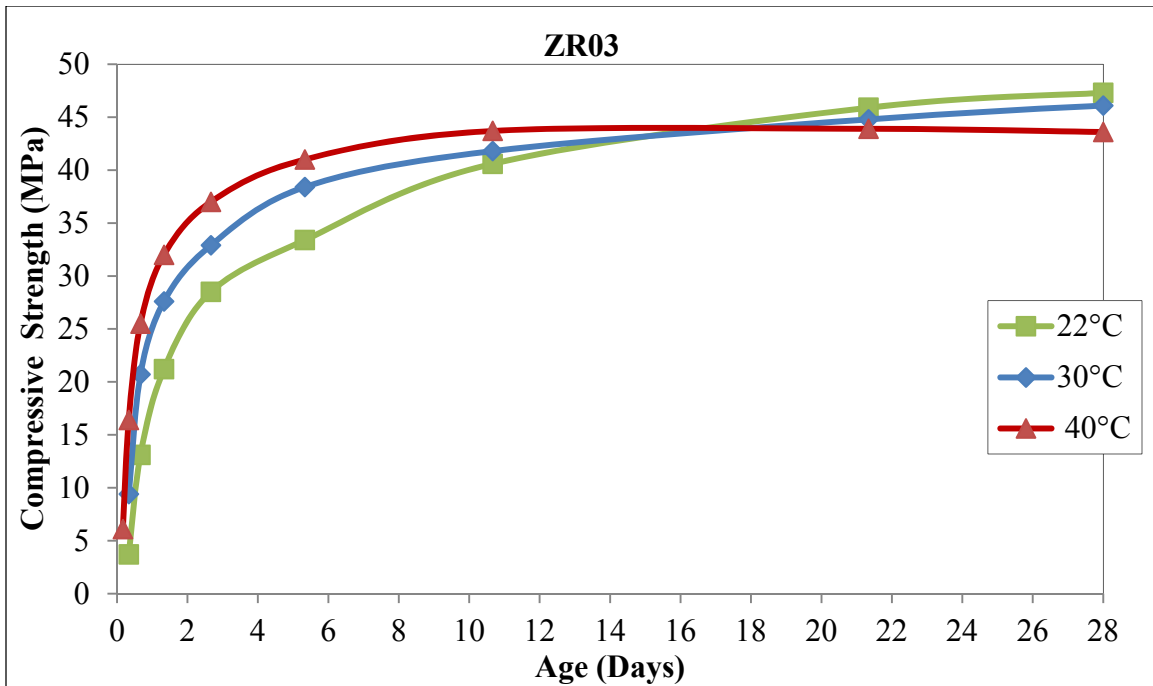


Figure 4.21: Effect of Curing Temperature on Compressive Strength Gain with Time for AC03 Cement



**Figure 4.22: Effect of Curing Temperature on Compressive Strength Gain with Time for ZR02 Cement**



**Figure 4.23: Effect of Curing Temperature on Compressive Strength Gain with Time for ZR03 Cement**

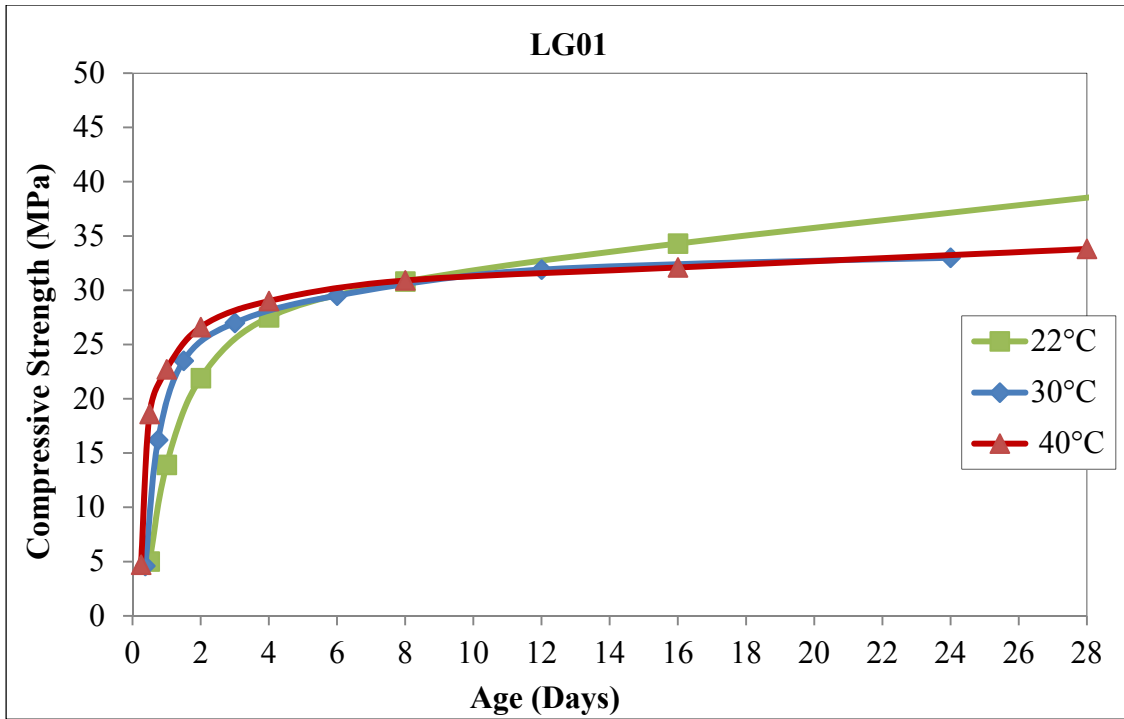


**Figure 4.24: Effect of Curing Temperature on Compressive Strength Gain with Time for LG01 Cement**

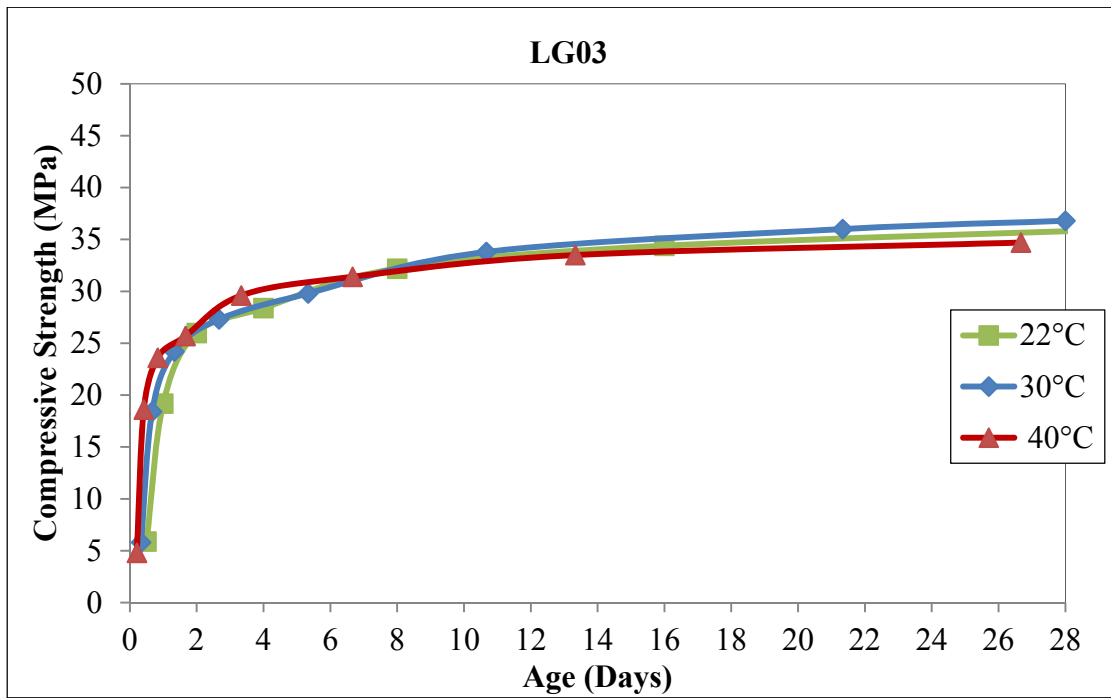


**Figure 4.25: Effect of Curing Temperature on Compressive Strength Gain with Time for LG03 Cement**

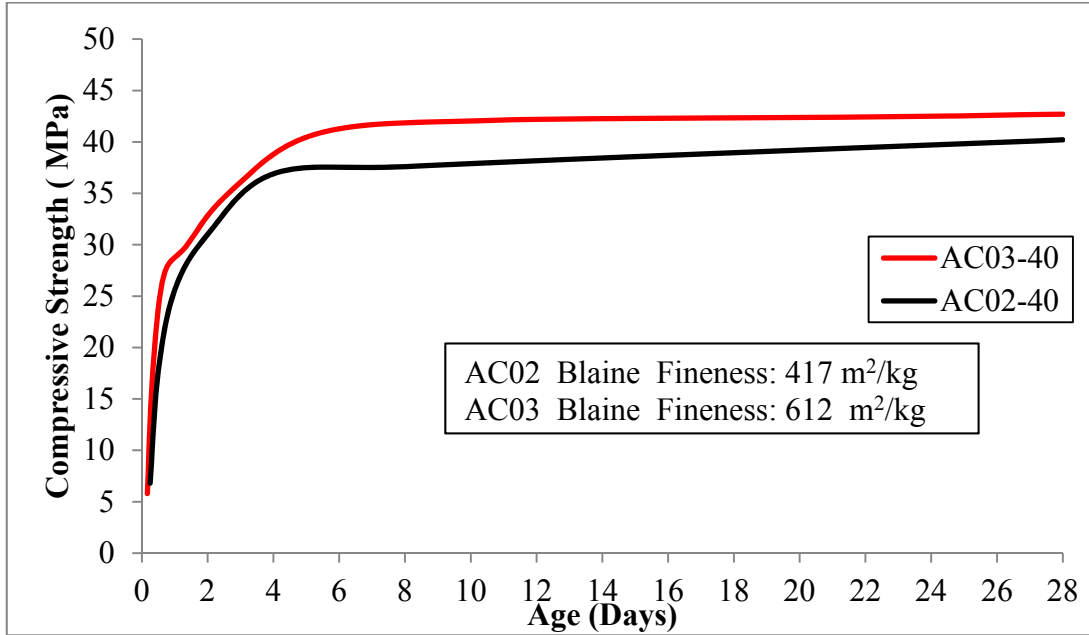


**Figure 4.26: Effect of Cement Fineness on Compressive Strength Gain with Time for AC Cements**

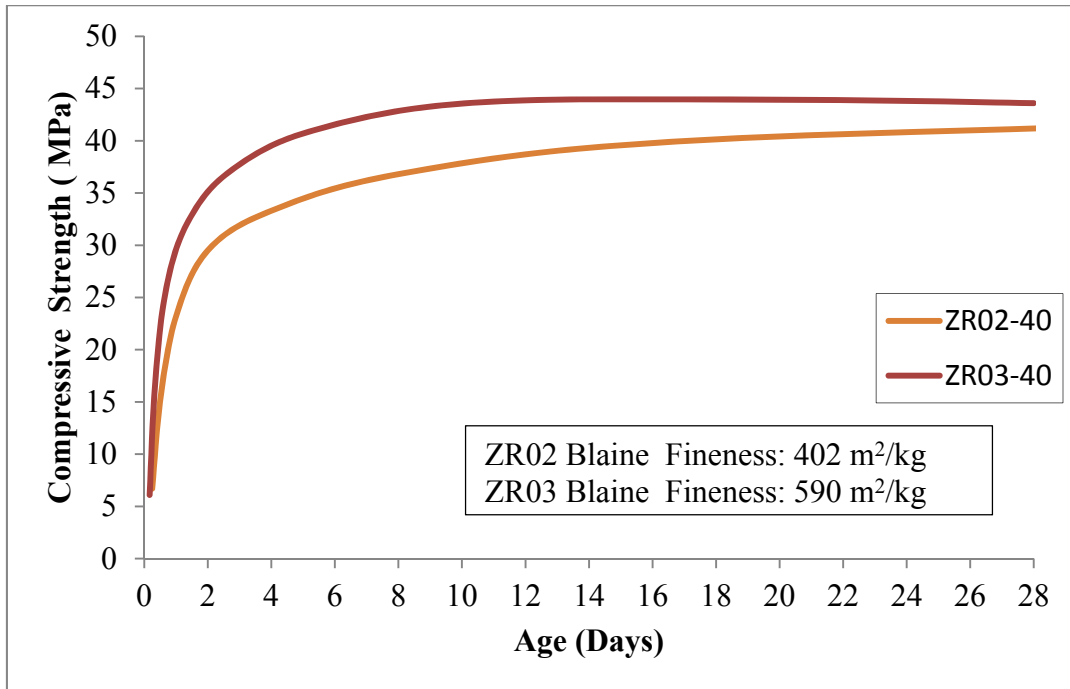


**Figure 4.27: Effect of Cement Fineness on Compressive Strength Gain with Time for ZR Cements**

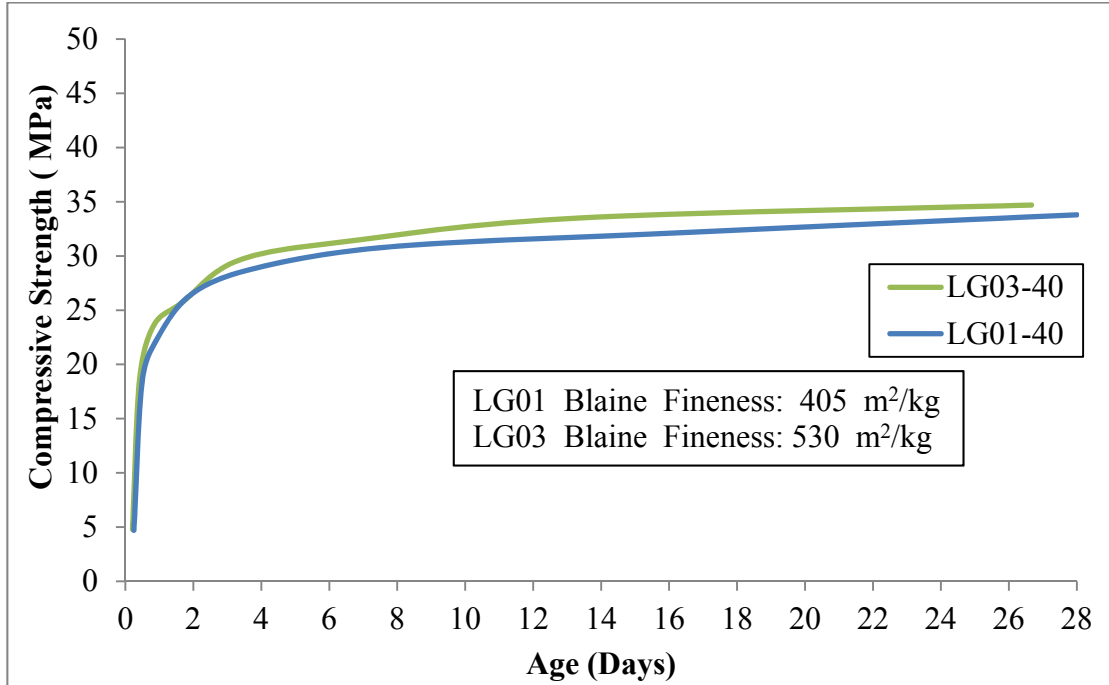


Figure 4.28: Effect of Cement Fineness on Compressive Strength Gain with Time for LG Cements

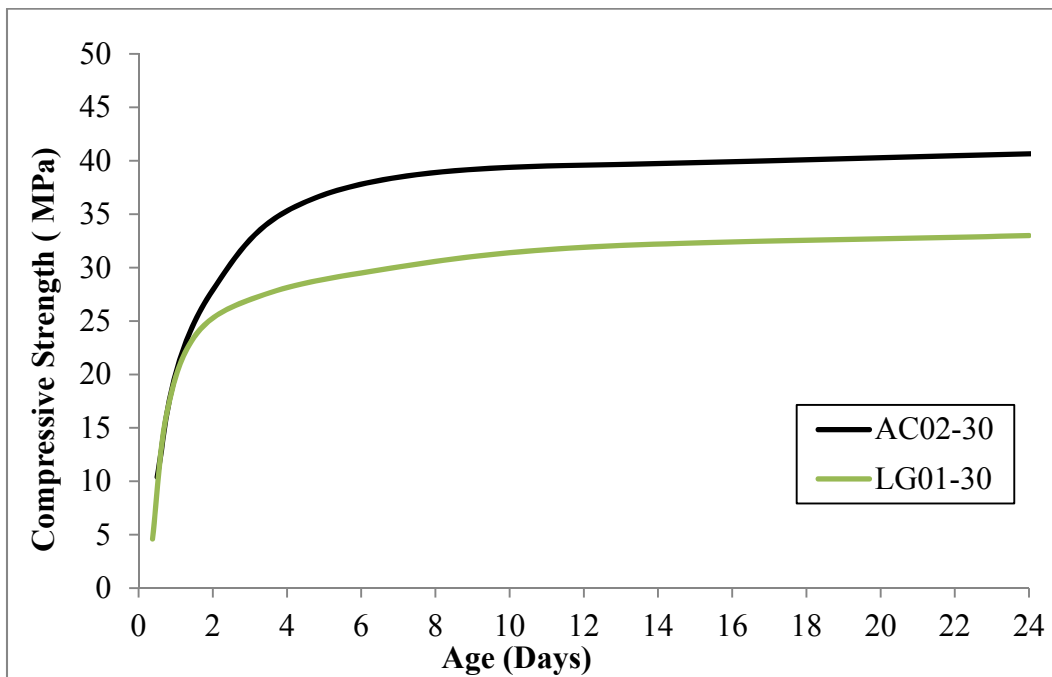


Figure 4.29: Effect of Cement Composition on Compressive Strength Gain with Time

The process of determining the activation energy based on strength measurements is outlined in Annex A1 of ASTM C1074-11 [31]. Two functions have been proposed and extensively used in activation energy determination; namely an exponential function presented in Equation 4.1 (same as Equation 2.4) and a hyperbolic function presented in Equation 4.2 (same as Equation 2.2) and adopted in the ASTM specifications:

$$S = S_u e^{-\left(\frac{\tau}{t}\right)^\beta} \quad \text{Equation 4.1 (2.4)}$$

where  $S$  = Average compressive strength at age  $t$  (MPa)  
 $t$  = Test age (days)  
 $S_u$  = Limiting strength (MPa)  
 $\tau$  = Time constant (days) [ $1/k$  in the hyperbolic function]  
 $\beta$  = Curve shape parameters (dimensionless)

$$S = S_u \frac{k(t-t_0)}{1+k(t-t_0)} \quad \text{Equation 4.2 (2.2)}$$

where  $S$  = Average compressive strength at age  $t$  (MPa)  
 $t$  = Test age (days)  
 $S_u$  = Limiting strength, (MPa)  
 $k$  = Rate constant or rate of reaction, (days<sup>-1</sup>)  
 $t_0$  = Age at which strength development is assumed to begin (days)

In this work, the parameters for both functions were determined using the Solver module of Microsoft Excel. Each function was fitted using the strength gain data at each curing temperature. The solver minimizes the sum of the squares of the residuals to obtain the best fit for the collected data. The coefficient of correlation ( $R^2$ ), which is a statistical measure of how well the regression line approximates the real data points, was calculated for each function at each curing temperature.  $R^2$  values for the cements studied here exceeded 0.97, which indicates a good

fit using either function. Tables 4.7 and 4.8 depict the fitted parameters for the hyperbolic and exponential functions, respectively. Once the parameters were determined, the calculated strengths determined through each function were plotted along with the actual collected data points. Figures 4.30 through 4.32 show an example of the analysis procedure using AC02 cement. The actual data and the predicted values at each curing temperature for both functions are presented. The same procedures were adopted for each cement and the data are presented in Table 4.7 and 4.8.

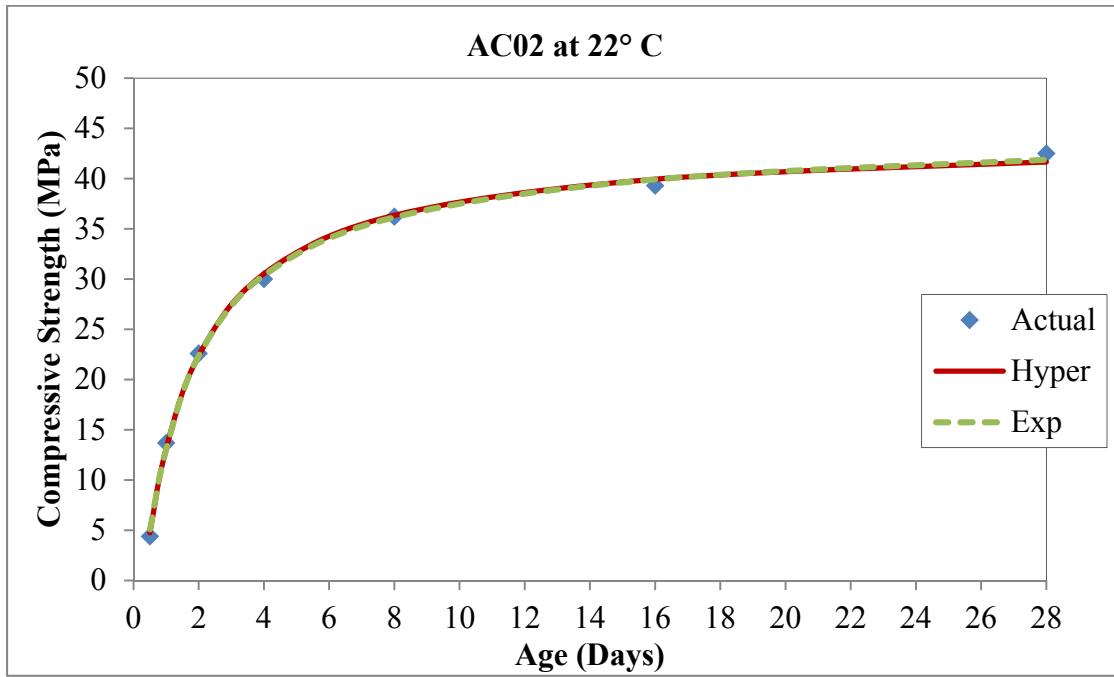


**Figure 4.30: Strength Data Fitting Using Exponential and Hyperbolic Functions on AC02 at 22°C**

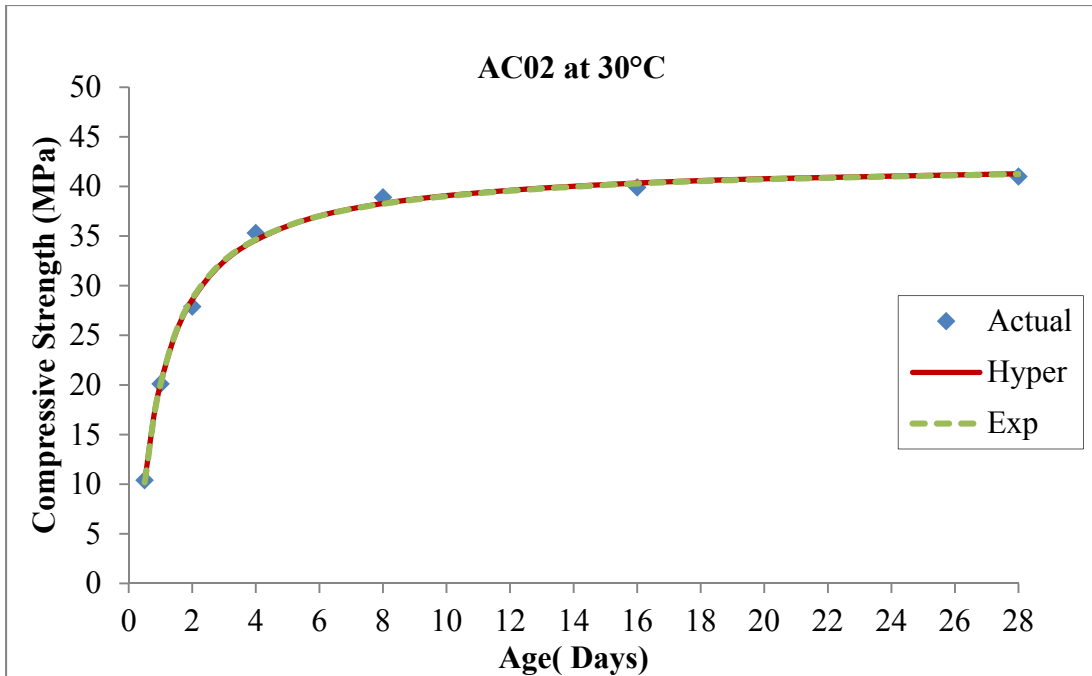


Figure 4.31: Strength Data Fitting Using Exponential and Hyperbolic Functions on AC02 at 30°C

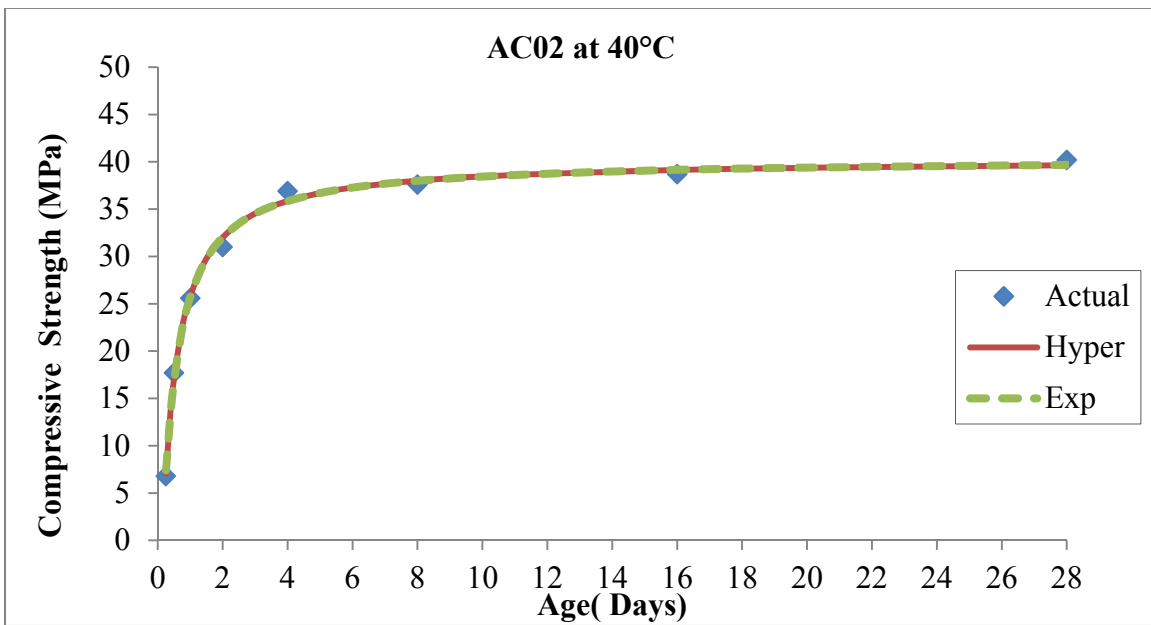


Figure 4.32: Strength Data Fitting Using Exponential and Hyperbolic Functions on AC02 at 40°C

**Table 4.7: Summary of Hyperbolic Function Parameters**

Cement	Temperature (°C)	$S_u$ (MPa)	$k$ (1/day)	$t_0$ (hr)	$R^2$
AC02	22	44.13	0.61	7.22	0.998
	30	42.58	1.15	5.29	0.998
	40	40.33	2.08	3.56	0.997
AC03	22	45.68	0.84	5.37	0.999
	30	42.34	1.64	3.42	0.988
	40	42.86	2.52	2.22	0.986
ZR02	22	41.97	0.52	4.66	0.999
	30	42.45	0.85	2.30	0.995
	40	41.34	1.32	2.16	0.995
ZR03	22	48.95	0.54	2.48	0.988
	30	46.10	1.13	2.51	0.989
	40	44.57	2.22	2.14	0.998
LG01	22	36.05	0.90	7.60	0.998
	30	32.93	2.00	6.97	0.997
	40	32.29	3.50	4.68	0.982
LG03	22	35.41	1.67	8.92	0.988
	30	35.69	1.83	5.00	0.974
	40	33.14	3.83	3.77	0.975

**Table 4.8: Summary of Exponential Function Parameters**

Cement	Temperature (°C)	$S_u$ (MPa)	$\tau$ (hr)	$\beta$	$R^2$
AC02	22	45.50	31.45	0.81	0.998
	30	42.70	17.69	0.93	0.998
	40	40.43	10.46	0.95	0.996
AC03	22	46.56	22.52	0.84	0.999
	30	42.79	12.06	0.88	0.988
	40	43.80	7.90	0.83	0.987
ZR02	22	43.89	33.30	0.74	0.999
	30	44.81	19.61	0.70	0.998
	40	43.19	13.19	0.73	0.998
ZR03	22	55.85	33.50	0.58	0.994
	30	48.89	14.69	0.68	0.994
	40	45.24	8.54	0.84	0.998
LG01	22	36.16	23.62	0.95	0.998
	30	32.41	14.42	1.21	0.992
	40	32.29	8.97	1.14	0.971
LG03	22	35.19	17.78	1.15	0.981
	30	36.72	13.03	0.87	0.973
	40	33.49	7.66	1.03	0.966

Once the rate of reaction ( $k$ ) for the hyperbolic function and the time constant ( $\tau$ ) for the exponential function were calculated, the respective activation energies were determined as shown in Figures 4.33 and 4.34. The slope of this line was the negative quotient of the universal gas constant  $R$  (8.3144 J/mol-K) and the activation energy  $E_a$  (kJ/mol). This procedure was followed in quantifying  $E_a$  for all the cements. As seen in Figure 4.33 and 4.34, for both functions the natural logarithm of the rate constants ( $k$ ) or ( $1/\tau$ ) were plotted against the reciprocal of the absolute curing temperature (K).

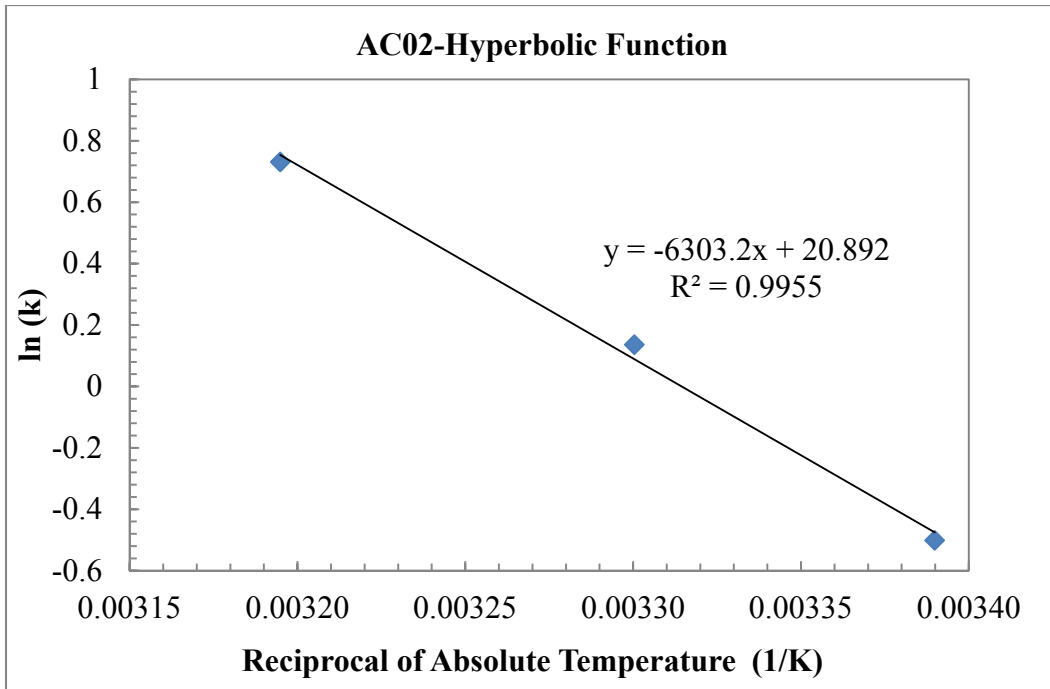


Figure 4.33: Activation Energy Determination  $E_a$  Using Hyperbolic Function on AC02

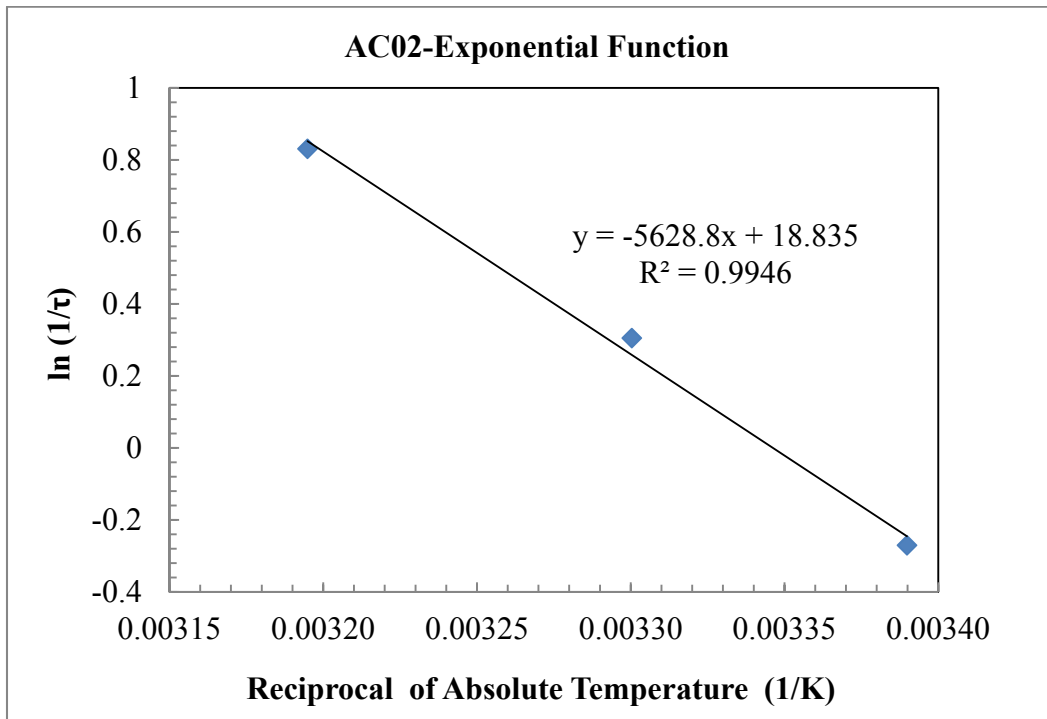


Figure 4.34: Activation Energy Determination  $E_a$  Using Exponential Function on AC02

The results presented in Table 4.9 indicate that the activation energy values determined for six of the as-received cements using mortar strength data showed similar trends regardless of the function used in calculating activation energy. It was also observed that in general, increasing cement fineness decreased activation energy except for ZR03. According to models presented in the literature [20], incorporation of some mineral admixtures will increase activation energy.

**Table 4.9: Activation Energy for As-Received Cements**

Cement	E <sub>a</sub> -Hyperbolic (kJ/mol)	R <sup>2</sup>	E <sub>a</sub> -Exponential (kJ/mol)	R <sup>2</sup>	E <sub>a</sub> Difference (kJ/mol)
AC02	52.4	0.996	46.8	0.995	5.6
AC03	46.3	0.971	44.3	0.975	2.0
ZR02	39.8	0.992	39.3	0.983	0.5
ZR03	60.0	0.995	57.8	0.973	2.1
LG01	57.5	0.978	41.2	0.997	16.3
LG03	36.2	0.866	36.1	0.990	0.1

In order to verify the mineralogical composition of ZR cements further, calibration curves were used in quantifying tricalcium silicates of this series. The results indicated that both ZR02 and ZR03 cements have a tricalcium silicate content of 52%. This C<sub>3</sub>S content is about 5% lower than the amount quantified using Rietveld analysis.

For AC cements and LG cements, it was found that for the same cement mineralogy, increasing cement fineness or decreasing cement mean particle size decreased the activation energy determined through both exponential and hyperbolic functions. It is well established in the literature that increasing cement fineness results in an increase in the rate of reaction. This is due to an increase in the surface area of cement particles that is available to react with water. The findings are in agreement with the models proposed in the literature as to the effect of increased fineness reducing the magnitude of the calculated activation energy [20]. However, the range of activation energy values for cements with the same mineralogy, but different fineness, appeared to be more pronounced when using the hyperbolic function (ASTM specified). Analysis using the hyperbolic function produced an activation energy range of 36.2-57.5 kJ/mol, whereas the exponential function produced a range of 36.1-46.8 kJ/mol. The published literature [28-30, 81]

indicates that the exponential function is not sensitive enough to reflect the combined effect of time and temperature on strength development.

Since Blaine fineness and mean particle size significantly affect the activation energy calculated from mortar strength, it is imperative, when addressing the effect of cement mineralogy on activation energy, that the fineness values and particle sizes are similar. This is a challenging task given the chemical, physical and mineralogical characteristics of the cements studied here. Comparison of AC03 and ZR03 cements (Blaine fineness values of 612 and 590 m<sup>2</sup>/kg, respectively, and MPS of 10.1 and 9.6 μm, respectively) reveals that for cements of the same tricalcium aluminate content, increasing C<sub>3</sub>S (QXRD-Rietveld) from 57% (ZR03) to 62% (AC03) decreased the strength-based activation energy from 60 kJ/mol to 46 kJ/mol. This effect appeared to be overshadowed if the mean particle size was simultaneously increased, as in the case of ZR02 and AC02. This observation appears to sustain the significance of cement particle size for activation energy. Also, comparing AC03 and LG03 (similar MPS of 10.1 and 10.3 μm, respectively, but different Blaine fineness values of 612 and 530 m<sup>2</sup>/kg, respectively) reveals that increasing C<sub>3</sub>A decreased the activation energy.

In conclusion, this section presented quantification of activation energy based on strength measurements at 3 curing temperatures per ASTM C1074-11 [31]. Two functions, the hyperbolic and exponential were used in determining the activation energy based on mortar strength data. The findings of this study indicated that cement fineness and mean particle size have a significant effect on the strength-based activation energy. The general observed trend was that an increase in cement fineness and a decrease in mean particle size decreased the activation energy when considering cements from the same source (clinker) and therefore cements of similar mineralogy. Additionally, increasing the C<sub>3</sub>S or decreasing the SO<sub>3</sub>/C<sub>3</sub>A ratio for cements of similar Blaine fineness and mean particle size was found to lower the activation energy determined through mortar cube strength.

#### **4.7 Density of As-Received Cements**

The measured densities for all cements used in this study are presented in Table 4.10, where it can be seen that ZR03 had the lowest density. In general, the densities reported here are within the ranges published for portland cements.

**Table 4.10: Density of As-Received Cements**

<b>Cement</b>	<b>Density (Mg/m<sup>3</sup>)</b>	<b>Cement</b>	<b>Density (Mg/m<sup>3</sup>)</b>
CLEP	3.16	ZR02	3.14
CLE02	3.16	ZR03	3.12
CLE03	3.16	ERD06	3.17
CHC	3.15	LG01	3.14
AC02	3.14	LG03	3.14
AC03	3.14		

#### **4.8 Hydration Process and Cement Fineness**

To relate cement fineness and composition to their effects on cement hydration, the progress of the hydration process was followed through semi-quantitative x-ray analysis of the hydration product calcium hydroxide using x-ray diffraction (XRD). The results are depicted in Figures 4.35 through 4.37 for AC, ZR and LG cements. Rutile was used as a reference material for semi-quantification purposes. The data indicate that for coarse cements (AC02, ZR02, and LG01), it appears that the calcium hydroxide formed during the first few hours of hydration is less than that in the finer cements. This is to be expected, as more surface area is available for reaction in finer cements. However, at an age of 7 days, the amount of calcium hydroxide appears to be higher in coarser cements, indicating that the effect of cement fineness on hydration kinetics dominates the reaction during the early stages of hydration. It is also noticed that AC cements had the highest calcium hydroxide content at 7 days due to their higher tricalcium silicate contents. While the amount of calcium hydroxide appears to continue to increase with hydration time for AC and ZR cements, the pattern appears to be different for LG cements due to possible secondary reactions with calcium aluminates present in those cements.

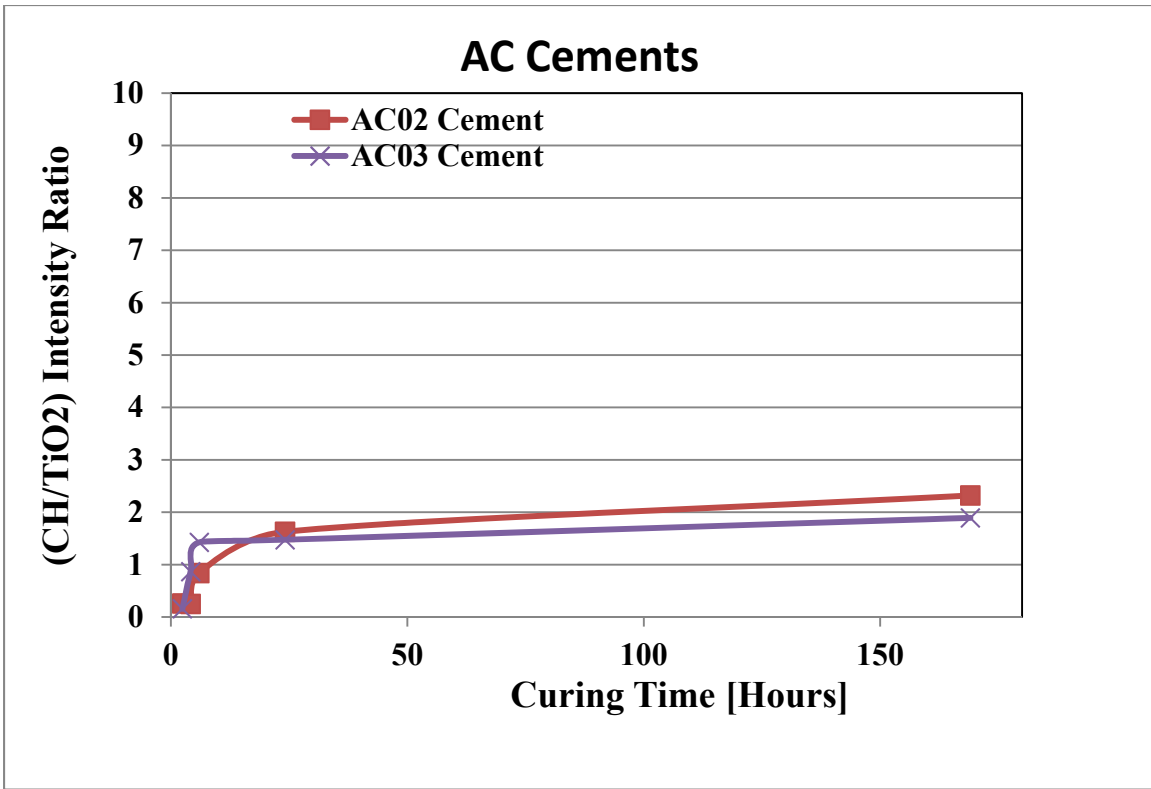


Figure 4.35: Relative Calcium Hydroxide Content with Hydration Time for AC Cements

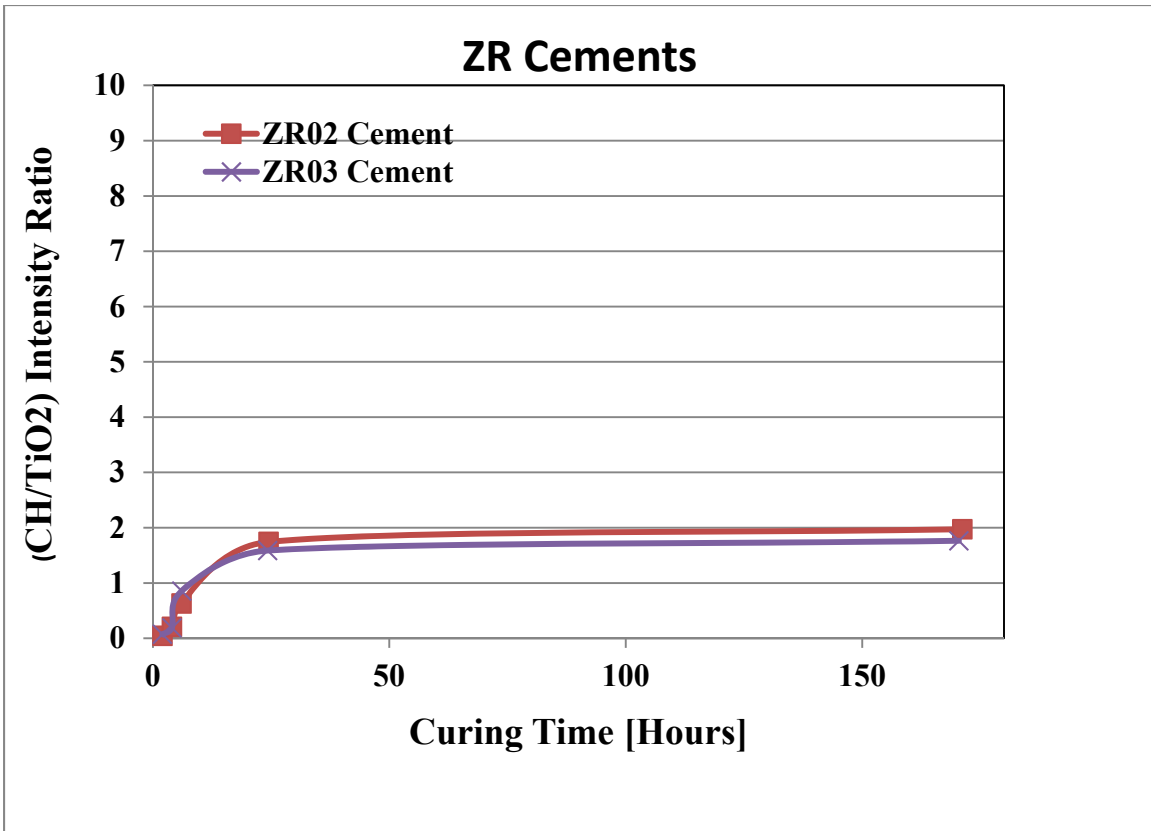


Figure 4.36: Relative Calcium Hydroxide Content with Hydration Time for ZR Cements

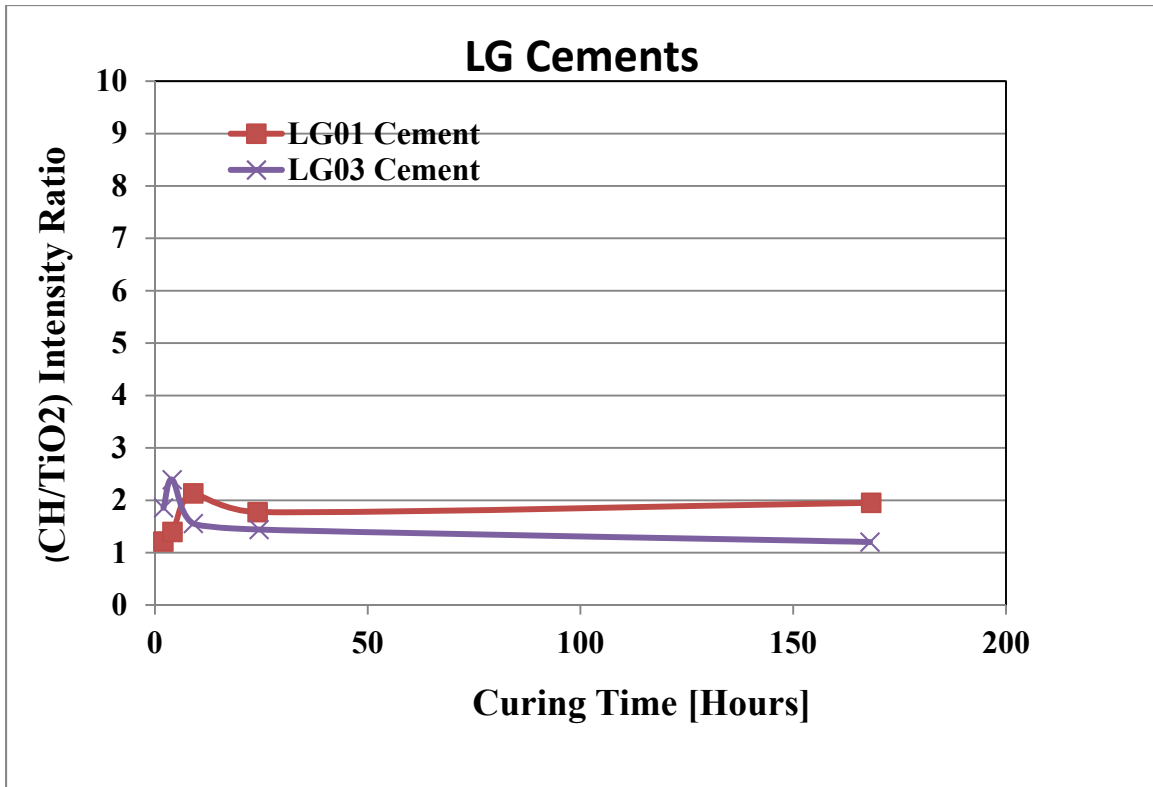


Figure 4.37: Relative Calcium Hydroxide Content with Hydration Time for LG Cements

#### 4.9 Restrained Shrinkage Measurements and Cement Fineness

Three rings per mortar mix were prepared for restrained shrinkage measurements in accordance to ASTM C1581-09a [77]. The specimens were cured for 24 hours using wet burlap followed by air-drying. The results for restrained shrinkage experiments are presented in Table 4.11 for mixes using  $w/c=0.485$  and Table 4.12 for mixes prepared with  $w/c=0.45$

Table 4.11: Restrained Shrinkage for AC Cement Mortar ( $w/c=0.485$ )

Specimen	Average Age at Cracking (days)
AC02	7
AC03	5

**Table 4.12: Restrained Shrinkage for LG, AC, and ZR Cement Mortars (w/c=0.45)**

Specimen	Average Age at Cracking (Days)
LG01	3
LG03	3
AC02	6
AC03	5
ZR02	6
ZR03	5

The findings of this study indicate that the coarser cement mixes cracked at longer times in agreement with the published literature [13]. According to Benz et al., coarser cements have a lower risk for cracking at early ages compared to finer cements. Comparing the strain as a function of time data for the AC03 and AC02 mixes, plotted in Figures 4.38 and 4.39, respectively, the time to cracking appeared to have decreased by approximately 25-30% when cement fineness increased from 417 to 612 m<sup>2</sup>/kg for AC02 and AC03, respectively. However, the differences did not result in a different classification of cracking potential for the cements studied here. Based on the definitions set in ASTM C1581-09a [77] for the criteria for cracking potential, all cements were classified as having a high potential for cracking. Cements that were high in tricalcium aluminates appear to have cracked at the shortest times as evident from the performance of LG cements.

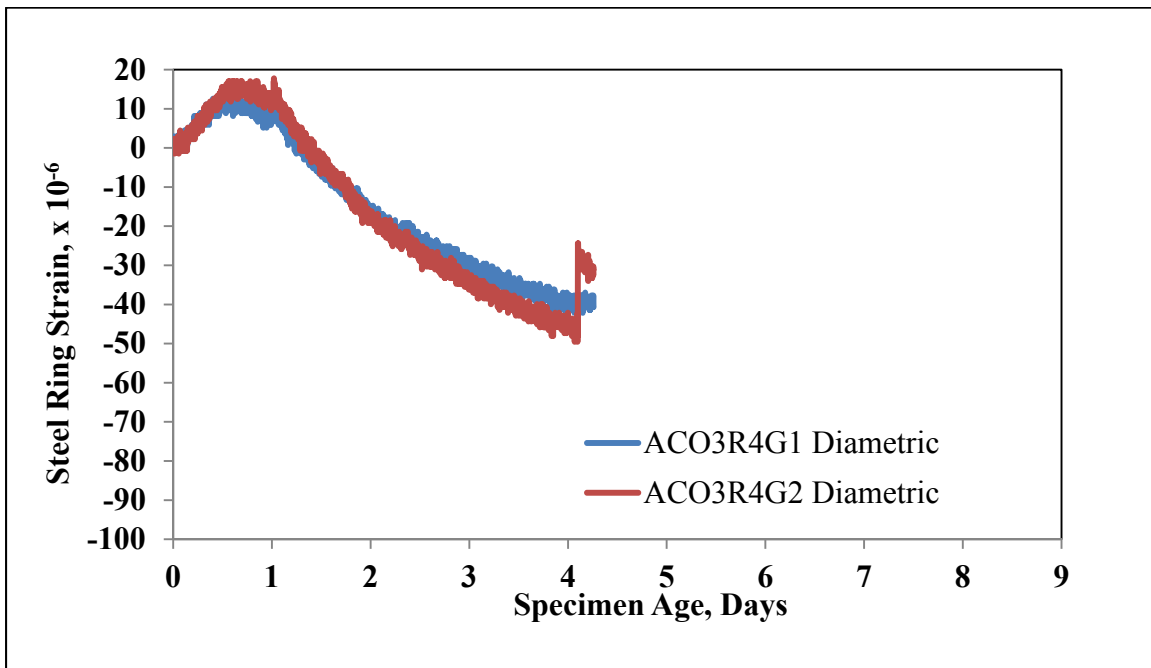


Figure 4.38: Development of Steel Ring Strain as a Function of Age for AC03 Mortar Mix

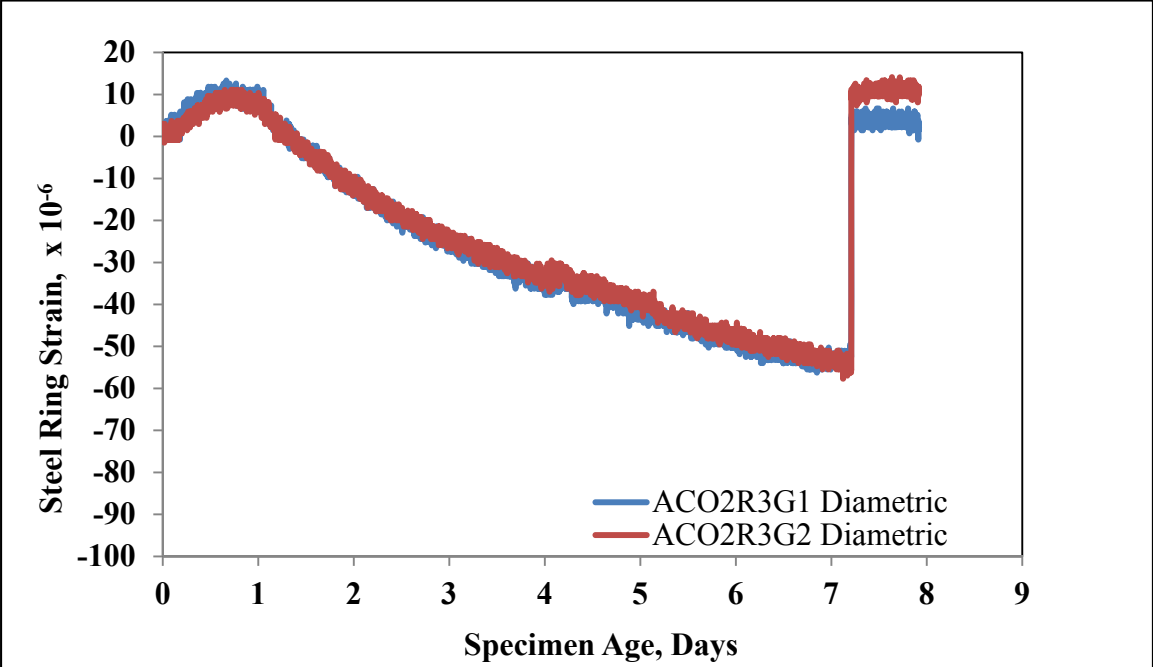


Figure 4.39: Development of Steel Ring Strain as a Function of Age for AC02 Mortar Mix

## CHAPTER 5: CONCLUSIONS AND RECOMMENDATIONS

This investigation primarily addressed the effects of cement particle size and mineralogy on the heat of hydration of portland cement. The findings of this study can be summarized as follows:

1. For portland cements with the same mineralogy (same source), the measured heat of hydration (HOH) was affected by cement Blaine fineness and particle size distribution. For cements from the same source, grinding to higher Blaine fineness or lower mean particle size increased the measured heat of hydration. This effect was confirmed with 7-day heat of hydration measurements using a TAM Air isothermal conduction calorimeter (internal mixing) per ASTM C1702.
2. The effect of portland cement fineness and/or mean particle size on the heat of hydration was also assessed using ASTM C186. The results indicate that for cements of the same mineralogy, increasing cement fineness and/or decreasing its mean particle size increased its heat of hydration. Fineness effects were observed on the measured heat at 7 days as well as 28 days.
3. Comparison of 2 cements, CLEP and ZR03, with the same heat index of 85, showed that the large differences in their fineness and particle sizes resulted in a 13-14 cal/g difference in the 7-day HOH.
4. Cements of similar Blaine fineness and heat index, in the range of 87-89, had HOH difference of about 14 cal/g at hydration time of 7 days.
5. Increasing tricalcium silicate and/or tricalcium aluminate contents of portland cements increased the measured heat of hydration at 7 days.
6. Portland cements produced from the same clinker (same mineralogy) showed that activation energy was affected by cement fineness. Both AC and LG portland cements showed a general trend of a decrease in the activation energy with an increase in cement fineness.
7. Increasing tricalcium silicate content or decreasing the  $\text{SO}_3/\text{Al}_2\text{O}_3$  ratio decreased the activation energy determined through mortar compressive strength measurements.
8. Increasing cement fineness reduced the age at cracking for Type II cements tested under conditions of restrained shrinkage.

9. Increasing cement fineness increased the rate of hydration as assessed by calcium hydroxide analysis.

Based on the findings of this study the following are recommended:

1. Require a maximum heat of hydration and a maximum fineness for Type II MH portland cements.
2. Determine heat of hydration of portland cement by direct measurement using the methods specified in ASTM C186 and/or ASTM 1072. The method used for heat determination should be noted.
3. For the acceptance of concrete mix designs, heat of hydration measurements of the cementitious system, including mineral and chemical admixtures, is recommended. The composite heat of hydration should be more useful in predicting the thermal behavior when evaluating the cracking tendency of a mix design.
4. Evaluate which method of determining heat of hydration of portland cement, ASTM C186 or ASTM C1702, is most applicable for predicting the thermal behavior of cementitious structures that are susceptible to cracking from thermal stresses.
5. Investigate further the effects of particle size and fineness on the shrinkage of portland cements and blended portland cements.
6. Study the effects of blending portland cements with commonly used pozzolanic materials on the hydration kinetics, heat evolution, strength development, and microstructural development.
7. Evaluate the use of Rietveld analysis and electron scanning microscopy coupled with energy dispersive spectroscopy for mineralogical characterization of cementitious systems.

## REFERENCES

1. Ferraro, C.C., Ishee, C. A., & Bergin, M. (2010). *Report of Changes to Cement Specifications AASHTO M85 and ASTM C150 Subsequent to Harmonization* (FL/DOT/SMO/10-536). Tallahassee, FL: Florida Department of Transportation
2. Poole, T. (2009). Predicting 7-Day Heat of Hydration of Hydraulic Cement from Standard Test properties. *Journal of the ASTM International*, 6 (6), p. 10.
3. Woods, H., Steinour, H. H., & Stark, H.R. (1932). Effect of Composition of Portland Cement on Heat Evolved During Hardening. *Industrial and Engineering Chemistry*, 24 (11), p. 1207-1224.
4. ASTM C150-12. (2012). "Standard Specification for Portland Cement" *Annual Book of ASTM Standards*, V. 04.01, ASTM International, West Conshohocken, PA.
5. Mehta, P. & Monteiro, P. (1993). *Concrete: Structure, Properties, and Materials*. 2nd ed. Englewood Cliffs, NJ: Prentice-Hall International Series in Civil Engineering and Engineering Mechanics, p. 43-77.
6. Lea, F. M. (1970). *The Chemistry of Cement and Concrete*. London, Edward Arnold
7. Lea, F. M., & Hewlett, P. C. (1998). *Lea's Chemistry of Cement and Concrete*. London: Arnold.
8. ASTM C186-05. (2005). "Standard Test Method for Heat of Hydration of Hydraulic Cement" *Annual Book of ASTM Standards*, V. 04.01, ASTM International, West Conshohocken, PA.
9. Poole, T. (2004). Predicting Heat of Hydration in Hydraulic Cement, unpublished report, *Research and Development Center*. Published (2009) in: *Journal of ASTM International (JAI)*, 6 (6), p. 10
10. ASTM C1702-13. (2013). "Standard Test Method for Measurement of Heat of Hydration of Hydraulic Cementitious Materials Using Isothermal Conduction Calorimetry" *Annual Book of ASTM Standards*, V. 04.01, ASTM International, West Conshohocken, PA.
11. Verbeck, G. J. & Foster, C. W. (1950). Long-Time Study on Cement Performance in Concrete: Chapter 6-The Heats of Hydration of the Cements. *Proceedings of the American Society for Testing and Materials*, 50 (1), p. 1-28.

12. Azari, H. (2010). Statistical Modeling of Cement Heat of Hydration Using Phase and Fineness Variables. *National Cooperative Highway Research Program, Transportation Research Board of the National Academies*, NCHRP web-only Document 167, p. 1-73.
13. Bentz, D.P., Sant, G., & Weiss, J. (2008). Early Age properties of Cement-Based Materials: I. Influence of Cement Fineness. *ASCE Journal of Materials in Civil Engineering*, 20(7), p. 502-508
14. Brewer, H.W. & Burrows, R.W. (1951). Coarse-Ground Cement Makes More Durable Concrete. *Journal of the American Concrete Institute*, 22(5), p. 353-360.
15. Burrows, R.W. (1988). The Visible and Invisible Cracking of Concrete. *American Concrete Institute*, Monograph No. 11, Farmington Hills, MI.
16. Tennis, P.D. & Bhatti, J. I. (2005). Portland Cement Characteristics-2004. *Concrete Technology Today, PCA*, 26 (3).
17. Bentz, D.P. & Haecker, C.J. (1999). An Argument for using Coarse Cements in High Performance Concretes. *Cement and Concrete research*, 29 (4), p. 615-618.
18. Laidler, K. (1969). *Theories of Chemical Reaction Rates*. New York: McGraw-Hill, Inc., p. 1-12.
19. Schindler, S. (2002). *Concrete Hydration, Temperature Development, and Setting at Early-Ages*. PhD. University of Texas.
20. Poole, J. L. (2007). *Modeling Temperature Sensitivity and Heat Evolution of Concrete*. PhD, University of Texas, Austin.
21. Poole, J. L., Riding, K.A., Folliard, K. J., Juenger, M.C. G, & Schindler, A.K. (2007). Methods for Calculating Activation Energy for Portland Cement. *ACI Journal*, 104 (1), p. 303-311.
22. Kjellsen, K. O. & Detwiler, R. J. (1993). Later-Age Strength Prediction by a Modified Maturity Model. *ACI Materials Journal*, 90 (3), p. 20-227.
23. Kjellsen, K. O. & Detwiler, R. J. (1992). Reaction kinetics of PC Mortars Hydrated at Different Temperatures. *Cement and Concrete Research*, 22 (1), p. 112-120.
24. Kada-Benameur, H., Wirquin, E., & Duthoit, B. (2000). Determination of Apparent Activation Energy of Concrete by Isothermal Calorimetry. *Cement and Concrete Research*, 30 (2), p. 301-305.

25. D'Aloia, L. & Chanvillard, G. (2002)., Determining the "Apparent" Activation Energy of Concrete:  $E_a$  - Numerical Simulation of the Heat of Hydration of Cement. *Cement and Concrete Research*, 32 (8), p. 1277-1289.
26. Bien-Aime, A. (2013). *Effect of Cement Chemistry and Properties on Activation Energy*. MS, University of South Florida.
27. Juenger, M. C. G., Winnefeld, F., Provis, J. L., & Ideker, J. H. (2011). Advances in Alternative Cementitious Binders. *Cement and Concrete Research*, 41 (12), p. 1232-1243.
28. Carino, N. (1991). The Maturity Method. In: Malhotra, V. and Carino, N. eds. (1991) *Handbook on Nondestructive Testing of Concrete*. Boca Raton, FL: CRC Press, p. 101-146.
29. Carino, N. J & Lew, H. (2001). The Maturity Method: From Theory to Application: In: *Proceedings of the 2001 Structures Congress and Exposition*, Washington, D.C. May 2001. Reston, VA: *American Society of Civil Engineers (ASCE)*, p. 1-20.
30. Carino, N. J. (1984). The Maturity Method: Theory and Application. *Journal of Cement, Concrete, and Aggregates (ASTM)*, 6 (2), p. 61-73.
31. ASTM C1074-11. (2011). "Standard Practice for Estimating Concrete Strength by the Maturity Method" *Annual Book of ASTM Standards*, V. 04.01, ASTM International, West Conshohocken, PA.
32. McIntosh, J. (1949). Electric Curing of Concrete. *Magazine of Concrete Research*, 1 (1), p. 21-28.
33. Nurse, R. (1949). Steam Curing of Concrete. *Magazine of Concrete Research*, 1 (2), p. 7-88.
34. Saul, A. (1951). Principles Underlying the Steam Curing of Concrete at Atmospheric Pressure. *Magazine of Concrete Research*, 2 (6), p. 127-140.
35. Ishee, C. A. (2011). *Evaluating the Performance of Portland Cement Under Differing Hydration Conditions*, PhD, McGill University.
36. Ferraro, C. C. (2009). *Determination of Test Methods for the Prediction of the Behavior of Mass Concrete*. PhD, University of Florida.

37. Freiesleben Hansen, P. & Pedersen, E. J. (1984). Curing of Concrete Structures. In: CEB-General Task Group 20. (eds.) (1985) *Draft CEB Guide to Durable Concrete Structures*. 1st ed. Switzerland: Comité Euro-International du Béton (CEB), p. 1-42.
38. Pinto, R.C.A & Schindler, A. K. (2010). Unified Modeling of Setting and Strength Development. *Cement and Concrete Research*, 40 (1), p. 58-65.
39. Verbeck, G. J. & Helmuth, R. A. (1968). Structures and Physical Properties of Cement Pastes. *Proceedings of the International Symposium on the Chemistry of Cement*, III (1), p. 1-32.
40. Maekawa, K., Chaube, R., & Kishi, T. (1999). *Modeling of Concrete Performance, Hydration, Microstructure Formation, and Mass Transport*. London: E & FN Spon.
41. Hooton, R. D., Boyd, A. J., & Bhadkamkar, D. D. (2005). Effect of Cement Fineness and C<sub>3</sub>S Content on Properties of Concrete: A Literature Review. *Portland Cement Association*, R&D Serial No.2781, p. 1-14.
42. Bentz, D.P, Garboczi, E.J., Claus, J., Haecker, C.J, & Jensen, O.M. (1999). Effects of Cement Particle Size Distribution on Performance Properties of Portland Cement-Based Materials. *Cement and Concrete Research*, 29 (10), p.1663–1671.
43. ASTM C778-13. (2013). "Standard Specification for Standard Sand" *Annual Book of ASTM Standards*, Vol. 4.02, ASTM International, West Conshohocken, PA.
44. ASTM C114-13. (2013). "Standard Test Methods for Chemical Analysis of Hydraulic Cement" *Annual Book of ASTM Standards*, Vol. 4.02, ASTM International, West Conshohocken, PA.
45. ASTM C188-09. (2009). "Standard Test Method for Density of Hydraulic Cement" *Annual Book of ASTM Standards*, Vol. 4.02, ASTM International, West Conshohocken, PA.
46. Stutzman, P. E. (2005). Powder Diffraction Analysis of Hydraulic Cements: ASTM Rietveld Round Robin Results on Precision. *ICDD-Advances in X-ray Analysis*, 48 (1), p. 33-38.
47. Stutzman, P. E. (1996). Guide for X-Ray Powder Diffraction Analysis of Portland Cement and Clinker (NISTIR 5755). *National Institute of Standards and Technology, Building and Fire Research Laboratory*, p. 1-38.

48. Leng, Y. (2008). *Materials Characterization: Introduction to Microscopic and Spectroscopic Methods*. Singapore, J. Wiley & Sons, p. 45-79.
49. Maqsood, A., & Iqbal, K. (2010). Materials Characterization by Non-Destructive Methods. *Journal of the Pakistan Materials Society*, 4 (1), p. 31-38.
50. ASTM C1365-06. (Reapproved 2011). "Standard Test Method for Determination of the Proportion of Phases in Portland Cement and Portland-Cement Clinker Using X-Ray Powder Diffraction Analysis" *Annual Book of ASTM Standards*, V. 04.02, ASTM International, West Conshohocken, PA.
51. Saoût, G., Kocaba, V., & Scrivener, K. (2011). Application of the Rietveld Method to the Analysis of Anhydrous Cement. *Cement and Concrete Research*, 41 (1), p. 133-148.
52. Gutteridge, W. A. (1979). "On the Dissolution of the Interstitial Phases in Portland Cement." *Cement and Concrete Research*, Vol. 9, pp. 319-324.
53. Taylor, H. F. W. (1997). *Cement Chemistry, 2<sup>nd</sup> ed.*, Thomas Telford Publishing, London, UK.
54. Taylor, J. C., Hinczak, I., Matulis, C. E. (2000). "Rietveld Full-Profile Quantification of Portland Cement Clinker: The Importance of Including a Full Crystallography of the Major Phase Polymorphs." *Powder Diffraction*, Vol. 15, No. 1, pp. 7-18.
55. Courtial, M., de Noirfontaine, M. -N., Gasecki, G., Signes-Frehel, M. (2003). "Polymorphism of Tricalcium Silicate in Portland Cement: A Fast Visual Identification of Structure and Superstructure." *Powder Diffraction*, Vol. 18, No. 1, pp. 7-15.
56. Chung, F. H. (1974). "A New X-Ray Diffraction Method for Quantitative Multicomponent Analysis." *Advances in X-ray Analysis*. New York, NY: Springer, pp. 106-115.
57. Wilson, William, K J Krakowiak, and F J Ulm. (2012). "Crystallinity of Cement Clinkers: Application of Rietveld Refinement." *Concrete Sustainability Hub@MIT - Research Profile Letter*. [http://cshub.mit.edu/sites/default/files/documents/04-2012\\_CSHub-News-Brief-Final.pdf](http://cshub.mit.edu/sites/default/files/documents/04-2012_CSHub-News-Brief-Final.pdf).
58. Jansen, D., C. Stabler, F. Goetz-Neunhoeffler, S. Dittrich, and J. Neubauer. (2011). "Does Ordinary Portland Cement Contain Amorphous Phase? A Quantitative Study Using an External Standard Method." *Powder Diffraction*. Vol. 26, pp. 31-38.

59. Klug, H. P. & Alexander, L.E. (1974). *X-ray Diffraction Procedures: For Polycrystalline and Amorphous Materials*. 2nd ed. Hoboken, NJ: John Wiley & Sons.
60. Mindess, S., Young, J. F., & Darwin, D. (2003). *Concrete*. 2nd ed. Upper Saddle River, NJ: Prentice-Hall.
61. ASTM C204-11. (2011). "Standard Test Method for Fineness of Hydraulic Cement by Air-Permeability Apparatus" *Annual Book of ASTM Standards*, V. 04.01, ASTM International, West Conshohocken, PA.
62. Mehta, P. & Monteiro, P. (1993). *Concrete: Structure, Properties, and Materials*. 2nd ed. Englewood Cliffs, NJ: Prentice-Hall International Series in Civil Engineering and Engineering Mechanics.
63. Malvern.com. (2009). *Why switch from Blaine to PSD?* [online] Available at: [http://www.malvern.com/processeng/industries/cement/blaine\\_to\\_PSD.htm](http://www.malvern.com/processeng/industries/cement/blaine_to_PSD.htm) [Accessed on 16 Nov 2012].
64. Jilavenkatesa, A., Dapkunas, S. J., & Lum, L. (2001). Particle Size Characterization. *National Institute of Science and Technology (NIST)*, Special Publication 960-1, p. 1-49.
65. HORIBA Instruments. (2001). *LA-950 Instructional Manual (2001)*, Irvine, CA, p. 1-96.
66. HORIBA Instruments. (2012). *A Guidebook to Particle Size Analysis*. [online] Available at: [http://www.horiba.com/fileadmin/uploads/Scientific/Documents/PSA/PSA\\_Guidebook.pdf](http://www.horiba.com/fileadmin/uploads/Scientific/Documents/PSA/PSA_Guidebook.pdf) [Accessed: 14 Nov 2012].
67. Wadsö, L. (2005). Applications of an Eight-channel Isothermal Conduction Calorimeter for Cement Hydration Studies. *Cement International*, issue 5, p. 94–101.
68. TA Instruments. (2008). *TAM Air Calorimeter Operator's Manual (2008)*, New Castle, p. 1-64.
69. Sedaghat, A. R., Zayed, A. and Sandberg, P. (2013). "Measurements and Predictions of Heat of Hydration of Portland Cement Using Isothermal Conduction Calorimetry." *ASTM Journal of Testing and Evaluation*. Vol. 41, No. 6, pp. 1-8.
70. Wadsö, L. (2010). Operational Issues in Isothermal Calorimetry. *Cement and Concrete Research*, 40 (7), p. 1129-1137.

71. ASTM C403-08. (2008). "Standard Test Method for Time of Setting of Concrete Mixtures by Penetration Resistance" *Annual Book of ASTM Standards*, V. 04.02, ASTM International, West Conshohocken, Pa
72. Dodson, V.H. (1994). Time of Setting. In: Klieger, P. & Lamond, J. F. eds. (1994) *Significance of Test and Properties of Concrete and Concrete-Making Materials (STP; 169C)*. 4th ed. Philadelphia, PA: ASTM, p. 77-87.
73. ASTM C305-13. (2013). "Standard Practice for Mechanical Mixing of Hydraulic Cement Pastes and Mortars of Plastic Consistency" *Annual Book of ASTM Standards*, V. 04.01, ASTM International, West Conshohocken, PA.
74. ASTM C109-13. (2013). "Standard Test Method for Compressive Strength of Hydraulic Cement Mortars (Using 2-in. or [50-mm] Cube Specimens)" *Annual Book of ASTM Standards*, V. 04.01, ASTM International, West Conshohocken, PA.
75. Taylor, H. F. W. (1990). *Cement chemistry*. New York and London, Thomas Telford, p. 123-166.
76. Wang, A., Zhang, C., & Ningsheng, Z. (1999). The Theoretic Analysis of the Influence of the Particle Size Distribution of Cement System on the Property of Cement. *Cement and Concrete Research*, 29 (11), p. 1721–1726.
77. ASTM C1581/C1581M-09a. (2009). "Standard Method for determining Age at Cracking and Induced Tensile Stress Characterization of Mortar and Concrete under Restrained Shrinkage" *Annual Book of ASTM Standards*, V. 04.01, ASTM International, West Conshohocken, PA.
78. See, H.T., Attiogbe, E. K., & Miltenberger, M. A. (2004). Potential for Restrained Shrinkage Cracking of Concrete and Mortar. *Cement, Concrete, and Aggregate*, 26 (2), p. 123-130.

## APPENDIX A

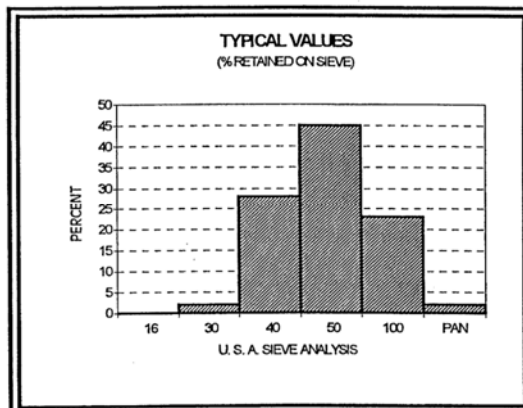
## Appendix A: Characteristics of Sand



### PRODUCT DATA

**ASTM<sup>(1)</sup> GRADED SAND**  
**UNGROUND SILICA**  
**PLANT: OTTAWA, ILLINOIS**

(1) American Society for Testing and Materials



USA STD SIEVE SIZE	MILLIMETERS	% RETAINED		CUMULATIVE % PASSING
		INDIVIDUAL	CUMULATIVE	
16	1.180	0.0	0.0	100.0
30	0.600	2.0	2.0	98.0
40	0.425	28.0	30.0	70.0
50	0.300	45.0	75.0	25.0
100	0.150	23.0	98.0	2.0
PAN		2.0	100.0	

### TYPICAL PHYSICAL PROPERTIES

COLOR..... WHITE	MINERAL..... QUARTZ
GRAIN SHAPE..... ROUND	pH..... 7.0
HARDNESS (MOHS)..... 7	SPECIFIC GRAVITY (g/cc)..... 2.65
MELTING POINT (DEGREES F)..... 3100	

### TYPICAL CHEMICAL ANALYSIS, %

SiO <sub>2</sub> (SILICON DIOXIDE)..... 99.7	MgO (MAGNESIUM OXIDE)..... < 0.01
Fe <sub>2</sub> O <sub>3</sub> (IRON OXIDE)..... 0.02	Na <sub>2</sub> O (SODIUM OXIDE)..... < 0.01
Al <sub>2</sub> O <sub>3</sub> (ALUMINUM OXIDE)..... 0.06	K <sub>2</sub> O (POTASSIUM OXIDE)..... < 0.01
TiO <sub>2</sub> (TITANIUM DIOXIDE)..... 0.012	LOI (LOSS ON IGNITION)..... 0.1
CaO (CALCIUM OXIDE)..... < 0.01	

### CONFORMS TO ASTM C778

12-15-97

U.S. Silica Company • P.O. Box 187, Berkeley Springs, WV 25411-0187 • (800) 243-7500